OZONOLYSIS OF AQUEOUS PHENOL AND ACETIC ACID

IN A PRESSURIZED BUBBLE COLUMN

By

VICTORIA LYNN MILAM

Bachelor of Science in Chemical Engineering

Oklahoma State University

Stillwater, Oklahoma

1981

Submitted to the Faculty of the Graduate College
of the Oklahoma State University
in partial fulfillment of the requirements
for the Degree of
MASTER OF SCIENCE
July, 1984

OZONOLYSIS OF AQUEOUS PHENOL AND ACETIC ACID

IN A PRESSURIZED BUBBLE COLUMN

Thesis Approved:

Archibald D. Hill
Thesis Adviser

Rob G. Will

Mayis Seapan

Norman N. Durha
Dean of the Graduate College

ACKNOWLEDGMENTS

TABLE OF CONTENTS

LIST OF TABLES

LIST OF FIGURES

NOMENCLATURE

a   interfacial area per unit volume

A   surface area of gas-liquid contact

c_{AG} concentration of component A in the gas phase

c_{Ai} concentration of component A at the interphase

c_{AL} Concentration of component A in the bulk liquid

c_{A_1} liquid bulk concentration of component A entering the reactor

c_{A_2} liquid bulk concentration of component A leaving the reactor

c_A^* equilibrium concentration of component A

$c_{A_1}^*$ equilibrium concentration of component A entering the reactor

$c_{A_2}^*$ equilibrium concentration of component A leaving the reactor

$[COD]_f$ final chemical oxygen demand

$[COD]_i$ initial chemical oxygen demand

$[COD]_m$ chemical oxygen demand at the half-hour

ΔCOD change in the chemical oxygen demand

d_B bubble diameter

D   ozone dose rate parameter

D_A molecular diffusion of component A

D_{O_3} molecular diffusion of ozone D_{O_2} molecular diffusion of oxygen

D_{Ph} molecular diffusion of phenol

E   enhancement factor

F   ozone gas flowrate

G   gas flowrate

h	gas holdup
H	Henry's Law constant for ozone
H_{O_2}	Henry's Law constant for oxygen
k	kinetic rate constant for phenol
k_D	kinetic rate constant for ozone decomposition
k_G	gas film coefficient
k_L	liquid film coefficient
$k_L a$	liquid side mass transfer coefficient with effective interfacial area
$k_L' a$	liquid side mass transfer coefficient with effective interfacial area for chemical absorption
k_{O_2}	rate constant for phenol in the wet air oxidation process
k'	kinetic reaction rate constant for phenolate ions
K_G	overall mass transfer coefficient based on gas phase concentrations
K_H	Henry's Law constant in units of atm M^{-1}
K_L	overall mass transfer coefficient based on liquid phase concentrations
K_2	equilibrium constant for Equation (40) of the literature survey
L	length of liquid film
L_f	height of the liquid in the column when there is recycling and gas bubbling
L_o	height of the liquid in the column when there is recycling and no gas bubbling
M_{O_3}	molar concentration of ozone in the liquid phase
N_A	quantity of A transferred per unit of time

$[O_2]$	oxygen concentration
$[O_3]$	ozone concentration
$[O_3]_f$	final ozone concentration
$[O_3]_i$	ozone concentration at the interface
$[O_3]_o$	initial ozone concentration
$[O_3]_t$	ozone concentration at time t
$[OH^-]$	hydrozyl concentration
ΔO_3	moles of ozone consumed
P_{AG}	partial pressure of component A in the gas phase
P_{Ai}	partial pressure of component A at the interface
P_{AL}	partial pressure of component A which is in equilibrium with the bulk liquid
P_{H_2O}	partial pressure of water
P_{O_3}	partial pressure of ozone
P	total pressure of system
$[Ph]$	phenol concentration in the bulk liquid
$[Ph]_m$	phenol concentration at the half-hour
$[Ph]_o$	initial phenol concentration
$[Ph]_{oxid}$	amount of phenol oxidized in one hour
$[Ph]_t$	phenol concentration at time t
$[Ph^-]$	concentration of phenolate ions
r	stoichiometric ratio of ozone to phenol
Re	Reynolds number
S	interfacial area
Sc	Schmidt number
Sh	Sherwood number

S_o rate at which a fraction of the surface is renewed in Danck-werts' theory

S_{O_2} stoichiometric ratio of phenol to oxygen

t reaction time

t_o length of time the surface element is exposed to the solute

T temperature in Kelvin

U_s slip velocity of the bubble with respect to the liquid

v_m amount of liquid drained at the half-hour

V reaction time

V_i initial reaction volume

V_{SL} velocity of the recycle liquid

W_o initial oxidation rate for phenol in the wet air oxidation process

X_A mole fraction of component A in the bulk liquid

Y_{O_3} mole fraction of ozone in the gas phase

y_1 ozone mole fraction at column inlet

y_2 ozone mole fraction at column outlet

θ residence time in reactor

μ molar ionic strength

CHAPTER I

INTRODUCTION

Phenol is used as a reaction compound for many manufacturing processes such as insulation, paint, plastics, and pharmaceuticals. It is also found as a side product in coal gasification, shale oil recovery, catalytic cracking units, foundries, and many other processes. The wastewater from the different types of processes contain a high concentration of phenol, causing phenol to be one of the most common aqueous pollutants. Phenol produces a "medicinal" taste and affects the skin of fish at concentrations as low as 2.5 ppb [30]. Larger concentrations not only kill fish, but completely destroy all life in the stream. Pollution of municipal water supplies by phenol-bearing wastes has become a serious problem in almost every major city in the United States [30].

The use of ozone has been proven to be one of the effective measures of eliminating phenol. Ozone is a powerful oxidant second only to fluorine among the readily available water treatment chemicals [35]. The use of ozone in treating drinking water has long been accepted in Europe, and is gaining acceptance in the United States. For wastewater treatment, ozone is able to destroy the phenolic compounds but, in general, is considered to be uneconomical compared to biological treatment [16, 33]. In certain cases, however, such as scarce availability of land, poor climate, and short operating periods, the biological treatment may not be practical.

The reaction of phenol with ozone is a mass transfer limited reaction, with ozone being transferred from the gas phase to the liquid phase. Subsequent reaction of ozone with oxidation products may be kinetically limited. The phenol is considered to react quickly with the ozone but many of the reaction products of phenol react much more slowly. The reaction between ozone and phenol is very complex. There are several multiple reaction pathways between the phenol compound and the final carbon dioxide product with the exact pathways not being quite clear. Among the products of phenol ozonation are low molecular weight organic acids. Some of these acids are stable and resistant to further oxidation with ozone. They are considered to be nontoxic [30] and are very easily biodegraded. In general, it is considered inefficient to oxidize phenol completely to carbon dioxide.

Wet air oxidation is a process that uses high temperatures (200-315°C) and high pressures (4-15 MPa) to oxidize organic compounds with oxygen. Usually for the process to be economical a minimal organic concentration of 1 to 4 percent is needed. At these concentrations the wet air oxidation process can become thermally autogeneous. The wet air oxidation process is similar to the ozonation process because it is a mass transfer limited reaction. Additional similarities are that phenol is easily oxidized and both produce low molecular weight organic acids that resist further oxidation.

With the pollution laws becoming more stringent, there is a need for more scientific information on the methods available for phenol destruction. The purpose of the present research is to attempt to improve the efficiency of the ozonation process. Temperatures of 65, 70, and 90°C are used. A pressure of 756 kPa is used. These conditions are used for

the following reasons. Pressure is increased to improve the absorption of ozone and the concentration of dissolved diatomic oxygen. Temperature is raised to increase reaction rates and to approach conditions similar to wet air oxidations. The initial phenol concentration in the experiments is 0.01 m. Acetic acid is added in some experiments to increase the organic concentration. The stoichiometry of the reaction, the reaction products, and the mass transfer coefficients are studied to determine if the efficiency of the process is improved.

CHAPTER II

REVIEW OF THE LITERATURE

Stoichiometry

Niegowski [31] was one of the earliest to study the oxidation of phenol with ozone. A 500 mL gas washing bottle was used for the reactor. Pure phenol was found to easily oxidize with ozone over a wide range of pH. For a 100 mg/L solution at a pH of 12, 2.2 moles of ozone per mole of phenol reduced the phenol concentration by 50 percent and 3.7 moles of ozone per mole of phenol reduced the phenol concentration by 99 percent. A 1000 mg/L solution of pure phenol with pH 12 was used to study the chemical oxygen demand (COD) reduction. The COD reduction was found to be around 1.4 mg ozone per mg of change in chemical oxygen demand.

The oxidation of complex waste solutions was also studied by Niegowksi [31]. To achieve a 99 percent phenol reduction, the lowest ozone to phenol ratio was 1.96 moles ozone per mole of phenol for a refinery waste, and the highest ratio was 39.2 moles of ozone per mole of phenol for one of the coke plant waste. The initial pH was found to influence the oxidation of phenols in waste solutions. For example, the ozone required at pH 12 for a phenolic waste solution was only one-half that of the ozone required at pH 7 for 99 percent oxidation of phenol. Up to 50 percent oxidation, however, the ozone-phenol reaction was still very rapid and pH adjustment had little if any effect.

4

Peppler and Fern [33] studied phenol ozonation using a 4.5 liter reactor with an ozone flow rate of 3 g/hr. For pure phenol solutions, the initial concentration was approximately 500 mg/L. It was assumed that the theoretical requirement for phenol destruction was 3 moles of ozone per mole of phenol. The experimental stoichiometric ratio at pH 5.7 was 4.7 moles ozone per mole phenol and at pH 12.3 was 3.1 moles ozone per mole phenol. For unstripped catalytic cracker condensate water, the moles of ozone per mole of phenol ratio was very high and the change in pH had little if any effect on the stoichiometric ratio. It was surmised that the oxidation of sulphides to sulphites and sulphates proceeded in preference to the oxidation of phenol.

McPhee and Smith [28] had samples of highly oxidized refinery waste and of pure phenol solutions treated with ozone. The initial phenol concentrations were 500 ppb for the pure phenol solution and 800 ppb for the refinery waste solution. The efficiency of the ozone absorbed per ozone applied ranged from 23.3 to 64.4 percent for pure phenol, and from 76.4 to 91.3 percent for refinery waste. The stoichiometric ratio for the pure phenol was 5.2 moles of ozone per mole of phenol at 50 percent reduction of phenol and 18.8 moles of ozone per mole of phenol at 99 percent reduction. The oxidation ratio for the refinery waste was 53.4 moles of ozone per mole of phenol at 96 percent phenol reduction.

Eisenhauer [9] studied the effect that different parameters had on the oxidation of phenol with ozone. He used a 1000 ml reactor with phenol concentration varying from 50 to 300 mg/L, ozone concentration varying from 15 to 30 mg/L, and ozone flow rate varying from 0.1 to 0.5 L/min. The amount of ozone consumed per ozone supplied was around 50 percent for all of the varying experimental conditions. Furthermore,

from the data given in the paper, after consumption of about four molecules of ozone, substantially all of the phenol present initially had disappeared.

Eisenhauer, in later studies [10], conducted experiments on the pH and temperature effects. The absorption of ozone at initial pH 11.0 was quantitative until about 2.3 moles ozone per mole of phenol had been consumed. After this the ozone absorption for pH 11.0 was similar to the ozone absorption for pH 3.0 to 9.0, having an efficiency of 57.0 percent. When the moles of ozone supplied per mole of phenol was approximately 22, at pH 3.0 to 9.0, all the ozone supplied to the reaction was consumed.

The increase in temperature affected the carbon dioxide production. At 20°C the efficiency of moles ozone consumed per carbon dioxide formed was 30 percent, whereas at 50°C the efficiency was 65 percent. At 20°C after an ozone consumption greater than 15 moles ozone per mole phenol, the carbon dioxide production ceased. Similar results were found at 50°C, but instead of carbon dioxide production ceasing, the production continued but at a much reduced rate.

Anderson [1] used a continuous reactor to study the stoichiometry of the reaction with pure phenol and the efficiency of the ozone absorption. At an initial pH of 6.6 to 7.4 the efficiency of the ozone absorbed per ozone fed was around 76 percent, and at an initial pH of 11.4 the efficiency was greater than 99 percent. For 50 percent phenol conversion, the stoichiometry of moles ozone fed per mole reacted was around 4.6 at the lower pH and around 1.9 at the higher pH. The mg ozone fed per mg change in COD was around 2.0 at the lower pH and around 1.0 at the higher pH.

Bauch, Burchard, and Arsovic [5] used a reactor with a length to diameter ratio of 20:1. The initial phenol concentration was 19 mg/L. Only by the end of the reaction could ozone be detected in small quantities at the reactor outlet. After reaction of 3 moles of ozone per mole of phenol, only 70 percent of the phenol had decomposed, and after 5.5 moles of ozone there was almost no residue of phenol.

Sharifov, Mamediarova, and Shults [39] studied the treatment of wastewaters containing petroleum products using ozone. Wastewater from an oil refinery that had undergone a single-stage biological treatment in an aeration tank was used. At pH 6.0 the COD reduction was around 75 percent, whereas at a pH of 12.0 the COD reduction was around 35 percent. This indicated that with increasing pH the oxidation rate begins to drop (contrary to what other observers have noted for pure phenol). However, the ozone consumption increased sharply with increasing pH. The amount of organic content left after ozonation was higher in acid medium than in neutral or alkaline medium. In alkaline mediums, sediments of metal hydroxides are formed which adsorb organic matter and which disturb the process of ozonation. Sharifov et al. concluded that a neutral regime was best for the refinery wastewater under study.

Yamamoto et al. [46] studied the ozonation of phenol in water at 30°C in a 100 ml reactor. The initial phenol concentration was 0.618 mmole phenol and the ozone flow rate was 0.12 mmole/min. After 90 minutes, substantially all of the phenol disappeared. This corresponds to a ratio of 17.5 moles ozone fed per mole phenol. At the same time, approximately a 30 percent decrease was observed in the total organic carbon content.

Baillod, Faith, and Masi [4] studied pure phenol ozonation in a 250 ml reactor with a phenol concentration of 50 mg/L and an ozone concentration of 25 mg/L. During the first two minutes of reaction, approximately 40 to 70 percent of the ozone supplied was utilized. However, this percentage decreased rapidly after four minutes, so that during the period of 10 to 30 minutes the ozone utilized was on the order of 5 percent of the amount fed. The value of the initial stoichiometric ratio for phenol at 6.0 was found to be 3.9 moles ozone consumed per mole phenol reacted.

Singer and Gurol [42] studied phenol ozonation in a 500 ml reactor at 20°C with a phenol concentration of 140 mg/L. After 16 minutes at pH 3.0, all of the phenol had been oxidized but only 21 percent of the total organic carbon (TOC) had been removed. At the end of two hours of ozonation, only 50 percent of the TOC was removed at pH 3.0 compared to 80 percent at pH 6.0.

Chen [6] used combinations of ultrasound, Raney-Nickel catalyst and ozone to oxidize phenol. Sonocatalytic ozonation (ultrasound, activated Raney-Nickel, and ozone) was found to be the best combination for removing COD in an initial solution of 500 mg/L of phenol. In an ozonation process alone 28 percent of the ozone was absorbed, whereas in a sono-catalytic ozonation process 83 percent of the ozone was absorbed.

Nakayama et al. [29] investigated the use of hydrogen peroxide as a catalyst for phenol ozonation. The efficiency of the process was dependent on the pH and hydrogen peroxide concentration. For a neutral pH and a hydrogen peroxide concentration of 30 mg/L, the ozone to TOC ratio was 9.6.

Experiments on the ozonation of organic compounds at high pressures were performed by Hill [15]. The pressure varied from 184 to 791 kPa.

The organic compounds studied were formic acid, methanol, glucose, and synthetic hospital waste. For all compounds, the ozone applied per change in COD was lower at the higher pressures. The effect that pressure had on the ratio of ozone absorbed per change in COD varied for the different compounds. For glucose and the synthetic laboratory waste the ratio increased with increasing pressure; for methanol the ratio decreased with increasing pressure; and for formic acid the ratio varied with increasing pressure.

The different investigators' findings on the stoichiometry of the reaction are summarized in Tables I, II, and III.

Reaction Products

Catechol and hydroquinone have been reported by several investigators [9, 12, 25, 27, 42, 46] as being reaction products of phenol ozonation. (For chemical structures see Appendix A.) Of these investigators, none reported finding resorcinal as a reaction product, indicating that the hydroxylation of phenol is an ortho-, para-directed reaction. Eisenhauer [9], Li et al. [27], and Gurol et al. [42] found catechol to be in much higher concentrations than hydroquinone at all times during the reaction but Gould et al. [12] found hydroquinone to be the major product. Li et al. [27] concluded that the production of catechol and hydroquinone is an electrophilic reaction. This would result in production of twice as much catechol as hydroquinone and very little resorcinal. Li et al. [27] further noticed from their experiments that the ratio of catechol to hydroquinone was more than two. It was proposed that a geometrical factor between the ozone and phenol existed which favored the catechol production.

TABLE I

PURE PHENOL STOICHIOMETRY

Researcher	Reactor Size (L)	Phenol Conc. (mg/L)	Ozone Conc.	pH	Phenol Oxidized (%)	Stoichiometry (Moles O_3/ Mole Phenol)
Niegowski	0.500	100	---	12.0	50.0	2.2
Niegowski	0.500	100	---	12.0	99.0	3.7
Peppler & Fern	4.500	500	3 g/hr	12.3	99.0	3.6
McPhee & Smith	---	0.50	---	---	50.0	5.2
McPhee & Smith	---	0.50	---	---	99.0	18.8
Anderson	CSTR Reactor	1000	30 mg/L	6.6	50.0	4.6
Anderson	CSTR Reactor	1000	30 mg/L	11.4	50.0	1.9
Bauch et al.	0.200	19	---	---	70.0	3.0
Bauch et al.	0.200	19	---	---	99.0	5.5
Yamamoto et al.	0.100	58	5.76 mg/L	---	99.0	17.5
Baillod et al.	0.250	50	25 mg/L	6.0	Initial	3.9
Eisenhauer	1.000	50	15 mg/L	---	99.0	4.1
Eisenhauer	1.000	200	21 mg/L	---	97.5	4.0

TABLE II

CHEMICAL OXYGEN DEMAND STOICHIOMETRY FOR PURE PHENOL

Researcher	Reactor Size (L)	Phenol Conc. (mg/L)	Ozone Conc.	pH	Phenol Oxidized	Stoichiometry mg $O_3/\Delta COD$
Niegowski	0.500	1000	---	12.0	---	1.4
Anderson	CSTR Reactor	1000	30 mg/L	6.6	---	2.0
Anderson	CSTR Reactor	1000	30 mg/L	11.4	---	1.0

TABLE III

STOICHIOMETRY FOR WASTE SOLUTIONS

Researcher	Waste Solution	Reactor Size (L)	Phenol Conc. (mg/L)	Ozone Conc.	pH	Phenol Oxidized	Stoichiometry (Moles O_3/Mole Phenol)
Niegowski	Coke Plant	0.500	1240	---	---	99%	3.92
Niegowski	Refinery	0.500	11600	---	---	99%	1.96
Peppler & Fern	Stripped Cat Cracker	4.500	114	---	7	99%	11.75
Peppler & Fern	Stripped Cat Cracker	4.500	114	---	12	99%	11.75
McPhee & Smith	Oxidized Refinery Waste	---	0.80	---	---	96%	53.40

Gould and Weber [12] assumed that catechol and hydroquinone under-
went ring cleavage instead of further hydroxylation since the addition
of a second hydroxyl group would make the ring double bonds more suscep-
tible to the ozone. This was supported by the fact that only one inves-
tigation reported finding quinones as product [25]. Furthermore, Yama-
moto et al. [46] concluded from their experiments that catechol and hy-
droquinone were more reactive toward ozone than phenol.

Catechol and hydroquinone were initial reaction products that reach-
ed a maximum early in the reaction and decreased rapidly [9, 12, 42].
Baillod et al. [4] did experiments to determine the catechol and hydro-
quinone concentrations in their phenol ozonation experiments but were un-
able to find any. From this, it was concluded that either these products
were formed very early in the reaction and were missed or could not be
detected at such low concentrations. In Eisenhauer's experiments [9],
the maximum catechol concentration reached approximately 10 mg/L at 5
minutes of reaction time when the initial phenol concentration was 50
mg/L and reached approximately 30 mg/L at 10 minutes reaction time when
the initial phenol was 300 mg/L. The catechol concentration was below
detection at the same time the phenol concentration was below detection.
Gould and Weber [12] found a maximum concentration of hydroxyl products
of 10 percent at 5 minutes of reaction time. The maximum concentrations
of catechol and hydroquinone were found to vary with varying pH in
Singer and Gurol's experiments [42]. At a pH of 3, the maximum amount
of catechol and hydroquinone observed was less than 1 percent whereas at
higher pH values, significant amounts of hydroxyl products were formed.

Muconaldehyde and muconic acid were the only six-carbon products of
ring cleavage reported by the different investigators [4, 42, 46]. Of

the four-carbon products, Bauch et al. [5] found maleic acid and tartaric acid, Yamamoto et al. [46] found maleinaldehyde, Legube et al. [25] found maleic acid and maleinaldehyde, and Baillod et al. [4] found maleic acid. Propionic acid and cetomalonic acid were the only three-carbon compounds found [5, 25]. Of the two-carbon products, Bauch et al. [5] reported finding glyoxylic acid, acetic acid, glycolic acid, and oxalic acid; Gould and Weber [12] and Yamamoto et al. [46] reported finding glyoxal, glyoxylic acid, and oxalic acid; and Legube [25] and Baillod et al. [4] reported finding oxalic acid. Yamamoto et al. [46], Li et al. [27], and Baillod et al. [4] reported finding formic acid, a one-carbon compound.

Glyoxal and glyoxylic acid accounted for the bulk of the organic carbon during most of the reaction time in Gould and Weber's experiments [12]. Figure 1 shows the intermediate products versus time in the experiment. The glyoxal reached a maximum value around 10 minutes and was at a very low value after 30 minutes. At its maximum value the glyoxal accounted for over 25 percent of the organic carbon. Glyoxylic acid had two peaks during the reaction. The first peak was around 5 minutes and the second peak was around 18 minutes. Gould and Weber surmised that the first peak was probably due to ring cleavage and the second peak was probably due to glyoxal oxidation. Glyoxylic acid accounted for virtually all of the organic carbon after 20 minutes of reaction time. The oxalic acid rose very slowly and reached only around 20 percent of the organic carbon at the end of 30 minutes.

In Yamamoto's et al. [46] experiments, the major product throughout the reaction was found to be formic acid. Figure 2 shows the concentration of the reaction product throughout the experiment. The formic acid
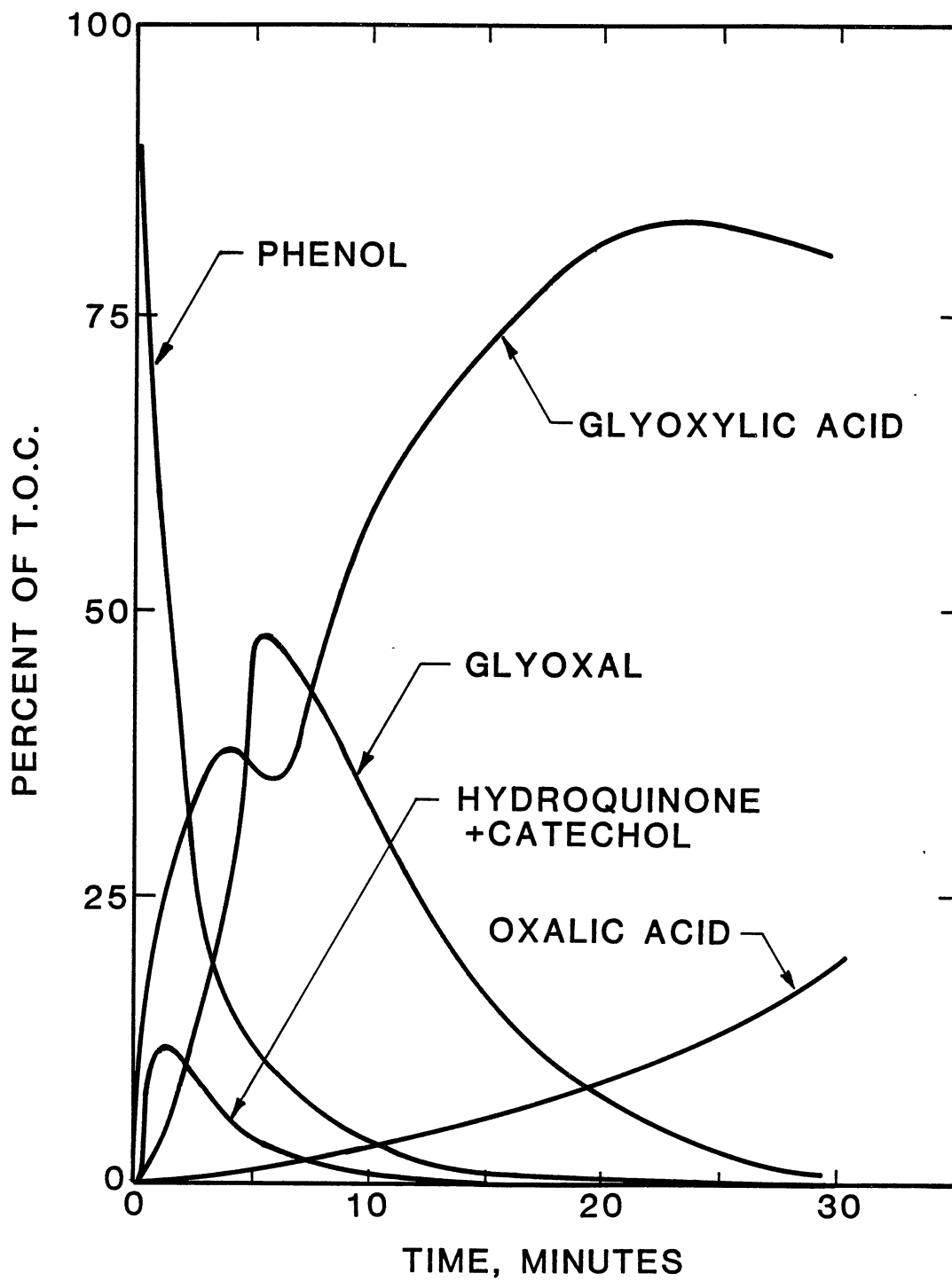
Figure 1. Gould and Weber's Reaction Products
as a Function of Time [12]
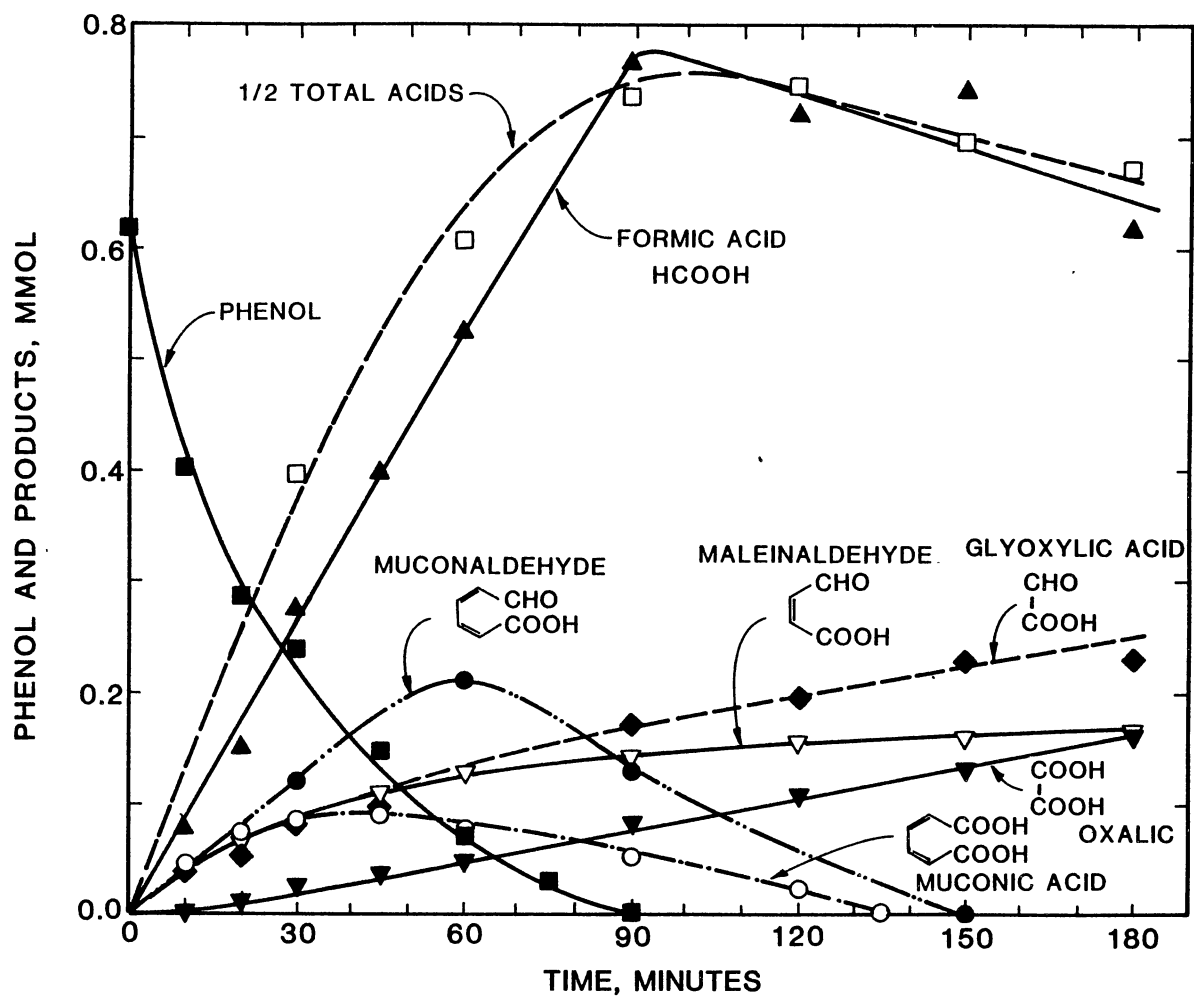
Figure 2.   Yamamoto's et al. Reaction Products as a
Function of Time [46]

reached a maximum of about 0.77 mmole at 90 minutes reaction time. The muconaldehyde reached a maximum value above 0.2 mmole at 60 minutes reaction time and decreased to very low amounts after 150 minutes. The muconic acid reached a maximum value around 0.08 mmole at 35 minutes reaction time and decreased to very low amounts after 135 minutes. The glyoxylic acid, maleinaldehyde, and oxalic acid concentrations continued to rise throughout the reaction. Initially, the maleinaldehyde concentration was close to the concentration of glyoxylic acid but by the end of the reaction the maleinaldehyde concentration was close to the concentration of oxalic acid. For example, at 60 minutes reaction time the concentrations of glyoxylic acid, maleinaldehyde, and oxalic acid were approximately 0.11, 0.11, and 0.04 mmole, respectively, and at 180 minutes reaction time the concentrations were approximately 0.24, 0.17, and 0.16 mmole, respectively. This showed that the production of maleinaldehyde decreased during the reaction.

In Baillod's et al. [4] studies, the major products were formic acid and oxalic acid. The reaction products versus time are shown in Figure 3. The initial phenol concentration was 50 mg/L and decreased below 1 mg/L after 6 minutes of reaction time. The formic acid reached a value around 30 mg/L after 6 minutes and remained approximately constant throughout the reaction. The oxalic acid reached a maximum concentration around 33 mg/L after 21 minutes reaction and decreased to below 1 mg/L after 60 minutes. Maleic acid reached a maximum slightly below 10 mg/L and decreased to below 1 mg/L after 6 minutes reaction time. Muconic acid reached a steady-state concentration around 4 mg/L. After 40 minutes it began to decrease and after 57 minutes it was below 1 mg/L.
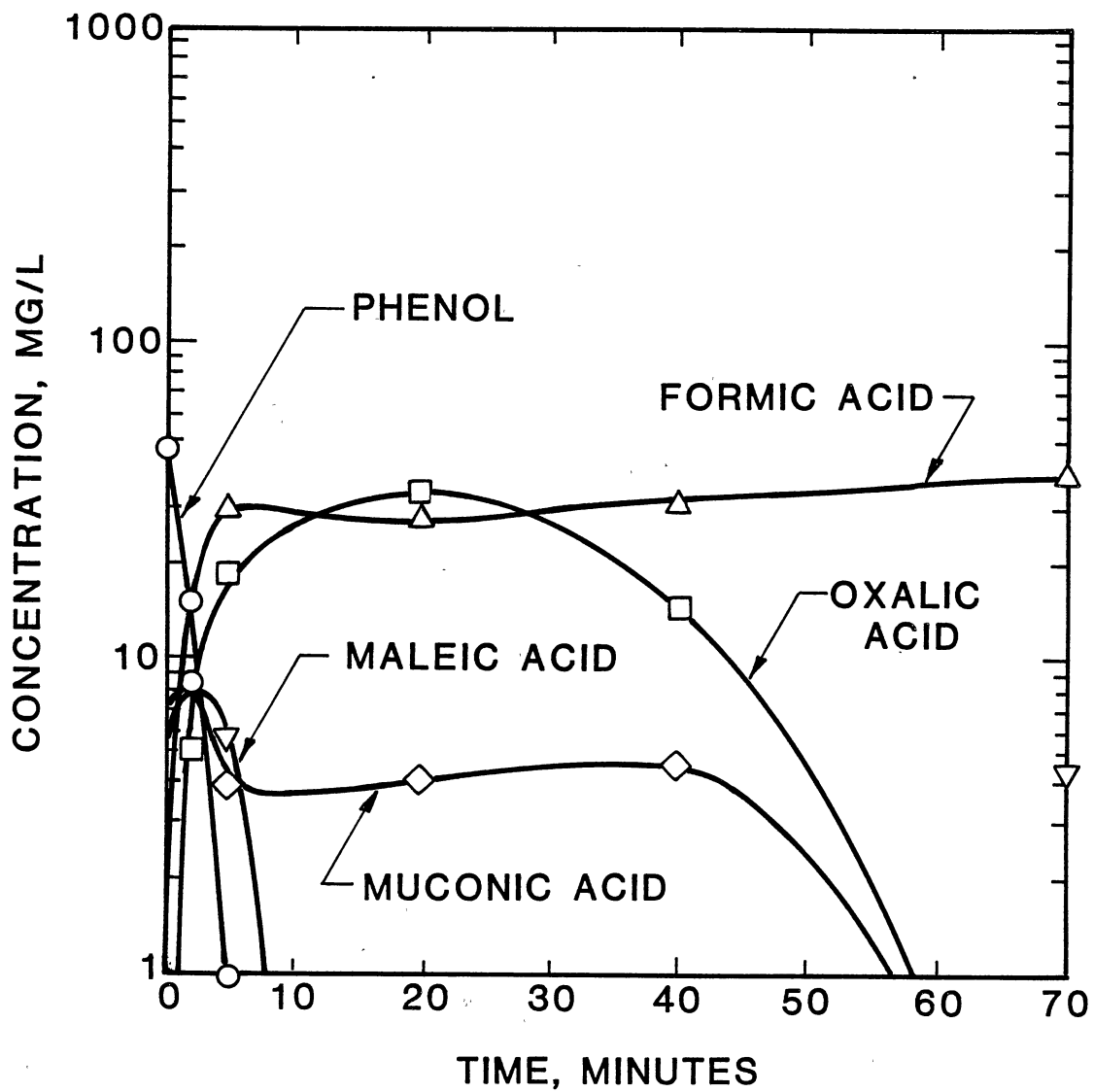
Figure 3. Baillod's et al. Reaction Products
as a Function of Time [4]

Kinetics

Empirical Kinetics

Eisenhauer [9] was one of the first to study the kinetics of phenol oxidation with ozone. He used a semi-batch reactor that operated at room temperature with phenol concentrations of 50 to 300 mg/L. An empirical parameter, the "ozone dose rate," was defined as follows:

$$D = \frac{[O_3] F}{[Ph]_o V} \qquad (1)$$

Assuming first order with respect to the phenol concentration and with respect to the ozone concentration, and using the ozone dose rate parameter, the kinetic equation was:

$$\frac{-d [Ph]}{dt} = kD [Ph] \qquad (2)$$

Integrating yielded

$$\ln \frac{[Ph]_o}{[Ph]_t} = kDt \qquad (3)$$

When D was constant, the experimental results showed a linear relationship between $\ln ([Ph]_o/[Ph]_t)$ and Dt up to 30 minutes reaction time.

In later experiments, Eisenhauer [10] studied the effect that pH had on the rate constant. From pH 3 to 9, the rate constant changed very little. However, at an initial pH of 11, the reaction rate more than doubled.

Gould and Weber [12] did experiments similar to Eisenhauer. The phenol concentration ranged from 110 to 1,100 mM/L and all the runs

were operated at room temperature. The experimental results agreed with Equation (3) which Eisenhauer had derived.

Gould and Weber also studied the effect that the pH had on the rate constant. The rate constant ranged from about 0.11 at lower pH values to about 0.28 at higher pH values. Most of the increase of the rate constant occurred between pH 4 and 7.5 and was essentially complete by pH 8. This disagreed with Eisenhauer's result.

Anderson [1] used a continuous stirred tank reactor with a phenol concentration of 1000 mg/L. Based on Eisenhauer's results, two kinetic equations were assumed:

$$\frac{d[Ph]}{dt} = k \ (A) \ [Ph] \ [O_3] \tag{4}$$

and

$$\frac{d[Ph^-]}{dt} = k' \ (A) \ [Ph^-] \ [O_3] \tag{5}$$

One set of experiments was performed at neutral conditions and the other set was performed at a pH of 11.4. For both equations a log mean concentration of ozone and a continuous stirred system for the liquid phase were assumed. At the high pH, a pKa value of 10.0 was used to determine the concentration of phenolate ion. A rate constant of 2.31 ±0.28 x 10^{-6} L^2/mg-min-cm^2 was calculated for phenol and a rate constant for phenolate ion was calculated to be 6.78 ±0.03 x 10^{-5} L^2/mg-min-cm^2. From this information the rate constant between phenolate and ozone was 27 times larger than the rate constant between phenol and ozone.

In Eisenhauer's [9] experiments, the value of the rate constant changed when the flow rate changed. This showed that the kinetic equations (Equations (3), (4), and (5)) combined the effects of mass

transfer and kinetics and, because of this, the combined rate constant is system specific. A summary of the different experimental values of the rate constant from Equation (3) is listed in Table IV.

Homogeneous Kinetics

Li, Kuo, and Weeks [27] studied the kinetics of ozone-phenol reaction in a homogeneous solution. They used the stopped-flow technique where solutions of ozone and phenol were stored in two separate drive syringes and were rapidly mixed in a mixing jet. This eliminated the mass transfer part of the reaction.

With mass transfer effects eliminated, the kinetic equation was written as

$$\frac{-1}{r} \frac{d[O_3]}{dt} = \frac{-d[Ph]}{dt} = k \, [Ph]^m \, [O_3]^n \tag{6}$$

When phenol was in large excess, Equation (6) could be approximated as

$$\frac{d[O_3]}{dt} = rk' \, [O_3]^n \tag{7}$$

where $k' = k \, [Ph_o]^m$. Integrating when $n = 1$ yielded

$$\frac{[O_3]_t}{[O_3]_o} = \exp \, (-r \, k' \, t) \tag{8}$$

The experimental data were found to fit Equation (8) best, implying first order with respect to ozone.

The order with respect to phenol concentration, m, was determined by plotting k' versus the initial concentration of phenol on a logarithmic scale. A straight line could be obtained in such a plot as indicated by Equation (9):

TABLE IV

EMPIRICAL RATE CONSTANTS FOR PHENOL OZONATION

Researcher	Reactor Size (L)	Phenol Conc. (mg/L)	Ozone Conc. (mg/L)	Gas Flowrate (L/min)	Initial pH	Rate Constant (Mole Phenol/ Mole O_3)
Eisenhauer	1.0	50-300	15-30	0.20	---	0.42
Eisenhauer	1.0	50-300	15-30	0.30	---	0.38
Eisenhauer	1.0	50-300	15-30	0.40	---	0.36
Eisenhauer	1.0	50-300	15-30	0.50	---	0.33
Eisenhauer	1.0	---	---	---	3.00	0.23
Eisenhauer	1.0	---	---	---	5.01	0.25
Eisenhauer	1.0	---	---	---	5.57	0.26
Eisenhauer	1.0	---	---	---	9.14	0.31
Eisenhauer	1.0	---	---	---	11.06	0.66
Gould & Weber	0.5	88,900	99	1.33	2.27	0.11
Gould & Weber	0.5	89,900	99	1.33	2.61	0.11
Gould & Weber	0.5	93,800	101	1.33	3.34	0.11
Gould & Weber	0.5	95,700	101	1.33	4.11	0.15
Gould & Weber	0.5	91,000	100	1.33	5.68	0.12
Gould & Weber	0.5	90,600	100	1.33	6.32	0.18
Gould & Weber	0.5	94,600	101	1.33	7.22	0.28
Gould & Weber	0.5	94,900	101	1.33	8.09	0.27
Gould & Weber	0.5	93,800	101	1.33	8.86	0.26
Gould & Weber	0.5	91,700	101	1.33	9.15	0.28
Gould & Weber	0.5	94,600	101	1.33	11.03	0.25
Yamamoto et al.	0.1	4,120	---	---	---	0.39
Yamamoto et al.	0.1	60	---	---	---	0.15
Baillod et al.	0.25	50	25	0.60	6.00	0.19
Baillod et al.	0.25	50	25	0.60	10.00	0.27

$$\log k' = \log k + m \log [Ph]_o \tag{9}$$

Using the method of least squares, the average value of m was calculated to be 0.85. This result was assumed to suggest that phenol was a first order reaction.

At constant temperature the only thing that affected the rate constant was the pH of the system. At a temperature of 25°C, the average rate constant for pH 1.5, 2.7, 3.7, and 5.2 was calculated to be 895.4, 2097, 4393, and 29,520 $M^{-1} s^{-1}$, respectively [16]. The rate constant increased with increasing pH and the increase was faster at the higher pH values. This seemed to indicate that Anderson's [1] theory of ozone reacting with phenol molecules and phenolate ions was correct.

Hoigné and Bader [18, 19, 20] proposed a two-path reaction model as shown to explain the pH effect (see Figure 4).
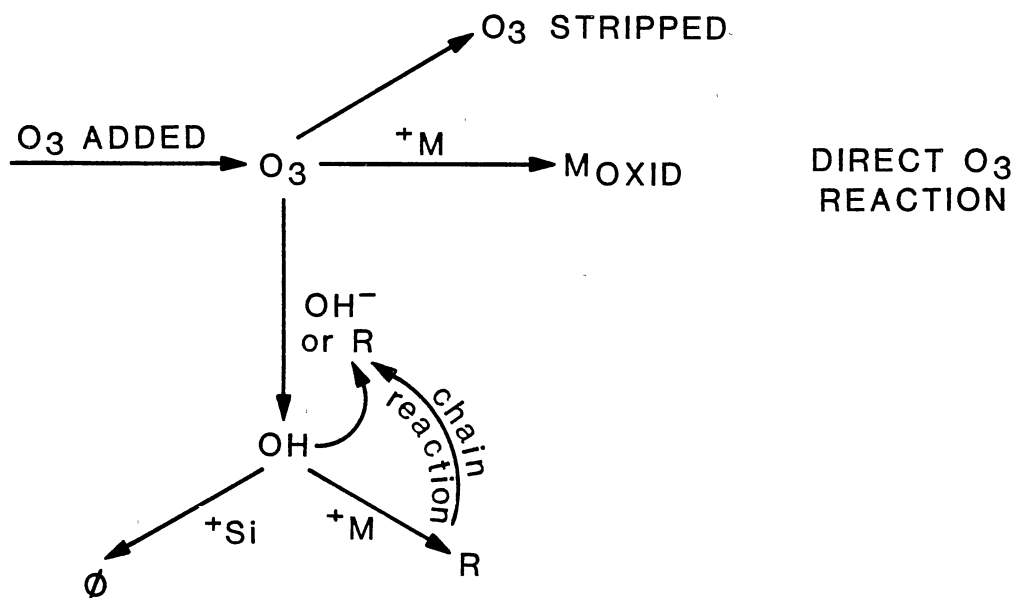
Figure 4. Phenol Ozonation Reaction Pathway

When the ozone is absorbed by the solution, it can follow three different pathways. The ozone can be stripped off before any reaction takes place, it can react directly with M to form M_{oxid}, or it can decompose. Hoigné proposed that the decomposition of ozone was catalyzed by hydroxide ions and other solutes. Part of the decomposition products form highly reactive secondary oxidants such as OH˙ radicals. Some types of solutes react with OH˙ radicals to form secondary radicals, R˙, which act as chain carriers of the ozone decomposition. Other solutes transform the primary radicals to inefficient species, ϕ, and thereby act as inhibitors of the chain reaction. The direct reaction is predominant under acidic conditions and is labeled the slow reaction. The radical reaction is predominant in basic solutions and is labeled the fast reaction.

Hoigné and Bader [19] measured the direct reaction of phenol by using a pH between 1.7 to 2.0 and a n-propanol scavenger of 1 mM concentration. These conditions helped minimize the ozone decomposition. The ozone was also injected below the liquid level of the solution to eliminate the mass transfer effects. The phenol concentration was in large excess compared with the ozone concentration so that the reaction rate becomes pseudo-first order. The rate constant was calculated to be 1300 ±300 M^{-1} s^{-1} at a temperature of 23 ±2°C.

Mass Transfer

Theory

A gas-liquid reaction system consists of the transport of solute from one phase to another caused by a concentration gradient. At steady-state the rate of mass transfer in terms of the gas phase is:

$$N_A = K_G \, S(p_{AG} - p_{AL}) = k_G \, S(p_{AG} - p_{Ai}) \qquad (10)$$

and in terms of the liquid phase is:

$$N_A = K_L \, S(C_{AG} - C_{AL}) = k_L \, S(C_{Ai} - C_{Al}) \qquad (11)$$

At a fixed temperature and a dilute solution the partial pressure of A varies linearly with the mole fraction of A in solution (x_A) in accordance with Henry's law:

$$p_A = Hx_A \qquad (12)$$

Equations (10), (11), and (12) can be rearranged to show the relationship between the film and overall mass transfer coefficients:

$$\frac{1}{K_L} = \frac{1}{k_L} + \frac{1}{H \, k_G} \qquad (13)$$

and

$$\frac{1}{K_G} = \frac{1}{k_G} + \frac{H}{k_L} \qquad (14)$$

If the component A is only slightly soluble (such as ozone), the Henry's law coefficient, H, is large. When H is large, from Equations (13) and (14) most of the resistance occurs in the liquid phase and

$$\frac{1}{K_L} \approx \frac{1}{k_L} \qquad (15)$$

There are many models that explain the mass transfer in the gas-liquid boundary region. The most noted models are the Lewis and Whitman two film theory, the Higbie penetration theory, and Danckwert's surface renewal theory [24, 32, 37].

The two film theory postulates that there is a gas film boundary and a liquid film boundary where the transport of mass is by diffusion only (see Figure 5). Outside the film boundaries the transport of mass is by convection and component A is at a bulk concentration.

INTERFACE
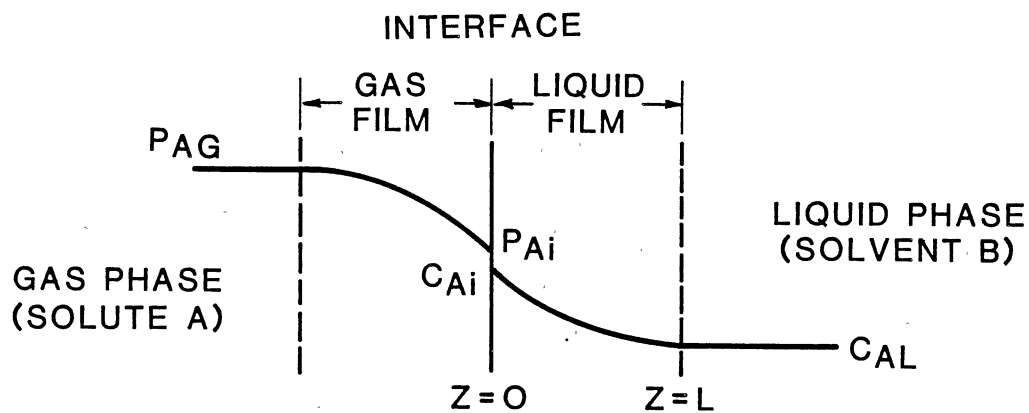
Figure 5. Two Film Theory

Since the mass transport in the film is by diffusion only, the unsteady-state continuity equation for one-dimensional transport is:

$$D_A \frac{\partial^2 C_A}{\partial z^2} = \frac{\partial C_A}{\partial t} \tag{16}$$

The liquid film is considered very thin without any accumulation of the diffusing mass [24]. Thus steady-state diffusion prevails and the concentration distribution is a linear function of the distance in the liquid film. Using this information the mass transfer can be written as:

$$N_A = D_A \, (C_{Ai} - C_{AL})/L \cdot S \tag{17}$$

Comparing Equations (11) and (17), k_L can be derived from the film theory as:

$$k_L = D_A/L \qquad (18)$$

The penetration theory as proposed by Higbie states that the surface film is continuously removed by the bulk [32]. The assumptions that he made are (a) the elements at the surface are stagnant, and (b) every surface element is exposed to the solute for the same length of time (t_o) before being replaced. The average mass flux can be derived to be:

$$N_A = 2(C_{Ai} - C_{AL}) \sqrt{[D_A/(\pi t_o)]} \cdot S \qquad (19)$$

The contact time, t_o, can be calculated using the following relationship for bubbles:

$$t_o = d_B/U_s \qquad (20)$$

Comparing Equations (11) and (19), k_L can be derived from penetration theory for bubble columns as shown:

$$k_L = 2\sqrt{D_A/(\pi t_o)} \qquad (21)$$

By using Equations (20) and (21), Higbie's result can be expressed in terms of dimensionless numbers as:

$$Sh = 1.13 \ Re^{1/2} \ Sc^{1/2} \qquad (22)$$

Danckwerts' theory is similar to the penetration theory except that instead of a constant time of exposure, the surface renewal theory describes the liquid phase as completely disturbed by numerous

infinitesimally small phase elements or eddies in the phase [24]. The probability for a given element to disappear from the surface was independent of its age; rather, it was proportional to the number of elements of that age that were present at the surface. The mass transfer according to Danckwerts' surface-renewal theory is:

$$N_A = \sqrt{D_A S_o} \ (C_{Ai} - C_{AL}) \cdot S \qquad (23)$$

Comparing Equations (11) and (23), k_L can be derived from the surface renewal theory as:

$$k_L = \sqrt{D_A S_o} \qquad (24)$$

Dimensional analysis indicates that the liquid-side mass-transfer coefficient can be correlated in terms of the Sherwood (Sh), Schmidt (Sc), and Reynolds (Re) numbers as shown by Higbie (Equation (21)). For the rise of swarms of gas bubbles in a reactor column, Hughmark [21] showed that the following correlation is applicable with an average deviation of 15 percent:

$$\frac{k_L \ d_B}{D_A} = Sh = 2 + 0.0187 \ [Re^{0.484} \ Sc^{0.339}$$
$$(d_B \ g^{33}/D_A^{0.667})^{0.072}]^{1.61} \qquad (25)$$

The rate at which the chemical reaction increases the mass transfer is called the enhancement factor, E, which is defined by:

$$E = k_L' \ a/k_L \ a \qquad (26)$$

The enhancement factor can be evaluated for a reaction of known kinetics. For a first order reaction, Danckwerts [7] derived the following result:

$$E = \sqrt{1 + M} \tag{27}$$

where

$$M = \frac{D_A \, k}{k_L^2} \cdot C_A \tag{28}$$

Gas-liquid mass transfer followed by an irreversible reaction can follow either of two regimes, labeled as fast reactions or as slow reactions [37]. The slow reaction is determined by the following equation:

$$\frac{D_A \, k}{k_L^2} \cdot C_A \ll 1 \tag{29}$$

The slow reaction can be further divided depending on whether the rate limiting step is kinetically controlled or mass transfer controlled. When the reaction is kinetically controlled, there will be a significant amount of the dissolved gas in the bulk liquid [37]. The mass transfer equation then becomes:

$$N_A = k_L \, a \, (C_{AG} - C_{AL}) \, V \tag{30}$$

When the reaction is mass transfer controlled, the dissolved gas in the bulk becomes approximately zero and the mass transfer equation can be written as:

$$N_A = k_L \, a \, C_{AG} \, V \tag{31}$$

A fast reaction is when an important fraction of the dissolved gas is reacted near the interface. The enhancement factor has an effect on the mass transfer and, because of this, the liquid side mass transfer coefficient with chemical reaction can be defined as:

$$k_L' a = \sqrt{D_A \, k} \; a \tag{32}$$

If all of the dissolved gas reacts in the film, then the concentration of dissolved gas in the bulk liquid is approximately zero and the mass transfer equation can be written as:

$$N_A = C_{AG} \sqrt{D_A \, k} \; (aV) \tag{33}$$

Mass Transfer With Kinetics

Baillod, Faith, and Masi [4] determined the $K_L a$ value for oxygen in a nonreactive system and used that value to estimate $K_L a$ for ozone. An oxygen $K_L a$ value was calculated and found to be 1.05 min^{-1} at an air flow rate of 0.6 ℓ/min. The following equation was used to estimate the $K_L a$ value for ozone:

$$(K_L a)_{O_3} = (K_L a)_{O_2} \, (D_{O_3}/D_{O_2})^{0.5} \tag{34}$$

The $(K_L a)_{O_3}$ value was computed to be 0.86 min^{-1}.

Using this value, the maximum possible ozone transfer rate without chemical reaction was calculated for the experimental conditions. The experimental ozone transfer rate was compared with the calculated maximum transfer rate without chemical reaction to find the apparent enhancement factor. An enhancement factor was calculated assuming that phenol and phenolate ions reacted with the ozone. At a pH of 6, for phenol, the apparent enhancement factor was 3.3 and the calculated enhancement factor was 1.06. Based on this, Baillod et al. concluded that ozone decomposition or reaction with intermediate products may cause the enhancement factor to be greater than the calculated enhancement factor for

phenol and phenolate ion. These conclusions lent support for Hoigné and Bader's theory [18].

Li and Kuo [26] developed a mass transfer model to describe the phenol concentration in a semi-batch reactor. The two-film model with the chemical reaction occurring in the liquid film was used. It was assumed that the ozone not only reacted with the phenol but decomposed by a 3/2 order. The simultaneous mass transfer and chemical reactions were, therefore, governed by the following set of differential equations:

$$D_{O_3} \frac{d^2[O_3]}{dz^2} = 2k \, [Ph] \, [O_3] + k_D \, [O_3]^{3/2} \tag{35}$$

and

$$D_{Ph} \frac{d^2[Ph]}{dz^2} = k \, [Ph] \, [O_3] \tag{36}$$

It was assumed at the interface that the concentration of ozone was in equilibrium with the gas phase. The reaction between ozone and phenol was observed to be fast and therefore no ozone existed in the main liquid stream. The phenol concentration was assumed to be zero at the interface, since the reaction was fast. At the edge of the film, the phenol was assumed to be the same as the concentration in the main stream. These assumptions were used as boundary conditions.

Using mass balances for ozone and phenol in the main liquid, assuming the phenol concentration varied linearly across the liquid film, and using Airy integrals, Equation (35) was used to derive the following equation:

$$\frac{d[Ph]}{dt} = -0.4592 \; k_L a \; [O_3]_i \; \frac{k \; D_{O_3}^{1/3}}{k_L^2} \; [Ph]^{1/3}$$

$$+ \; 0.1768 \; k_D \; k_L a \; [O_3]_i^{3/2} \tag{37}$$

Under acidic conditions the decomposition of ozone was negligible and, therefore, the last term on the right side was ignored. Integrating yielded:

$$\frac{[Ph]_t}{[Ph]_o}^{2/3} = 1 - 0.3061 \; k_L a \; N^{1/3} \; \frac{[O_3]_i}{[Ph]_o} \; t \tag{38}$$

where N is defined by:

$$N = \frac{k \; [Ph]_o \; D_{O_3}}{k_L^2} \tag{39}$$

For isothermal absorption of ozone with a constant flow rate and a fixed pH, the physicochemical properties of Equations (38) and (39) remain constant. Under this condition $([Ph]_t/[Ph]_o)^{2/3}$ should vary linearly with time as predicted by Equation (38). Li and Kuo [26] performed experiments measuring the phenol concentration with time. A straight line could be drawn for each experiment by plotting $([Ph]_t/[Ph]_o)^{2/3}$ against the absorption time. This concluded that the experimental data agreed well with the qualitative predictions of Equation (38).

Augugliaro and Rizzuti [3] used a wetted wall column to study the kinetics of phenol ozonation. In order to explain the pH dependence of the reaction, the assumption was made that the species attacked by the ozone was the phenate ion instead of phenol. Thus the reactions taking place in the phenol ozonation process would be:

$$C_6H_5OH \underset{}{\overset{k_1}{\rightleftharpoons}} C_6H_5O^- + H^+ \tag{40}$$

$$C_6H_5OH + OH^- \underset{}{\overset{k_2}{\rightleftharpoons}} C_6H_5O^- + H_2O \tag{41}$$

$$C_6H_5O^- + O_3 \xrightarrow{k_3} \text{Products} \tag{42}$$
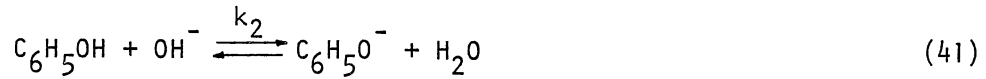
Using the kinetic equations for the above reactions and assuming steady-state, the phenate ion was eliminated from Equation (42) and the kinetic equation for Equation (42) became:

$$r_3 = K_2 \, k_3 \, [O_3][OH^-][Ph] \; \frac{1}{1 + \dfrac{K_2 k_3 \, [O_3][OH^-]}{k_1 + k_2 \, [OH^-]}} \tag{43}$$

In acidic solution the following two hypotheses were made: (i) the phenate ion present in the solution was essentially produced by the dissociation reaction (Equation (40)); (ii) the oxidation of the phenate ion was the rate determining step. Thus it can be written:

$$k_2 \, [OH^-] \ll k_1 \quad ; \quad \frac{K_2 \, k_3 \, [O_3][OH^-]}{k_1 + k_2 \, [OH^-]} \ll 1 \tag{44}$$

and Equation (43) became:

$$r_3 = K_2 \, k_3 \, [O_3][OH^-][Ph] \tag{45}$$

Augugliaro et al. [27] assumed that the absorption process was the so-called "fast reaction regime" and used Astarita's [2] equation to derive:

$$k_L = \sqrt{D_{O_3} \, K_2 \, k_3 \, [OH^-][Ph]} \tag{46}$$

In the experiments performed $[OH^-]$ and $[Ph]$ are constant throughout the column; therefore, k_L was constant.

Taking a mass balance over a differential volume of the column and integrating gave:

$$\frac{k_L \; S}{H \; G} = \frac{\ell n \; (y_1/y_2)}{1 - \frac{G}{S \; k_G} \ell n \; (y_1/y_2)}$$ (47)

Experimental values for y_1 and y_2 were measured and the value for k_L calculated from Equation (47). The values of k_L were plotted against the phenol concentration at a constant pH of 5.5 and were plotted against the pH at constant phenol concentrations. A straight line of slope 1/2 fit to a good approximation for the k_L versus phenol concentration and also a straight line of slope 1/2 could be drawn for the pH data in the range 4 to 6. These experimental results agreed well with Equation (46).

The following two hypotheses were made for ozone absorption in basic solutions: (i) the phenate ion present in the solution was essentially produced by the salification reaction (Equation (41)); and (ii) the salification reaction was also the rate determining step. Thus it can be written:

$$k_2 \; [OH^-] \gg k_1 \quad ; \quad \frac{K_2 \; k_3 \; [O_3][OH^-]}{k_1 + k_2 \; [OH^-]} \gg 1$$ (48)

and Equation (43) becomes:

$$r_3 = k_2 \; [OH^-][Ph]$$ (49)

Using Astarita's [2] "fast reaction regime" equation and the boundary condition that the ozone in the bulk is zero, the absorption coefficient equation for basic solutions became:

$$k_L \ [O_3]_i^{0.5} = \sqrt{(2D_{O_3} \ k_2 \ [OH^-][Ph]}$$ (50)

The values of $k_L \ [O_3]_i^{0.5}$ were calculated and plotted against the phenol

concentration at a constant pH of 9 and plotted against the pH value at

a constant phenol concentration. A straight line could be drawn with

slope of 1/2 for the phenol concentration graph and also a straight line

could be drawn with slope of 1/2 for the pH graph when the pH was in the

range of 8 to 9.5. The experimental results agreed with Equation (50).

Gurol and Singer [43] developed a mathematical model that described

the rate of change of phenol and ozone in a semi-batch column at low pH.

They assumed a reaction scheme as shown below (see Figure 6).

PHENOL
CATECHOL + O3 $\xrightarrow{k'}$ **OLEFINIC COMPOUNDS WITH**
HYDROQUINONE   **TWO DOUBLE BONDS (MUCONIC ACID, MUCONALDEHYDE, ETC.)**

\+

O3

$\downarrow k''$

GLYOXAL
OXALIC ACID $\xleftarrow{k'''}$ O3 + **OLEFINIC COMPOUNDS WITH**
GLYOXALIC   **ONE DOUBLE BOND (MALEIC**
ACID   **ACID, MALEINALDEHYDE, FUMARIC ACID, ETC.)**
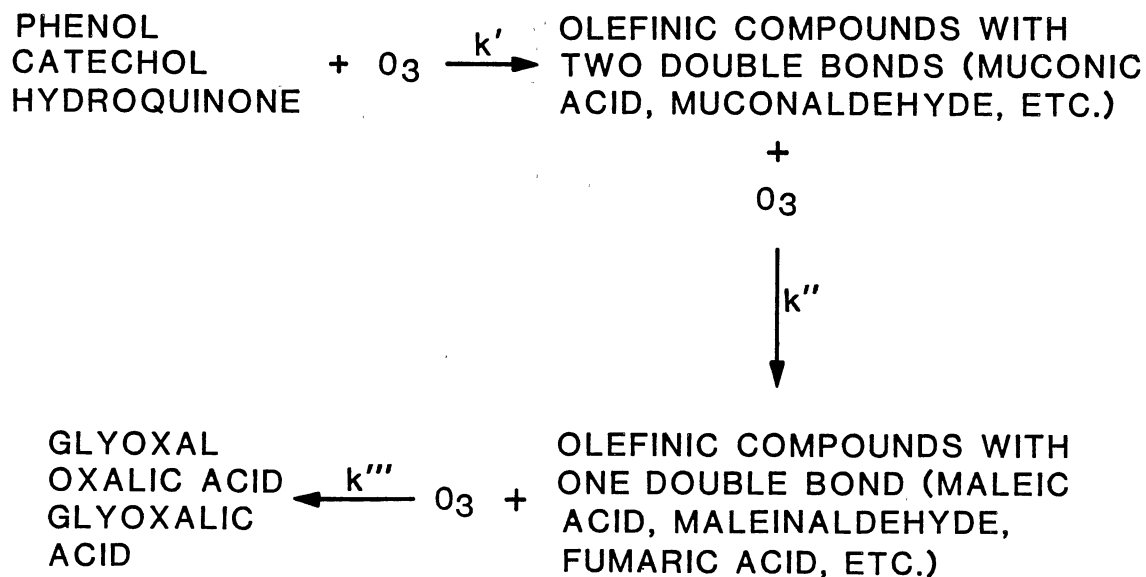
Figure 6. Reaction Scheme Illustrating the Ring Cleavage
of Phenol, Catechol, and Hydroquinone

It was assumed that k' was less than k'' and k''' in the reaction

scheme and, therefore, the first step was the rate controlling step.

Furthermore, the ozonation of the products oxalic acid, glyoxalic acid, and formic acid was assumed to be sufficiently slow so as not to influence the kinetics of phenol ozonation. The relevant chemical equations which were assumed to be significant in the acidic system were:

$$Ph + O_3 \xrightarrow{k_1} C \tag{51}$$

$$Ph + O_3 \xrightarrow{k_2} H \tag{52}$$

$$Ph + O_3 \xrightarrow{k_3} MA \tag{53}$$

$$P + 3O_3 \xrightarrow{k_4} \text{Stable Products} \tag{54}$$

$$C + 3O_3 \xrightarrow{k_C} \text{Stable Products} \tag{55}$$

$$H + 3O_3 \xrightarrow{k_H} \text{Stable Products} \tag{56}$$

$$MA + 2O_3 \xrightarrow{k_{MA}} \text{Stable Products} \tag{57}$$

In these equations C, H, and MA stand for catechol, hydroquinone, and muconic acid, respectively. The reaction rates of phenol, ozone, and the intermediate compounds can be written as:

$$\frac{d[Ph]}{dt} = -k_1 [Ph][O_3] - k_2 [Ph][O_3] - k_3 [Ph][O_3] - k_4 [Ph][O_3]$$

$$= -k_p [Ph][O_3] \tag{58}$$

where $k_p = k_1 + k_2 + k_3 + k_4$.

$$\frac{d[C]}{dt} = k_1 [Ph][O_3] - k_C [C][O_3] \tag{59}$$

$$\frac{d[H]}{dt} = k_2 [Ph][O_3] - k_H [H][O_3] \tag{60}$$

$$\frac{d[MA]}{dt} = k_3 [Ph][O_3] - k_{MA} [MA][O_3] \tag{61}$$

$$\frac{d[O_3]}{dt} = k_L a([O_3]_i - [O_3]) - k_1 [Ph][O_3] - k_2 [Ph][O_3]$$

$$- k_3 [Ph][O_3] - 3k_4 [Ph][O_3] - 3k_C [C][O_3]$$

$$- 3k_H [H][O_3] - 2k_{MA} [MA][O_3] \tag{62}$$

The value of k_p was reported by Hoigné [19] to be 400 M^{-1} sec^{-1}. This value was used to determine the values for k_C, k_H, and k_{MA} by the relative reaction rate method developed by Hoigné. To determine k_C, the inital concentrations of catechol in the mixtures were selected to be several times greater than that of the initial phenol concentration, in order to keep the amount of catechol formed from the oxidation of phenol small. The relative rate equation yields:

$$\frac{\ln ([C]_t/[C]_o)}{\ln ([Ph]_t/[Ph]_o)} = \frac{k_C}{k_p} \tag{63}$$

$\ln ([C]_t/[C]_o)$ and $\ln ([Ph]_t/[Ph]_o)$ were plotted for several sets of data with different $[C]_o$ and $[Ph]_o$ to determine the slope and hence k_C/k_p. The same analysis was done for hydroquinone and muconic acid. The values for k_C, k_H, and k_{MA} were calculated to be approximately 1000, 720, and 2200 M^{-1} s^{-1}, respectively, at pH 3.

To determine k_1, k_2, k_3, and k_4, the maximum concentration point for catechol, hydroquinone, and muconic acid were found. At this point the derivatives of Equations (59), (60), and (61) were equal to zero. For example, the catechol equation became:

$$k_1 \ [Ph]^* \ [O_3] = k_C \ [C]^* \ [O_3] \tag{64}$$

and

$$k_1 = k_C \ \frac{[C]^*}{[Ph]^*}$$

where $[Ph]^*$ and $[C]^*$ are the concentrations of phenol and catechol, respectively, at the point where $d[C]/dt = 0$. The values for k_1, k_2, k_3, and k_4 were experimentally observed to be 0.8, 6, 88, and 350 $M^{-1} s^{-1}$, respectively.

The mathematical model developed by Singer and Gurol adequately predicted the observed rates of phenol removal as well as the time at which the dissolved ozone appeared in solution. The model reflected the mass-transfer-limited nature of the reaction and, therefore, the rate of phenol removal was relatively insensitive to chemical kinetics. The model failed to predict the observed ozone profile after phenol was completely oxidized [43].

Wet Air Oxidation

Process Conditions

Teletzke [44] studied the effect of temperature on the wet air oxidation of organic compounds. He noted that the extent of oxidation is primarily determined by the maximum temperature reached during the reaction. The higher the temperature, the shorter the time it takes to reach equilibrium. In his data, at 300°C approximately, 98 percent of the material was oxidized after reaching equilibrium, whereas at 100°C only 15 percent of the material was oxidized after reaching equilibrium. The time required to reach equilibrium was one hour at 300°C and two hours

at 100°C. Similar results were obtained by Baillod, Faith, and Masi [4].
Hurwitz and Dundas [22] noted that below 150°C oxidation was slow and re-
action incomplete. In Schmidt's [38] experimental data, the rise in tem-
perature from 150° to 300°C lowered the COD and the phenol concentration.
Above 300°C, the rise of temperature continued to lower the COD but less
sharply.

In plant operations, oxidations have ranged from 30 to 40 percent
in the case of low pressure plants (500 psig) to 70 to 80 percent in the
higher pressure plants (1800 psig) [44]. Pruden and Le's [34] experimen-
tal studies with a continuous reactor showed that pressure had a signifi-
cant effect on the percent conversion of phenol. For a temperature of
250°C, residence time of 0.25 h, feed concentration of 3000 mg/ℓ, and
air flow rate of 0.014 m^3/h, the conversion of phenol was 67 percent at
5 MPa and 97 percent at 10 MPa. It was also shown that the higher the
pressure the more the change in temperature affected the reaction [41].
In Shibaeva, Metelitsa and Denisov's [40] study, the initial oxidation
rate of phenol increased linearly with an increase in the partial pres-
sure of oxygen.

Shibaeva et al. [40] did experiments on the effect that hydrogen
ion had on the oxidation of phenol. A semi-continuous reactor was used
with a temperature of 200°C and an oxygen pressure of 3.5 MPa. For these
conditions, the oxidation rate increased with an increase in pH reaching
a maximum at pH 3.2 and then decreased. The phenol consumption was
found to be first order in pH range 3.0 to 5.5 and zero order in the pH
range 2.0 to 0.7. Shibaeva et al. [40] then studied the effect that
temperature (180-200°C) had on the rate constant of phenol consumption
at the lower pH range. A linear equation was derived with the rate

constant being a function of the inverse of the hydrogen ion. The slope and intercept of the equation were exponential functions of the inverse temperature.

Reaction Products

Acetic acid is found to be a product of wet air oxidation (WAO). The Sterling Drug Company performed studies on different WAO processes [44]. They found acetic acid to be an intermediate product of oxidation and the concentration of acetic acid varied inversely with temperature with only traces remaining at 320°C [44]. In Pruden's et al. [34] study of continuous WAO of phenol at 250°C, the acetic acid was found in trace amounts.

Wastewater containing 34,000 mg/ℓ of phenol was oxidized and found to produce a substantial amount of volatile acids [38]. At temperatures of 150 to 200°C the concentration of acids increased, reaching a maximum of 6,250 mg/ℓ. The rise of temperature above 200°C led to a decrease in the concentrations of acids. Acetic acid (4800 mg/ℓ) was then added to the wastewater [38]. After treatment for 120 min at 150°C the acetic acid concentration was 3400 mg/ℓ and for 120 min at 300°C the acetic acetic acid concentration was 1700 mg/ℓ.

Day, Hudgins, and Silveston [8] studied the oxidation of propionic acid. They initially had intended to use acetic acid but the oxidation rate was too slow for measurement using the experimental conditions. The two main products from propionic acid oxidation were acetaldehyde and acetic acid. The acetic acid increased approximately linearly throughout the reaction whereas the acetaldehyde reached an approximate constant concentration. It was proposed that the acetaldehyde formed

a quasi-steady-state, the amount being produced equaling the amount being oxidized to acetic acid.

A carbon dioxide analysis was performed on the reaction products at 500°F and 500 psi, which indicated approximately 55 percent of the carbon in propionic acid formed carbon dioxide [8]. Acetic acid accounted for 40 percent of the carbon and the remaining 5 percent was carbon monoxide, acetaldehyde, and gaseous hydrocarbons. From this analysis, Day [8] proposed an overall oxidation scheme for propionic acid in terms of two simple parallel reaction paths shown below (see Figure 7). One path was the oxidation to acetaldehyde which further oxidized to acetic acid. One mole of carbon dioxide was produced for every mole of acetic acid produced. The other path is the complete oxidation of propionic acid to carbon dioxide and water. There is a side path that produced gaseous products that is probably a combination of several reaction mechanisms.

PROPIONIC ACID

ACETALDEHYDE   COMPLETE
                OXIDATION

ACETIC ACID   CARBON DIOXIDE   GASEOUS PRODUCTS
                AND WATER   (INCLUDING METHANE,
                                   PROPANE AND
                                   ETHYLENE)
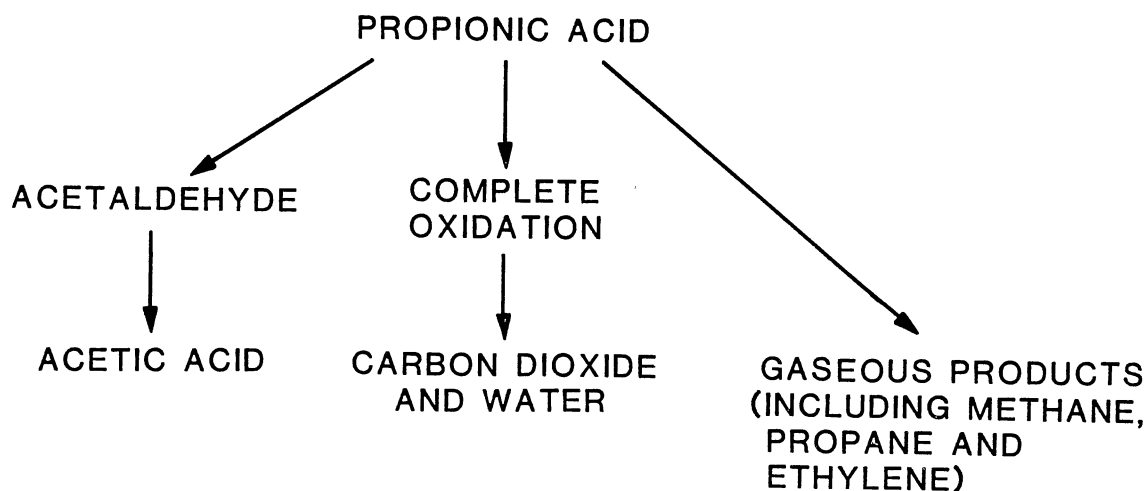
Figure 7. Proposed Scheme for the Wet Air
           Oxidation of Propionic Acid

The WAO products of phenol were analyzed by Baillod et al. [4]. The initial concentration of phenol was 5000 mg/ℓ and the process conditions were 5.2 MPa and 232°C. A significant amount of the total organic carbon remained in solution after the phenol had been completely oxidized. Approximately three-fourths of the carbon in solution was low molecular weight acids, acetaldehyde, and acetone. The reaction products measured accounted for 83 to 105 percent of the total organic carbon at 15 to 60 minutes.

The main products of phenol oxidation were formic acid and acetic acid, each measuring a little under 1000 mg/ℓ after 60 minutes of reaction time. Succinic acid, acetone, and acetaldehyde measured approximately 80, 15, and 9 mg/ℓ, respectively, after 60 minutes reaction time. Maleic acid and oxalic acid were formed, reaching a maximum concentration approximately 6 minutes into the reaction and disappearing after 13 minutes.

Mass Transfer With Kinetics

In Shibaeva's [40] study, the value of the initial oxidation rate (W_o) for phenol increased linearly with an increase in initial concentration of phenol (0.015-0.095 mole/ℓ) and increased linearly with an increase in the partial pressure of oxygen. The oxidation rate W_o did not vary with change in pH (1.5-2.7) and with change in temperature (180-200°C). This indicated that the initial oxidation rate equation was:

$$W_o = k_{O_2} [Ph][O_2] \qquad (65)$$

Day [8] varied the rate of agitation in the propionic acid oxidation study. Within experimental error the rate of agitation probably

did not affect the oxidation rate. Thus the oxidation of propionic acid appears to be kinetically controlled and not mass transfer controlled.

Pruden [34] developed a model which described the effect that residence time, pressure, and temperature had on a continuous WAO system. It was assumed that the gas phase resistance was negligible and derived an equation based on the rate of reaction for mass transfer in the liquid phase resistance, the rate of reaction for kinetics, and the basic definition of the rate of reaction. The oxygen equilibrium concentration was put in terms of the pressure of oxygen and Henry's law constant. The data for Henry's law constant were obtained from Himmelblau [17]. The final equation assuming first order for both the concentration of phenol and oxygen is

$$\frac{0.21 \ \theta \ (P - P_{H_2O})}{([Ph]_o - [Ph]_f) \ H_{O_2}} = \frac{1}{k_{O_2} \ [Ph]} + \frac{1}{k_L a \ S_{O_2}} \tag{66}$$

At constant temperature and pressure, the only variables that change are residence time and phenol concentration. For this condition $\theta/([Ph]_o - [Ph]_f)$ should vary linearly with $1/[Ph]$. Least square fitting of this line gave correlation coefficients that were 0.9987 and 0.9946 at 200°C and 250°C, respectively. The equation developed was found to be a good fit for the experimental work done. The results showed that phenol and oxygen are probably first order reaction.

Isotachophoresis

Isotachophoresis is electrophoresis carried out at a constant speed [41]. Only a compound that can be ionized can be detected by isotachophoresis. Since different ions are different from each other in

molecular weight, shape of molecules, and degree of electric charge, they travel at different speeds (mobility) even if an equal voltage is applied to the solution. This difference in speed is what separates the different ions. Initially, when the ions are not separated they travel at different speeds. After the ions are separated, they travel at the same speed since the amount of ions going in have to equal the amount of ions going out. In order to obtain good separation in isotachophoresis, the diffusion needs to be minimized. This is done by using a small capillary tube through which the component ions migrate. A diagram of the isotachophoresis is shown in Figure 8.

The leading electrolyte is an electrolyte which contains an ion having a larger effective mobility than that of any component ion in the sample [41]. The terminal electrolyte is an electrolyte which contains an ion having a smaller effective mobility than that of any component in the sample. A boundary is formed in the migration tube between the leading electrolyte and the terminal electrolyte at the position of the injection port. The sample with the leading and terminal electrolyte travels down the migration tube. Two platinum electrodes are installed near one end of the migration tube. They measure the potential gradients of the separated ion zones. First the leading ions are sensed, then the different ions of the sample are sensed, and then the terminal ions are sensed. The result is a stepwise record. The height of each step gives qualitative information. When this stepwise curve is differentiated, a peak will be recorded at each boundary between zones. The peak-to-peak difference corresponds to the length of the zone and gives quantitative information. Isotachopherograms are shown in Appendix B.
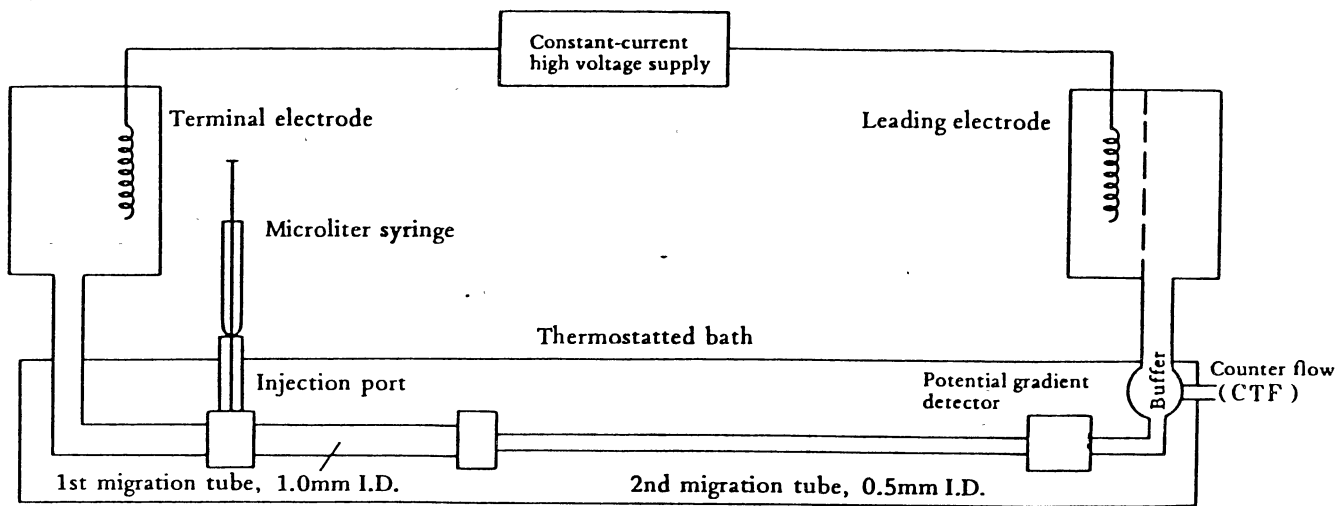
Figure 8.   Isotachophoresis

Isotachophoresis can be effectively used for inorganic ions of low molecular weight, metallic ions, and even proteins of extremely high molecular weight [41]. Any sample that can be electrically charged can be analyzed by isotachophoresis irrespective of molecular weight. Since isotachophoresis is not influenced much by the existence of impurities, it is rarely required to clean up samples before analyses. In analyzing low molecular weight organic acids, the isotachophoresis does not require pretreatment of the samples whereas the gas chromatograph does.

CHAPTER III

EXPERIMENTAL PROCEDURE AND EQUIPMENT

Description of Experimental Runs

The purpose of this study is to oxidize phenol with ozone at elevated temperatures and pressure. A total of 14 runs were made in the ozonation column. Runs 1 through 3 were at conditions of 65°C and 756 kPa (at the column base) and a concentration of 0.01 M phenol. Runs 4 through 6 were at conditions of 70°C and 756 kPa and concentrations of 0.01 M phenol and 0.15 M acetic acid. Runs 7 through 9 were at conditions of 70°C and 756 kPa and concentrations of 0.01 M phenol and 0.01 acetic acid. Runs 10 through 12 were at conditions of 90°C and 756 kPa, and concentrations of 0.01 M phenol and 0.01 M acetic acid. Run 13 was at the same conditions and concentrations as runs 4 through 6, except that no ozone was added. Run 14 was at conditions of 70°C and 756 kPa and a concentration of 0.15 M acetic acid (no phenol was added in this run). All runs were operated in the semi-batch mode and the time of each run was four hours.

Description of Equipment

A drawing of the bubble column is shown in Figure 9. The column consists of two lower sections 2.44 m in length and a top section 1.22 m in length. All sections have an inside diameter of 5.25 cm. The two lower sections are made of schedule 40 stainless steel pipe. The top
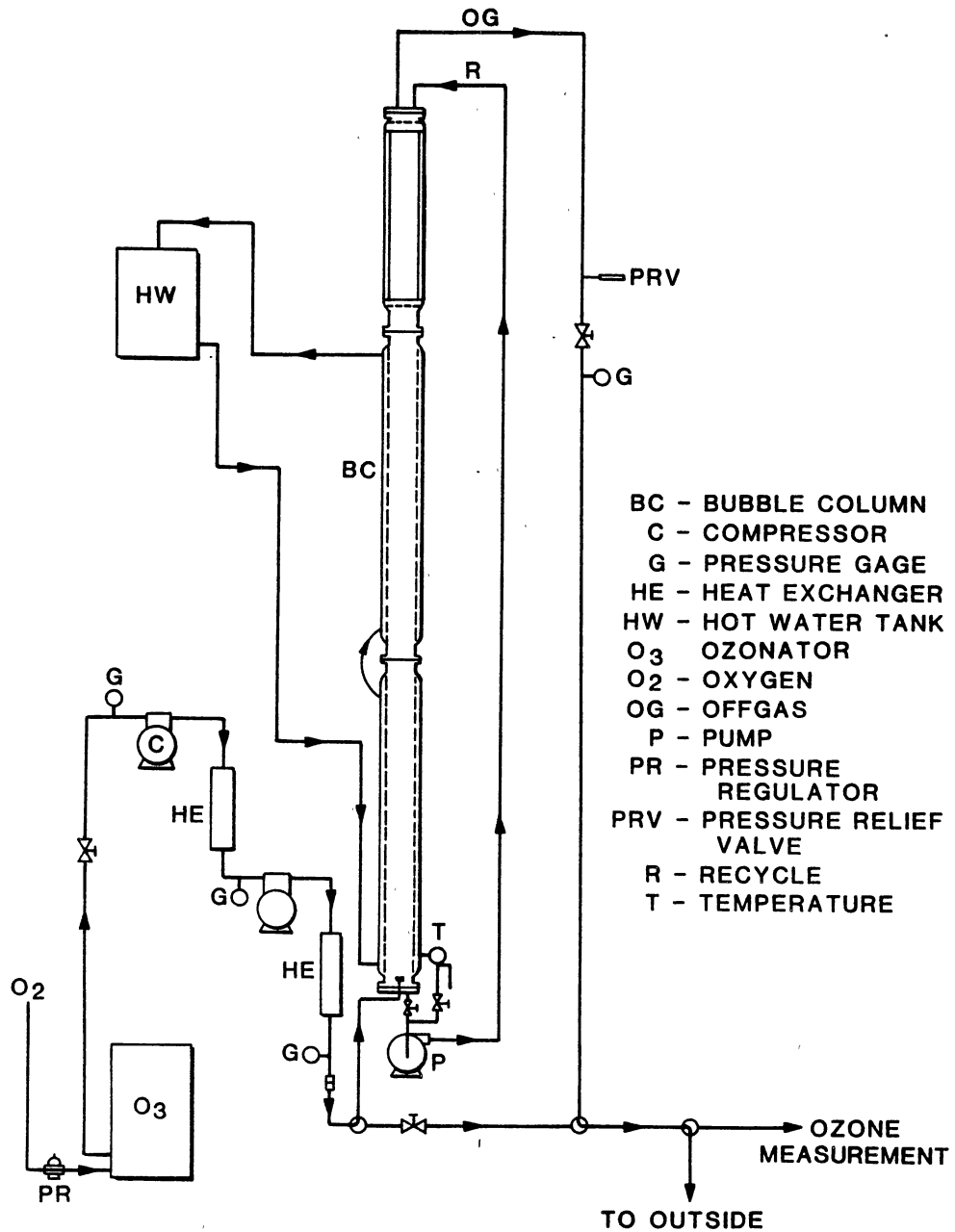
Figure 9. Pressure Ozonation System

section of the column was made transparent by adaptation of a used, nominal 5 cm diameter, stainless steel rotameter. The original rotameter glass was replaced with a heavy wall pyrex glass (6.35 cm outside diameter). The column sections were connected by flanged joints using Teflon gaskets (3.2 mm thick).

The two lower sections have heating jackets. A continuous flow of thermostated water originating from a constant temperature bath was fed to the heating jackets. The jackets are connected in sequence from bottom to top with the liquid overflow returning to the bath. Electric heating tape surrounds the lower 1 m of the column.

A liquid recycle line was used during all the runs. The liquid is drawn off the bottom of the column and reenters at the top. All of the liquid recycle line is 1.25 cm stainless steel. To circulate the flow an Eastern D-11 centrifugal pump is used. The flowrate of the recycle is 4.9 L/min (liquid volume of column about 12 L). A sample port is connected to the recycle line near the base of the column.

In all tests ozone was generated from oxygen. The gas from the ozonator goes through two compressors to reach operating pressures. Development of the compression process has been described in detail by Hill and Howell [14]. This consists of two Gast Model PAB-10 separate drive, oil-less piston compressors. Modified piston rings were installed in the compressors to enable them to operate at low RPM (maximum 300 RPM) and maintain a tight gas seal.

A metering valve before the compressors controls the flowrate. The average gas flowrate was 1.72 L/min. The gas enters the column at the center of the bottom blind flange through a sparger. The gas sparger consists of a porous Kellundite (ceramically bonded alumina) disk 33.3 mm in diameter, 6.3 mm thick, 50 μm nominal particle retention (Ferro

Corporation). A needle valve is connected to the offgas flow line to control the pressure of the column. The offgas goes through a three-way valve and is either vented to the outside or goes through a wet-test meter and bubbled through a KI solution for ozone measurement.

Column Operating Procedures

The experimental solution was made the day of the run. Distilled water, reagent grade phenol, and glacial acetic acid were used. The phenol had a purity of 88 percent and the acetic acid had a purity of 99 percent.

The heating element and pump to the hot water bath and the heating tape at the column base were turned on approximately four hours before the run. The solution was then added to the column and the recycle pump (4.9 L/min) started. This allowed time for the system to reach startup temperature. The ozone generators and compressors were turned on one hour before the run and the gas was vented to the outside air. This allowed for stabilization of the ozonator. The ozonator was set at conditions of 118 V, 207 W, and 2.0 slpm for all runs.

Before the run started, the ozone concentration of the gas leaving the compressor was measured by the KI analytical method and an initial sample of the solution was taken. The run was started when the gas leaving the ozonator was vented into the reaction column. It took approximately 15 minutes for the two-stage compressor to pressurize the column to 100 psig. The inlet pressure gage read 120 psig and the outlet pressure gage read 90 psig. The outlet pressure and inlet flowrate were controlled by two metering valves. The temperature was controlled manually by a switch which controlled the heating coils.

The gaseous ozone leaving the column and the dissolved ozone in the aqueous solution were measured by the KI analytical method on the half-hour. A sample of the solution was taken on the hour. The sample was later used for gas chromatograph analysis of phenol, pH measurement, chemical oxygen demand measurement, and isotachophoresis analysis of intermediate products. The concentration of ozone and flowrate of the inlet gas were measured again at the end of the run.

Ozonator

A Welsbach T-816 ozonator was used to produce the ozone needed for the experiments. The maximum capacity of the ozonator using dry oxygen is 16 grams/hr. The ozonator voltage capacity ranged from 0 to 118 V. The higher the voltage the higher the ozone/oxygen ratio. A Veriflow pressure regulator was used to control the inlet oxygen flow. The ozonator had a flowmeter that recorded the outlet flowrate from 0 to 2.0 slpm at 70°F and 8 psig. Water was used to keep the ozonator cool.

Ozone Analysis

To analyze the ozone in the gas streams, the standard potassium iodide test is used. This method prescribes that approximately 200 mL of a 10 percent solution of KI be mixed with 600 mL of distilled water. The gas bubbles through the mixture and then goes through a wet-test meter. The mixture is then titrated with 0.1 N $Na_2S_2O_3$. The $Na_2S_2O_3$ solution is standardized with 0.25 N $K_2Cr_2O_7$. The flowrate is also determined during the ozone analysis. When the gas goes through the wet-test meter, the time and volume are recorded.

To analyze the dissolved ozone in the liquid sample taken from the bottom of the column, a modified procedure of the process described in Standard Methods for the Examination of Water and Waterwater [11] is used. This method was described by Hill [15]. The following procedure was applied:

1. Place 10 mL of 10 percent KI solution and two drops of 5 percent KOH into a 100 mL graduated cylinder.

2. Purge the liquid sample line.

3. Draw the liquid sample rapidly to the 95 mL mark. Keep the opening of the sample line tubing near the bottom of the cylinder during this operation.

4. Add a few drops of 1.0 M H_2SO_4.

5. Titrate immediately with 0.02 N $Na_2S_2O_3$ (the sodium thiosulfate is standardized with potassium dichromate.)

Chemical Oxygen Demand

Chemical oxygen demand tests were performed based on the procedure in the Standard Methods for the Examination of Water and Wastewater [11]. This method prescribes that 20 mL of "liquid sample," 30 mL concentrated H_2SO_4, 0.4 x 0.4 g H_gSO_4, and 10 mL 0.025 N $K_2Cr_2O_7$ be placed in a refluxing apparatus. After a two-hour boiling period the mixture is cooled, diluted, and titrated with 0.01 N Fe $(NH_4)_2$ $(SO_4)_2$. The liquid sample is a mixture of distilled water and the hourly sample to be analyzed, with the amounts of each depending on the concentration of organic in the hourly sample.

Gas Chromatography

Gas chromatography was used to analyze the amount of phenol in the different samples. The gas chromatograph was a Varian Model 3700. The integrator was a 3390A Hewlett Packard. The injection and column temperatures were set at 220°C each and the flame ionization temperature was set at 300°C. The carrier gas was nitrogen and had a flowrate of 30 cc/min. The combustion gases were air and hydrogen having a flowrate of 300 and 30 cc/min, respectively. The column was 1/8 inch outer diameter stainless steel tubing 5 ft long with Porapak Q packing.

The gas chromatograph was turned on two hours before samples were analyzed. This allowed for stabilization of the system. Five microliters of sample were injected for each analysis.

A calibration curve was made from injecting different known concentrations of phenol. Usually three to four known samples of phenol were injected each time the gas chromatograph was operated to calibrate the column. There were at least two injections for each sample.

Isotachophoresis

The isotachoporetic analyzer was a Shimadzu model IP-2A. The temperature was set at 20°C. The capillary tube was 1 mm o.d. and 60 mm long. The current programming was set at 250 mA for five minutes and then switched to 125 mA. The recorder was turned on after six minutes and had a chart speed of 10 mm/min. The leading electrolyte was 0.01 M histidine HCl and 0.01 M histidine. The terminal electrolyte was 0.01 M glutamic acid. The injection sample was 5 μL.

CHAPTER IV

RESULTS

Stoichiometry

The gas flowrate and the ozone concentration in the gas are calculated at room temperature and then corrected for conditions of 20°C and 1 atm. The temperature-pressure correction factor, C, is calculated as shown below:

$$C = \frac{(293) \text{ K}}{(760 \text{ mm Hg})} \frac{P}{T} \tag{66}$$

where T is room temperature, and P is 760- vapor pressure of water. The equation for the gas flowrate is

$$\text{Gas Flow (L/min)} = \frac{C \text{ (liters gas) } 60}{t_{sec}} \tag{67}$$

The equation for the ozone concentration in the gas is:

$$\text{Gas } O_3 \text{ (mg/L)} = \frac{N_{Na_2S_2O_3} \times mL_{Na_2S_2O_3} \times 24}{C \times \text{(liters gas)}} \tag{68}$$

where $N_{Na_2S_2O_3}$ is normality of sodium thiosulfate, and $mL_{Na_2S_2O_3}$ is milliliters of sodium thiosulfate used as titrant. The factor 24 is to convert mmoles of sodium thiosulfate to milligrams of ozone. The equation for the dissolved ozone concentration does not have a temperature-pressure conversion factor, C, since it is a liquid measurement. The dissolved ozone equation is shown as:

$$\text{Diss. } O_3 \text{ (mg/L)} = \frac{N_{Na_2S_2O_3} \times mL_{Na_2S_2O_3} \times 24{,}000}{mL_{sample}} \qquad (69)$$

The factor 24,000 is used to convert moles of sodium thiosulfate to milligrams of ozone. The chemical oxygen demand (COD) is calculated as shown below:

$$\text{COD (mg/L)} = \frac{\left(mL_{[Fe(\ )]blank} - mL_{[Fe(\ )]sample}\right) \times N_{Fe(\ )} \times 8000}{mL_{sample}}$$

$$(70)$$

where

$mL_{[Fe(\ )]blank}$ = milliliters of ferrous ammonium sulfate $(Fe(NH_4)_2(SO_4)_2)$ used as a titrant when the COD was from the water only; and

$mL_{[Fe(\ )]sample}$ = milliliters of ferrous ammonium sulfate $(Fe(NH_4)_2(SO_4)_2)$ used as a titrant when the COD was from the water and the sample.

Equation (70) measures the COD from the sample only, eliminating the oxygen demand from the water. The factor 8,000 is used to convert moles of ferrous ammonium sulfate to milligrams of atomic oxygen. The ozone concentrations for the gas and liquid, COD concentrations, and pH values are listed in Tables V through XVI. The phenol concentration versus time is graphed for runs 1 through 12 in Figures 10 through 13.

The gas flowrate is used in calculating the amount of moles of ozone consumed. The gas flowrate was initially set at 2 L/min but when measured during the experiment, the flowrate was found to be consistently lower. In runs 7 through 14 the average value of the offgas flowrate is assumed to be the best value to use in the calculations for both the

TABLE V

SUMMARY OF RUN 1 (10/20/82)

| Time (hr) | Ozone Concentration | | | pH | Reaction Volume (L) | Ozone Consumed (moles/hr) | Phenol Oxidized (moles/hr) | COD Change (mg/hr) | COD (mg/L) |
	Inlet Gas (mg/L)	Offgas (mg/L)	Dissolved Gas (mg/L)						
0	49.4	---	---	7.50	12.50	0	0	0	2,220
0.5	---	0.42	25.80	---	12.40	---	---	---	---
1.0	---	---	---	3.05	12.26	0.107	0.0450	3,860	1,910
1.5	---	0.11	26.52	---	12.15	---	---	---	---
2.0	---	---	---	2.80	12.01	0.108	0.0330	3,780	1,570
2.5	---	0.15	51.86	---	11.90	---	---	---	---
3.0	---	---	---	2.65	11.76	0.108	0.0229	3,720	1,295
3.5	---	0.00	68.87	---	11.65	---	---	---	---
4.0	50.9	---	---	2.60	11.51	0.108	0.0113	3,630	975

0.01 M phenol (940 mg/L); T = 65°C; flowrate = 1.721 L/min; p = 756 kPa.

TABLE VI

SUMMARY OF RUN 2 (1/26/83)

Time (hr)	Ozone Concentration			pH	Reaction Volume (L)	Ozone Consumed (moles/hr)	Phenol Oxidized (moles/hr)	COD Change (mg/hr)	COD (mg/L)
	Inlet Gas (mg/L)	Offgas (mg/L)	Dissolved Gas (mg/L)						
0	38.2	---	---	7.00	12.50	0.0	0.0	0.0	2,320
0.5	---	1.55	22.44	---	12.40	---	---	---	---
1.0	---	---	---	3.05	12.26	0.0837	0.0457	3,630	2,010
1.5	---	0.21	0.0	---	12.16	---	---	---	---
2.0	---	---	---	2.85	12.02	0.0962	0.0361	3,875	1,695
2.5	---	0.17	2.40	---	11.91	---	---	---	---
3.0	---	---	---	2.65	11.77	0.1060	0.0285	3,965	1,345
3.5	---	0.06	13.51	---	11.66	---	---	---	---
4.0	56.2	---	---	2.65	11.52	0.1159	0.0037	4,075	1,010

0.01 M phenol (940 mg/L); T = 65°C; ozone flowrate = 1.721 L/min; p = 756 kPa.

TABLE VII

SUMMARY OF RUN 3 (4/1/83)

Time (hr)	Ozone Concentration Inlet Gas (mg/L)	Offgas (mg/L)	Dissolved Gas (mg/L)	pH	Reaction Volume (L)	Ozone Consumed (moles/hr)	Phenol Oxidized (moles/hr)	COD Change (mg/hr)	COD (mg/L)
0	51.21	---	---	6.35	12.50	0.0	0.0	0.0	2,155
0.5	---	0.90	0.00	---	12.39	---	---	---	---
1.0	---	---	---	3.05	12.25	0.1090	0.0503	3,810	1,865
1.5	---	0.51	6.73	---	12.14	---	---	---	---
2.0	---	---	---	2.80	12.00	0.1112	0.0359	3,870	1,545
2.5	---	0.00	0.00	---	11.90	---	---	---	---
3.0	---	---	---	2.65	11.76	0.1138	0.0335	4,165	1,215
3.5	---	0.00	0.00	---	11.65	---	---	---	---
4.0	53.91	---	---	2.60	11.51	0.1152	0.0623	3,910	865

0.01 M phenol (940 mg/L); T = 65°C; flowrate = 1.721 L/min; p = 756 kPa.

TABLE VIII

SUMMARY OF RUN 4 (6/29/83)

Time (hr)	Ozone Concentration			ph	Reaction Volume (L)	Ozone Consumed (moles/hr)	Phenol Oxidized (moles/hr)	COD Change (mg/hr)	COD (mg/L)
	Inlet Gas (mg/L)	Offgas (mg/L)	Dissolved Gas (mg/L)						
0	43.29	---	---	2.80	12.65	0.0	0.0	0.0	11,130
0.5	---	0.88	16.51	---	12.55	---	---	---	---
1.0	---	---	---	2.65	12.41	0.0934	0.0482	2,285	10,995
1.5	---	0.22	14.28	---	12.30	---	---	---	---
2.0	---	---	---	2.60	12.16	0.9960	0.0316	3,625	10,655
2.5	---	0.71	error	---	12.06	---	---	---	---
3.0	---	---	---	2.50	11.92	0.1025	0.0238	4,830	10,250
3.5	---	Undetected	5.39	---	11.81	---	---	---	---
4.0	51.44	---	---	2.45	11.67	0.1085	0.0101	3,120	9,985

0.15 M acetic acid; 0.01 M phenol; T = 70°C; flowrate = 1.721 L/min; p = 756 kPa.

TABLE IX

SUMMARY OF RUN 5 (7/6/83)

Time (hr)	Ozone Concentration			pH	Reaction Volume (L)	Ozone Consumed (moles/hr)	Phenol Oxidized (moles/hr)	COD Change (mg/hr)	COD (mg/L)
	Inlet Gas (mg/L)	Offgas (mg/L)	Dissolved Gas (mg/L)						
0	48.09	---	---	2.90	12.80	0.0	0.0	0.0	11,965
0.5	---	0.14	13.11	---	12.69	---	---	---	---
1.0	---	---	---	2.75	12.55	0.1055	0.0406	2,350	12,125
1.5	---	0.24	16.45	---	12.43	---	---	---	---
2.0	---	---	---	2.70	12.29	0.1053	0.0302	6,915	11,255
2.5	---	0.15	14.27	---	12.17	---	---	---	---
3.0	---	---	---	2.60	12.03	0.1054	0.0239	2,515	11,070
3.5	---	0.00	9.74	---	11.91	---	---	---	---
4.0	48.72	---	---	2.55	11.77	0.1058	0.0153	3,635	10,695

0.15 M acetic acid; 0.01 M phenol; T = 70°C; flowrate = 1.7488 L/min; p = 756 kPa.

TABLE X

SUMMARY OF RUN 6 (7/13/83)

Time (hr)	Ozone Concentration			pH	Reaction Volume (L)	Ozone Consumed (moles/hr)	Phenol Oxidized (moles/hr)	COD Change (mg/hr)	COD (mg/L)
	Inlet Gas (mg/L)	Offgas (mg/L)	Dissolved Gas (mg/L)						
0	47.30	---	---	2.85	12.94	0.0	0.0	0.0	11,110
0.5	---	0.44	13.62	---	12.82	---	---	---	---
1.0	---	---	---	2.75	12.68	0.1140	0.0446	4,475	10,770
1.5	---	0.00	11.05	---	12.56	---	---	---	---
2.0	---	---	---	2.65	12.42	0.1151	0.0336	1,713	10,630
2.5	---	0.00	10.69	---	12.31	---	---	---	---
3.0	---	---	---	2.60	12.17	0.1150	0.0303	6,090	10,135
3.5	---	0.00	10.23	---	12.05	---	---	---	---
4.0	49.59	---	---	2.55	11.91	0.1151	0.0174	3,495	9,850

0.15 M acetic acid; 0.01 M phenol; T = 70°C; flowrate = 1.90 L/min; p = 756 kPa.

TABLE XI

SUMMARY OF RUN 7 (7/20/83)

Time (hr)	Ozone Concentration			pH	Reaction Volume (L)	Ozone Consumed (moles/hr)	Phenol Oxidized (moles/hr)	COD Change (mg/hr)	COD (mg/L)
	Inlet Gas (mg/L)	Offgas (mg/L)	Dissolved Gas (mg/L)						
0	error	---	---	3.40	12.56	0.0	0.0	0.0	3,005
0.5	---	0.85	13.34	---	12.44	---	---	---	---
1.0	---	---	---	3.00	12.30	0.1186	0.0499	3,720	2,710
1.5	---	0.32	12.64	---	12.18	---	---	---	---
2.0	---	---	---	2.80	12.04	0.1198	0.0326	2,880	2,475
2.5	---	0.18	9.70	---	11.93	---	---	---	---
3.0	---	---	---	2.70	11.79	0.1201	0.0261	4,465	2,100
3.5	---	0.36	11.62	---	11.67	---	---	---	---
4.0	52.14	---	---	2.60	11.53	0.1197	0.0119	4,320	1,730

0.01 M acetic acid; 0.01 M phenol; T = 70°C; flowrate = 1.850; p = 756 kPa.

TABLE XII

SUMMARY OF RUN 8 (8/4/83)

Time (hr)	Ozone Concentration			pH	Reaction Volume (L)	Ozone Consumed (moles/hr)	Phenol Oxidized (moles/hr)	COD Change (mg/hr)	COD (mg/L)
	Inlet Gas (mg/L)	Offgas (mg/L)	Dissolved Gas (mg/L)						
0	47.70	---	---	3.35	12.50	0.0	0.0	0.0	2,700
0.5	---	1.76	13.74	---	12.39	---	---	---	---
1.0	---	---	---	2.90	12.25	0.0964	0.0450	2,950	2,460
1.5	---	0.49	20.62	---	12.13	---	---	---	---
2.0	---	---	---	2.70	11.99	0.1001	0.0286	3,535	2,170
2.5	---	0.00	14.78	---	11.88	---	---	---	---
3.0	---	---	---	2.65	11.74	0.1021	0.0216	2,360	1,975
3.5	---	0.00	9.16	---	11.61	---	---	---	---
4.0	49.65	---	---	2.55	11.47	0.1031	0.0090	3,290	1,690

0.01 acetic acid; 0.01 M phenol; T = 70°C; flowrate = 1.67 L/min; p = 756 kPa.

TABLE XIII

SUMMARY OF RUN 9 (8/8/83)

Time (hr)	Ozone Concentration			pH	Reaction Volume (L)	Ozone Consumed (moles/hr)	Phenol Oxidized (moles/hr)	COD Change (mg/hr)	COD (mg/L)
	Inlet Gas (mg/L)	Offgas (mg/L)	Dissolved Gas (mg/L)						
0	47.05	---	---	3.30	12.50	0.0	0.0	0.0	2,905
0.5	---	0.63	error	---	12.40	---	---	---	---
1.0	---	---	---	2.90	12.26	0.0955	0.0397	2,990	2,660
1.5	---	0.00	0.00	---	12.16	---	---	---	---
2.0	---	---	---	2.70	12.01	0.0980	0.0338	3,295	2,390
2.5	---	0.00	8.77	---	11.90	---	---	---	---
3.0	---	---	---	2.60	11.76	0.0991	0.0255	3,030	2,140
3.5	---	0.00	12.71	---	11.65	---	---	---	---
4.0	49.28	---	---	2.55	11.51	0.1002	0.0125	3,700	1,825

0.01 M acetic acid; 0.01 M phenol; T = 70°C; flowrate = 1.64 L/min; p = 756 kPa.

TABLE XIV

SUMMARY OF RUN 10 (7/25/83)

Time (hr)	Ozone Concentration			pH	Reaction Volume (L)	Ozone Consumed (moles/hr)	Phenol Oxidized (moles/hr)	COD Change (mg/hr)	COD (mg/L)
	Inlet Gas (mg/L)	Offgas (mg/L)	Dissolved Gas (mg/L)						
0	51.52	---	---	3.40	12.50	0.0	0.0	0.0	2,905
0.5	---	0.98	9.85	---	12.39	---	---	---	---
1.0	---	---	---	3.00	12.25	0.1069	0.0490	3,145	2,655
1.5	---	0.21	0.00	---	12.14	---	---	---	---
2.0	---	---	---	2.80	12.00	0.1086	0.0379	3,745	2,345
2.5	---	0.00	0.00	---	11.89	---	---	---	---
3.0	---	---	---	2.70	11.75	0.1090	0.0292	3,710	2,035
3.5	---	0.00	6.33	---	11.63	---	---	---	---
4.0	51.88	---	---	2.60	11.49	0.1090	0.0096	4,370	1,660

0.01 M acetic acid; 0.01 M phenol; T = 90°C; flowrate = 1.69 L/min; p = 756 kPa.

TABLE XV

SUMMARY OF RUN 11 (7/27/83)

Time (hr)	Inlet Gas (mg/L)	Offgas (mg/L)	Dissolved Gas (mg/L)	pH	Reaction Volume (L)	Ozone Consumed (moles/hr)	Phenol Oxidized (moles/hr)	COD Change (mg/hr)	COD (mg/L)
	Ozone Concentration								
0	52.47	---	---	3.45	12.50	0.0	0.0	0.0	2,875
0.5	---	0.81	11.64	---	12.39	---	---	---	---
1.0	---	---	---	3.00	12.25	0.1069	0.0496	4,065	2,555
1.5	---	0.78	14.00	---	12.14	---	---	---	---
2.0	---	---	---	2.80	12.00	0.1069	0.0377	3,920	2,180
2.5	---	0.00	0.00	---	11.88	---	---	---	---
3.0	---	---	---	2.65	11.74	0.1085	0.0216	4,230	1,870
3.5	---	0.00	error	---	11.63	---	---	---	---
4.0	52.79	---	---	2.65	11.49	0.1085	0.0069	4,370	1,470

0.01 M acetic acid; 0.01 M phenol; T = 90°C; flowrate = 1.65 L/min; p = 756 kPa.

TABLE XVI

SUMMARY OF RUN 12 (7/30/83)

Time (hr)	Ozone Concentration			pH	Reaction Volume (L)	Ozone Consumed (moles/hr)	Phenol Oxidized (moles/hr)	COD Change (mg/hr)	COD (mg/L)
	Inlet Gas (mg/L)	Offgas (mg/L)	Dissolved Gas (mg/L)						
0	53.72	---	---	3.45	12.50	0.0	0.0	0.0	2,790
0.5	---	0.37	9.20	---	12.39	---	---	---	---
1.0	---	---	---	2.95	12.25	0.1088	0.0523	2,885	2,555
1.5	---	0.83	9.72	---	12.13	---	---	---	---
2.0	---	---	---	2.75	11.99	0.1079	0.0357	4,515	2,185
2.5	---	0.00	8.74	---	11.88	---	---	---	---
3.0	---	---	---	2.60	11.74	0.1096	0.0248	3,750	1,870
3.5	---	0.00	4.40	---	11.61	---	---	---	---
4.0	54.08	---	---	2.55	11.47	0.1096	0.0087	4,110	1,520

0.01 M acetic acid; 0.01 M phenol; T = 90°C; flowrate = 1.63 L/min; p = 756 kPa.
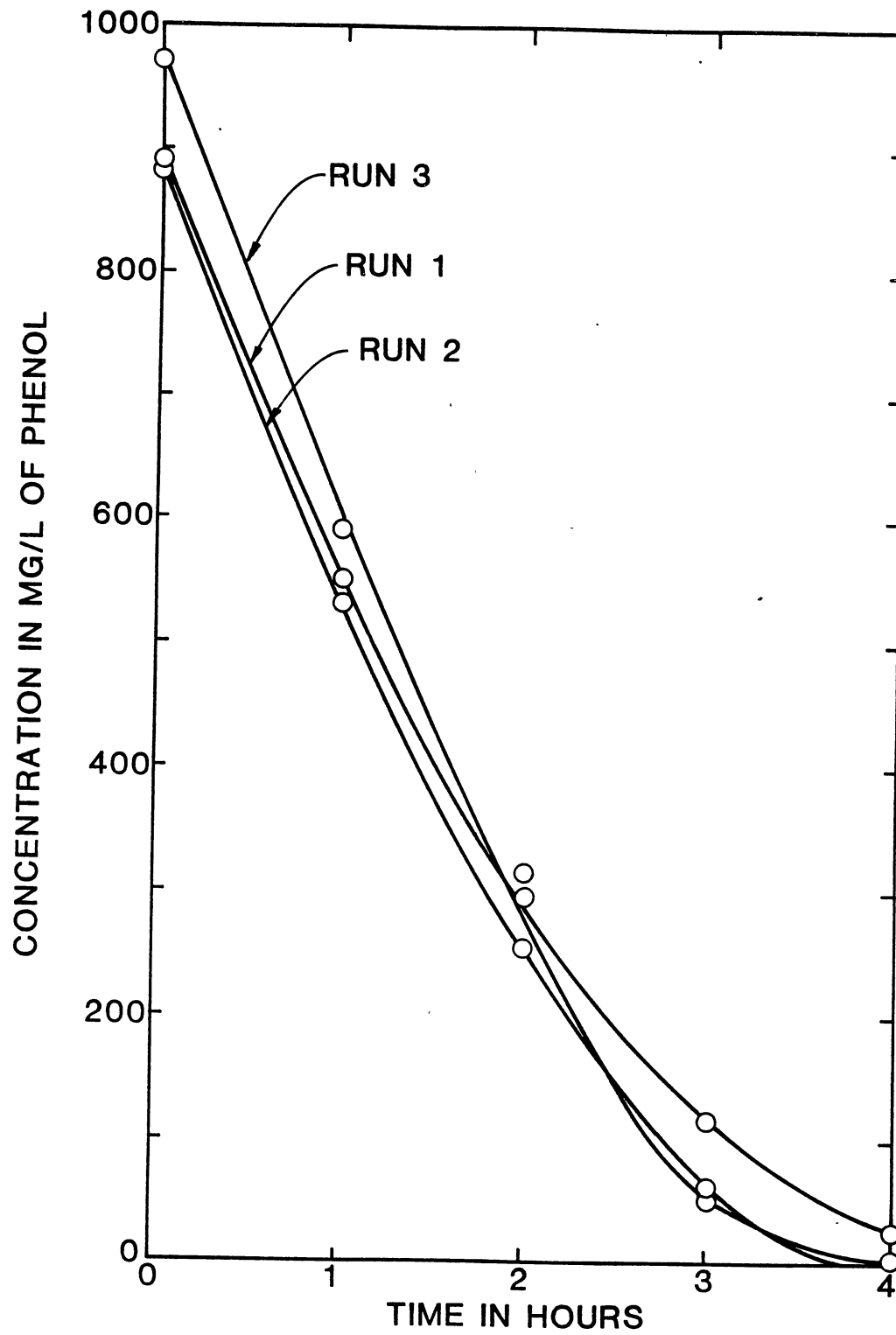
Figure 10. Phenol Concentration With Time
for Condition 1
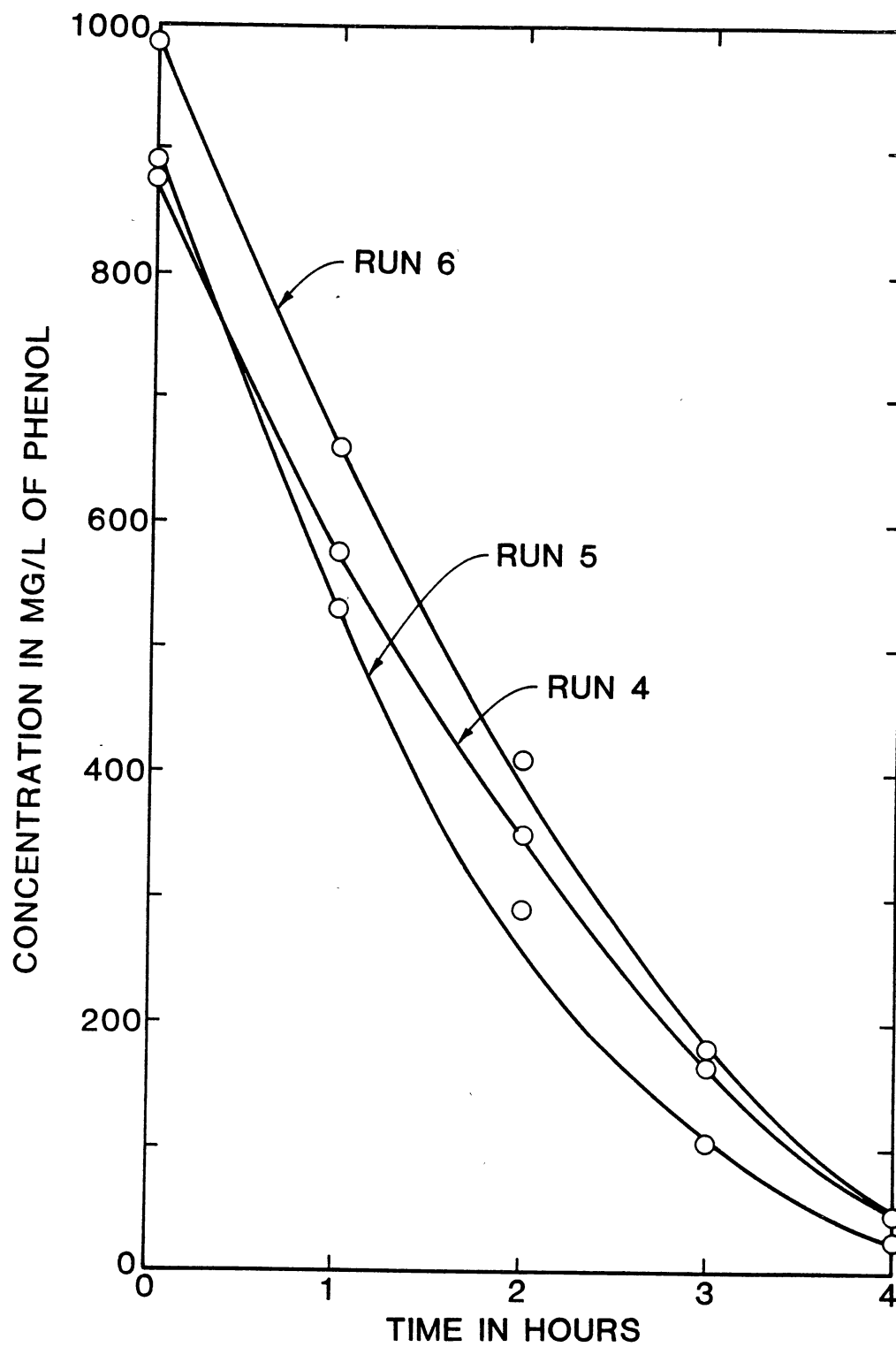
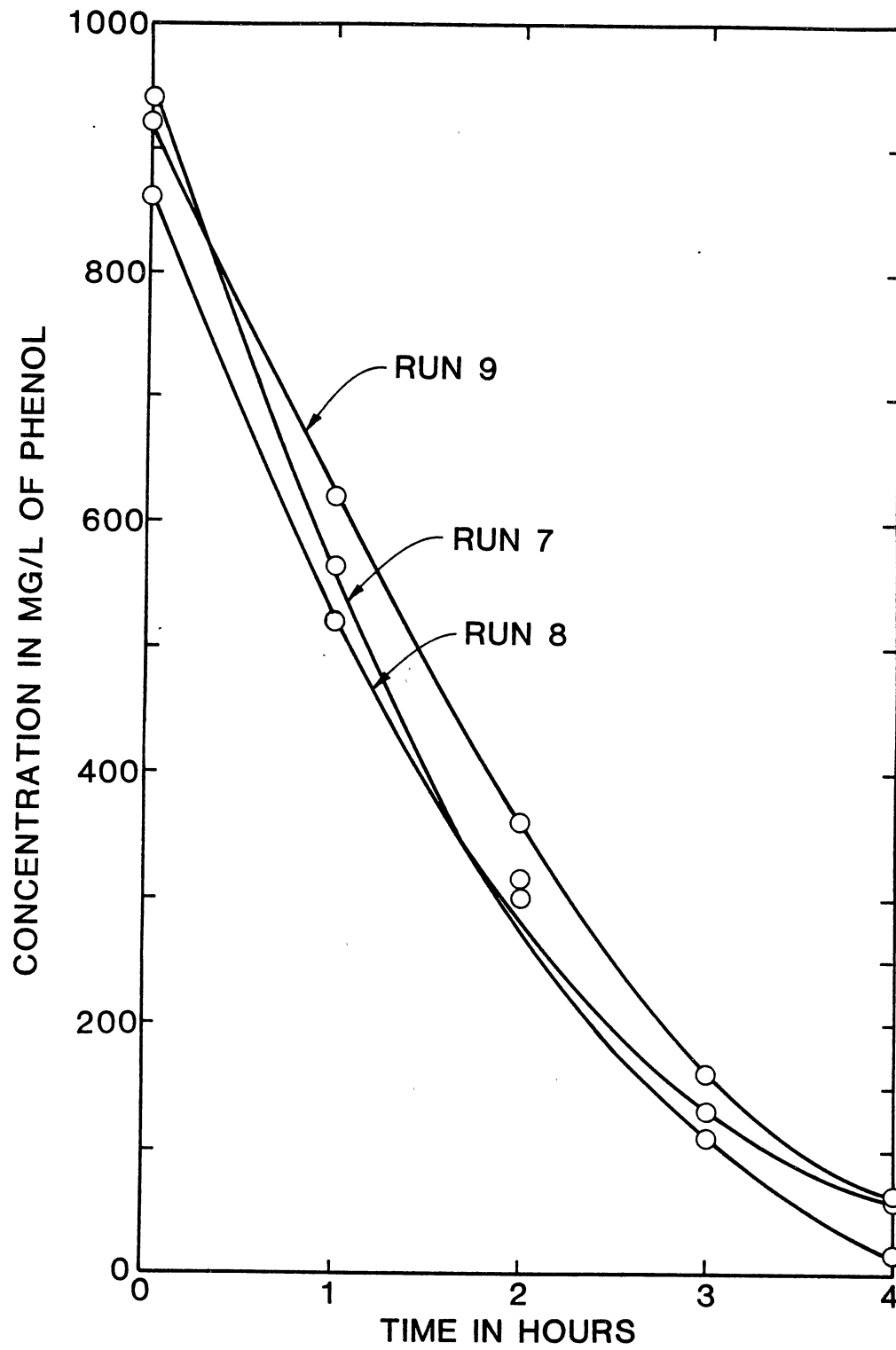Figure 11. Phenol Concentration With Time
for Condition 2

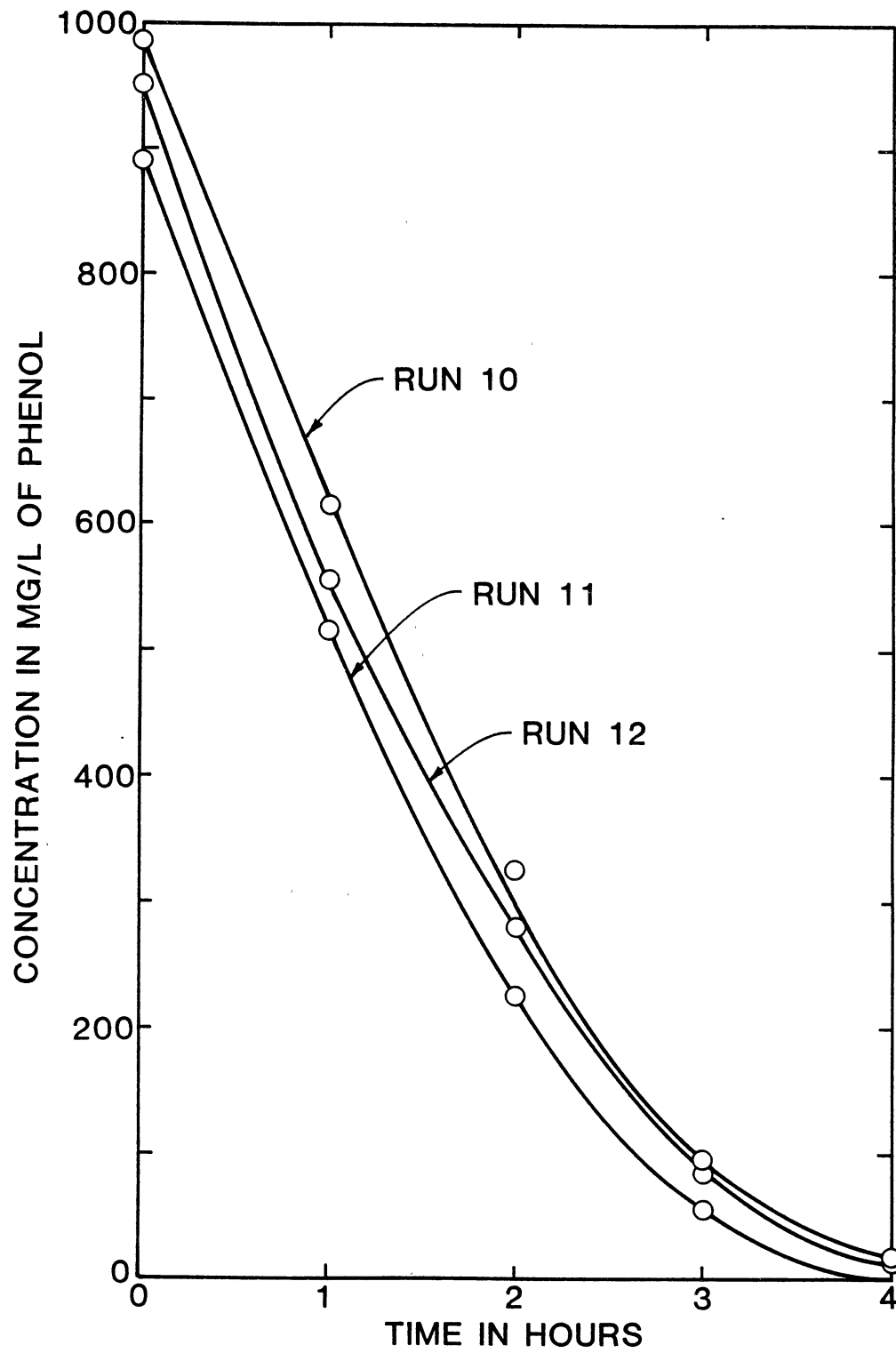Figure 12.   Phenol Concentration With Time
for Condition 3

Figure 13.   Phenol Concentration With Time
for Condition 4

inlet and outlet flows. The flowrate is assumed constant throughout the experiment. In runs 1 through 6, the gas flowrate was not measured. A collective average of the offgas flowrate from runs 7 through 14 is assumed to be the best value for the gas flowrate in runs 1 through 6. The moles of ozone consumed is calculated from the following equation:

$$\Delta O_3 \text{ (moles/hr)} = \frac{([O_3]_o - [O_3]_f)}{800} G \tag{71}$$

where G is gas flowrate in L/min. The factor 800 is a combination of converting milligrams of ozone to moles of ozone and of converting minutes to hours.

The volume of the liquid changed in the reaction every one-half hour during the experiment and is taken into consideration in calculating the moles of phenol oxidized and in calculating the change in COD. Volume changes are estimated as follows: 40 mL from purging the drain every half-hour, 100 mL from taking a liquid sample every hour, and a volume on the half-hour associated with the dissolved ozone analysis. The equation to calculate the amount of phenol oxidized in one hour is:

$$Ph_{oxid} \text{ (mole/hr)} = \frac{V_i [Ph]_i - V_m[Ph]_m - (V_i - V_m)[Ph]_f}{94,000} \tag{72}$$

where V_m is amount of liquid drained on the half-hour, and $[Ph]_m$ is phenol concentration on the half-hour. The factor 94,000 is used to convert milligrams of phenol to moles of phenol. The equation to calculate the change in COD per hour is similar to the phenol oxidized equation as shown:

$$\Delta COD \text{ (mg/L)} = V_i ([COD]_i - V_m[COD]_m - (V_i - V_m)[COD]_f \tag{73}$$

A summary of the ozone consumed, of the volume of the reaction, of the phenol oxidized, and of the change in COD is listed for each run in Tables V through XVI. A summary of runs 13 and 14 is listed in Tables XVII and XVIII. Run 13 is at a temperature of 70°C, a pressure of 756 kPa, and a concentration of 0.15 M acetic acid. There is no phenol in this run. Run 14 is at a temperature of 70°C, a pressure of 756 kPa, and a concentration of 0.15 M acetic acid and 0.01 M phenol. No ozone is used in this run. A summary of the stoichiometric ratios is listed in Tables XIX and XX.

Isotachophoresis

Six known compounds are analyzed with the isotachophoresis. These known compounds are oxalic acid, glyoxylic acid, acetic acid, tartaric acid, fumaric acid, and maleic acid. Their chemical structures are shown in Appendix A. To qualitatively identify the compounds, a ratio of the height of the known compound relative to the height of the terminal electrolyte is calculated. A summary of the relative peak heights for the known compounds is listed in Table XXI. The average relative peak height for oxalic acid, fumaric acid, tartaric acid, maleic acid, acetic acid, and glyoxylic acid is 0.165, 0.284, 0.303, 0.396, 0.589, and 0.722, respectively. The oxalic acid has two peaks when it is analyzed by isotachophoresis. The first peak is much smaller in quantity and is assumed to be an impurity. A sample isotachopherogram for each compound is shown in Appendix B.

Three runs are made with the isotachophoretic analyzer using a mixture of known compounds. The data from the runs are listed in Table XXII. The first run is a mixture of acetic acid, maleic acid, tartaric acid, and

TABLE XVII

SUMMARY OF RUN 13 (6/15/83)

Time (hr)	Ozone Concentration			pH	COD (mg/L)	N_A (mg/hr)	C_{A1}^* (mg/L)	C_{A2}^* (mg/L)
	Inlet Gas (mg/L)	Offgas (mg/L)	Dissolved Gas (mg/L)					
0	46.74	---	---	2.90	9,125	---	---	---
0.5	---	8.59	25.2	---	---	---	---	---
1.0	---	---	---	2.95	9,090	4,010	36.7	6.65
1.5	---	20.80	40.7	---	---	---	---	---
2.0	---	---	---	3.00	9,125	2,890	37.8	16.10
2.5	---	20.20	49.0	---	---	---	---	---
3.0	---	---	---	3.00	9,010	3,090	38.8	15.60
3.5	---	22.50	46.4	---	---	---	---	---
4.0	52.18	---	---	3.00	8,810	2,995	39.9	17.40

TABLE XVIII

SUMMARY OF RUN 14 (6/22/83)

Time (hr)	COD (mg/L)	pH
0	12,110	2.90
1	12,250	2.90
2	12,285	2.85
3	12,695	2.85
4	11,920	2.90

TABLE XIX

STOICHIOMETRIC RATIO OF MOLES OZONE CONSUMED
PER MOLE PHENOL OXIDIZED

Time (hr)	Run 1 (10/20/82)	Run 2 (1/26/83)	Run 3 (4/1/83)	Run 4 (6/29/83)	Run 5 (7/6/83)	Run 6 (7/13/83)	Run 7 (7/20/83)	Run 8 (8/4/83)	Run 9 (8/8/83)	Run 10 (7/25/83)	Run 11 (7/27/83)	Run 12 (7/30/83)
1	2.34	1.83	2.16	1.94	2.59	2.56	2.38	2.14	2.41	2.18	2.15	2.08
2	2.76	2.20	2.56	2.41	2.98	2.93	2.90	2.67	2.63	2.49	2.45	2.46
3	3.20	2.60	2.79	2.85	3.34	3.18	3.30	3.14	2.96	2.80	2.96	2.90
4	3.83	3.53	3.56	3.55	3.84	3.65	3.97	3.84	3.52	3.45	3.72	3.59

TABLE XX

STOICHIOMETRIC RATIO OF MG OZONE CONSUMED PER MG PHENOL OXIDIZED

Time (hr)	Run 1 (10/20/82)	Run 2 (1/26/83)	Run 3 (4/1/83)	Run 4 (6/29/83)	Run 5 (7/6/83)	Run 6 (7/13/83)	Run 7 (7/20/83)	Run 8 (8/4/83)	Run 9 (8/8/83)	Run 10 (7/25/83)	Run 11 (7/27/83)	Run 12 (7/30/83)
1	1.33	1.11	1.37	1.96	2.16	1.22	1.53	1.57	1.53	1.63	1.26	1.81
2	1.35	1.15	1.38	1.57	1.09	1.78	1.73	1.46	1.48	1.50	1.29	1.41
3	1.36	1.20	1.35	1.32	1.29	1.34	1.56	1.62	1.51	1.47	1.27	1.41
4	1.38	1.24	1.37	1.40	1.31	1.40	1.49	1.59	1.45	1.39	1.25	1.37

TABLE XXI

ISOTACHOPHORESIS DATA FOR PURE COMPONENTS

Sample	Relative Peak Height	Peak Width (cm)
Oxalic Acid	0.170	1.20
Oxalic Acid	0.152	1.10
Oxalic Acid	0.172	1.21
Oxalic Acid	0.164	1.19
Fumaric Acid	0.284	1.75
Tartaric Acid	0.298	1.40
Tartaric Acid	0.305	1.08
Tartaric Acid	0.307	1.11
Maleic Acid	0.382	1.40
Maleic Acid	0.403	1.00
Maleic Acid	0.404	1.09
Acetic Acid	0.593	1.65
Acetic Acid	0.581	1.08
Acetic Acid	0.593	0.92
Glyoxylic Acid	0.722	1.20

All sample concentrations are 1000 mg/L.

TABLE XXII

ISOTACHOPHORESIS DATA ON MIXTURES
WITH KNOWN COMPOUNDS

Relative Peak Height	Peak Width (cm)	Identification
Run 1. Acetic Acid, Maleic Acid, Tartaric Acid, and Fumaric Acid		
0.287	0.75	{ Tartaric Acid and Fumaric Acid
0.389	0.40	Maleic Acid
0.578	0.50	Acetic Acid
Run 2. Fumaric Acid, Acetic Acid, Glyoxylic Acid, and Oxalic Acid		
0.157	0.40	Oxalic Acid
0.287	0.50	Fumaric Acid
0.593	0.65	{ Acetic Acid and Glyoxylic Acid
Run 3. Glyoxylic Acid, Tartaric Acid, Oxalic Acid, and Maleic Acid		
0.157	0.40	Oxalic Acid
0.296	0.30	Tartaric Acid
0.389	0.40	Maleic Acid
0.657	0.20	Glyoxylic Acid

fumaric acid, each component having a concentration of 250 mg/L. The chromatograph for this run is shown in Appendix B. From the isotacho-pherogram it is shown that there are only three peaks for the four components. The relative peak heights are 0.287, 0.389, and 0.578. Based on previous single component runs, the first peak is determined to be a mixture of tartaric acid and fumaric acid. Therefore, in the prelimini-nary analysis of the components produced from phenol ozonation, no distinction can be made between fumaric acid and tartaric acid.

The second run is a mixture of fumaric acid, acetic acid, glyoxylic acid, and oxalic acid, with a concentration of 250 mg/L for each component. Again, there are only three peaks for the four components (Appendix B). From the analysis of the data, it is assumed that the glyoxylic acid and acetic acid formed one peak. This is verified by running a mixture of acetic acid and glyoxylic acid through the isotachophoresis and having only one peak appear on the isotachopherogram.

The third run is a mixture of glyoxylic acid, tartaric acid, oxalic acid, and maleic acid, with a concentration of 250 mg/L for each component. For this run, there are four peaks for the four components. The first three peaks are identified as oxalic acid, tartaric acid, and maleic acid, and the relative peak heights for the mixture correspond relatively closely with the relative heights of the pure components. The fourth peak is assumed to be glyoxylic acid. The relative peak height for glyoxylic acid in the mixture is 0.657 whereas the relative peak height of pure glyoxylic acid is 0.722, showing a slight discrepancy between the two.

To quantitatively analyze a sample, the width from peak to peak is measured. The ratio of a known concentration of a sample divided by the width is equal to an unknown concentration of the sample divided by the width. Example calculations are shown in Table XXIII. The example calculations are made on the three runs that had a mixture of components. The width for each component in the "mixture" runs is measured and used as the unknown concentration. The known concentration is the "single component" runs. The average width value for each single component is used in the calculations. Table XXIII shows a comparison of the calculated concentrations and the known concentrations.

The isotachopherograms for run 1 of phenol ozonation are shown in Appendix B. In the first hour isotachopherogram, two peaks are found. The first peak has a relative peak height close to formic acid (the relative peak height is also close to fumaric acid and tartaric acid). The second peak is unidentified. On the first hour isotachopherogram, there is an indication of a peak between the first and second peak. In the second hour isotachopherogram, three peaks are found. The first peak is again assumed to be formic acid. The second peak is assumed to be maleic acid, although the value of the relative peak height is slightly higher than the value found for pure maleic acid. The third peak is assumed to be the same unknown peak that was observed in the first hour isotachopherogram. In the second hour isotachopherogram, there is indication of a peak before the first peak (formic acid peak). The third and fourth hour isotachopherograms both have three peaks at similar locations. The peaks are tentatively identified as oxalic acid, formic acid, and maleic acid, respectively. In the fourth hour isotachopherogram, there is indication of a peak after the third peak. The data from the isotachophero-

TABLE XXIII

SAMPLE CALCULATIONS ON ISOTACHOPHORESIS DATA

Run	Sample	Peak Width of Known (cm)	Peak Width of Unknown (cm)	Calculations	Calculated Concentration (mg/L)	Actual Concentration (mg/L)
1	Tartaric Acid and Fumaric Acid	1.58	0.75	$\dfrac{(1000)(0.75)}{1.58} =$	476	500
	Maleic Acid	1.40	0.40	$\dfrac{(1000)(0.40)}{1.40} =$	286	250
	Acetic Acid	1.65	0.50	$\dfrac{(1000)(0.50)}{1.65} =$	303	250
2	Oxalic Acid	1.10	0.40	$\dfrac{(1000)(0.40)}{1.15} =$	348	250
	Fumaric Acid	1.75	0.50	$\dfrac{(1000)(0.50)}{1.75} =$	286	250
	Acetic Acid and Glyoxylic Acid	1.40	0.65	$\dfrac{(1000)(0.65)}{1.40} =$	456	500
3	Oxalic Acid	1.15	0.40	$\dfrac{(1000)(0.40)}{1.15} =$	348	250
	Tartaric Acid	1.40	0.30	$\dfrac{(1000)(0.30)}{1.40} =$	214	250
	Maleic Acid	1.40	0.40	$\dfrac{(1000)(0.40)}{1.40} =$	286	250
	Glyoxylic Acid	1.20	0.20	$\dfrac{(1000)(0.20)}{1.20} =$	167	250

gram for run 1 is summarized in Table XXIV. Figure 14 shows the approximate concentration of the identified compounds with respect to time. The phenol concentration and the total organic carbon concentration are also plotted in Figure 14.

A summary of the isotachophoresis data and analysis for run 2 is shown in Table XXV and in Figure 15. The first and second hour isotachopherograms have three peaks at similar locations. The peaks are identified as oxalic acid, formic acid, and maleic acid, respectively. The third and fourth hour isotachopherograms have five peaks at similar locations. The first, third, fourth, and fifth peaks are tentatively identified as oxalic acid, formic acid, maleic acid, and acetic acid, respectively. The second peak is unknown. This unknown is not the same unknown found in run 1.

A summary of the isotachophoresis data and analysis for run 3 is shown in Table XXVI and in Figure 16. Appendix B shows the isotachopherograms for run 3. The first and second hour isotachopherograms have peaks at similar locations. The peaks are tentatively identified as oxalic acid, formic acid, and maleic acid. On the second hour isotachopherogram, there is indication of a peak after the third peak. For the third and fourth hour isotachopherograms, there are four peaks at similar locations. The peaks are tentatively identified as oxalic acid, formic acid, maleic acid, and acetic acid.

Mass Transfer

To calculate the liquid mass transfer coefficient, $k_L a$, the equilibrium and operating lines are assumed to be linear. This assumption is possible because the ozone is dilute in both the gas phase and the liquid

TABLE XXIV

TENTATIVE IDENTIFICATION OF ISOTACHO-
PHORESIS DATA FOR RUN 1

Sample	Tentative Identification		Relative Peak Height	Peak Width (mm)
1:00	1.	Formic Acid	0.3077	2.50
	2.	Unknown #1	0.5385	1.65
2:00	1.	Formic Acid	0.3010	3.40
	2.	Maleic Acid	0.4175	2.25
	3.	Unknown #1	0.5437	1.50
3:00	1.	Oxalic Acid	0.1567	1.75
	2.	Formic Acid	0.3077	4.85
	3.	Maleic Acid	0.4231	4.25
4:00	1.	Oxalic Acid	0.1553	2.10
	2.	Formic Acid	0.3107	7.00
	3.	Maleic Acid	0.4253	4.10
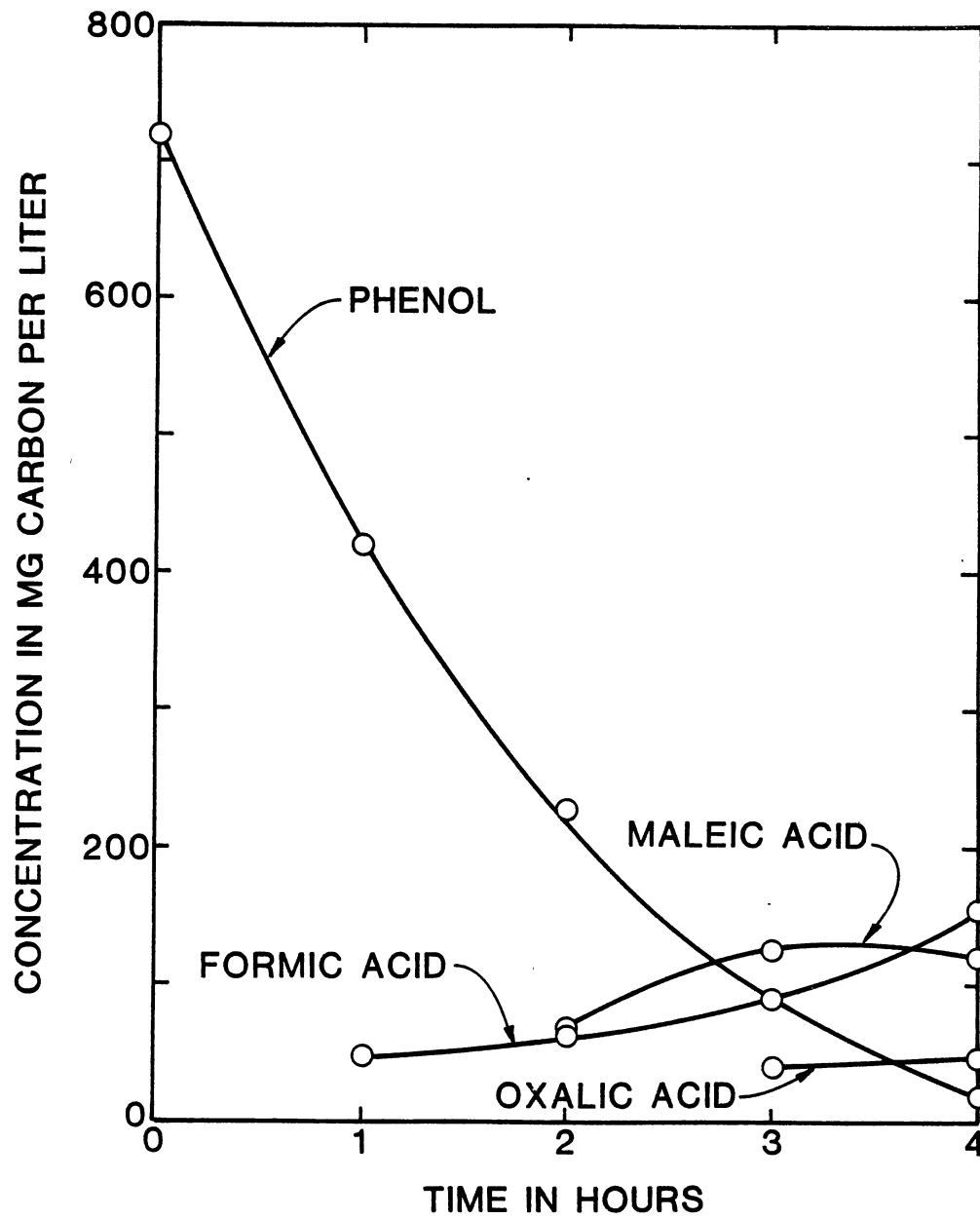
Figure 14.   Concentration With Time for Run 1

TABLE XXV

TENTATIVE IDENTIFICATION OF ISOTACHO-
PHORESIS DATA FOR RUN 2

Sample	Tentative Identification		Relative Peak Height	Peak Width (mm)
1:00	1.	Oxalic Acid	0.1521	4.00
	2.	Formic Acid	0.3119	0.95
	3.	Maleic Acid	0.4150	1.05
2:00	1.	Oxalic Acid	0.1495	4.35
	2.	Formic Acid	0.3085	1.50
	3.	Maleic Acid	0.4124	2.20
3:00	1.	Oxalic Acid	0.1454	7.45
	2.	Unknown #2	0.1747	1.00
	3.	Formic Acid	0.3073	2.50
	4.	Maleic Acid	0.4079	1.45
	5.	Acetic Acid	0.6197	1.15
4:00	1.	Oxalic Acid	0.1458	4.05
	2.	Unknown #2	0.1771	1.35
	3.	Formic Acid	0.3102	3.95
	4.	Acetic Acid	0.6247	1.70
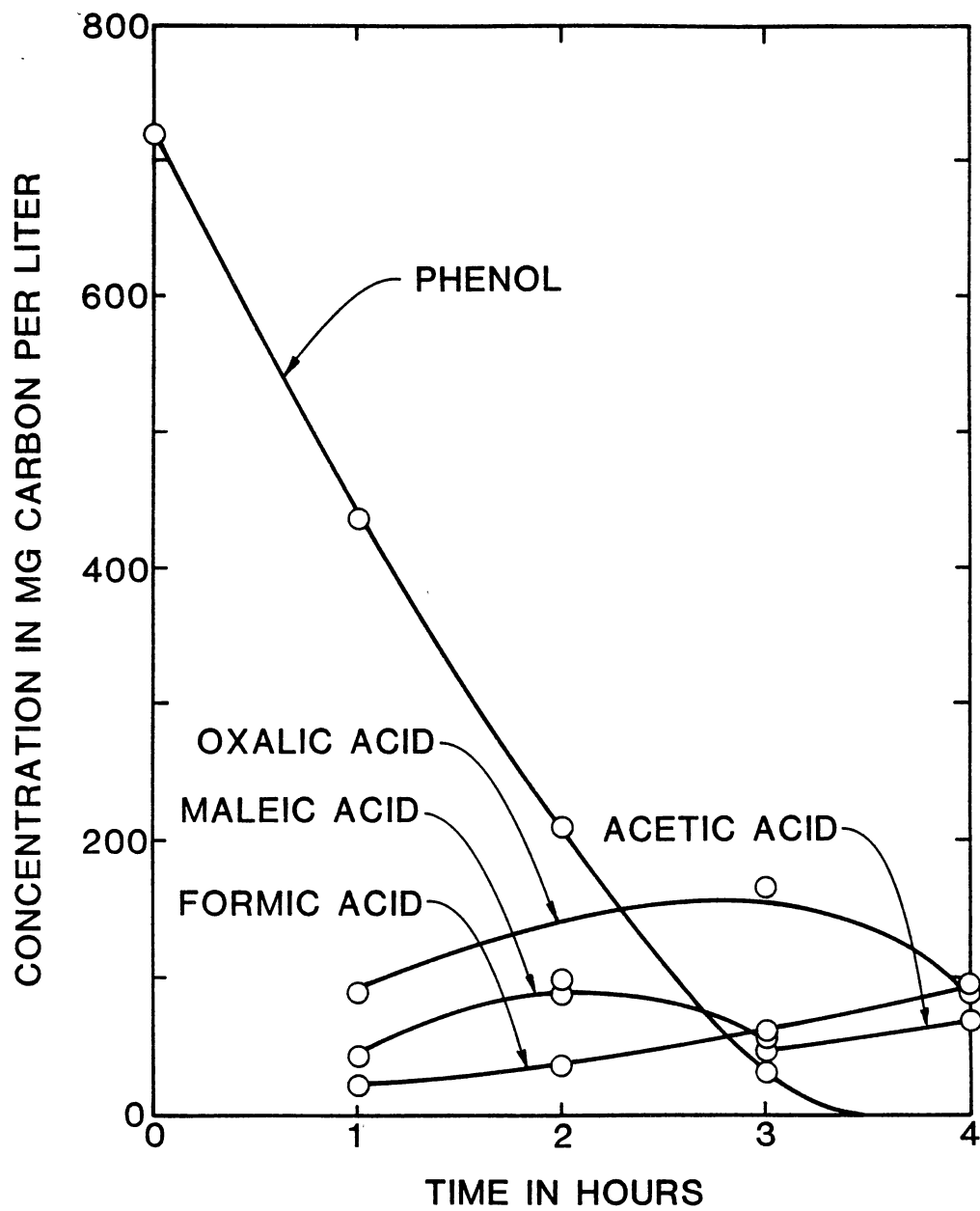
Figure 15. Concentration With Time for Run 2

TABLE XXVI

TENTATIVE IDENTIFICATION OF ISOTACHO-
PHORESIS DATA FOR RUN 3

Sample	Tentative Identification		Relative Peak Height	Peak Width (mm)
1:00	1.	Oxalic Acid	0.1545	1.00
	2.	Formic Acid	0.2816	1.25
	3.	Maleic Acid	0.4008	2.45
2:00	1.	Oxalic Acid	0.1539	1.05
	2.	Formic Acid	0.2830	3.00
	3.	Maleic Acid	0.3849	3.05
3:00	1.	Oxalic Acid	0.1500	1.60
	2.	Formic Acid	0.2939	4.50
	3.	Maleic Acid	0.3889	3.00
	4.	Acetic Acid	0.5789	1.65
4:00	1.	Oxalic Acid	0.1567	2.25
	2.	Formic Acid	0.2993	7.40
	3.	Maleic Acid	0.3891	2.35
	4.	Acetic Acid	0.6295	2.50
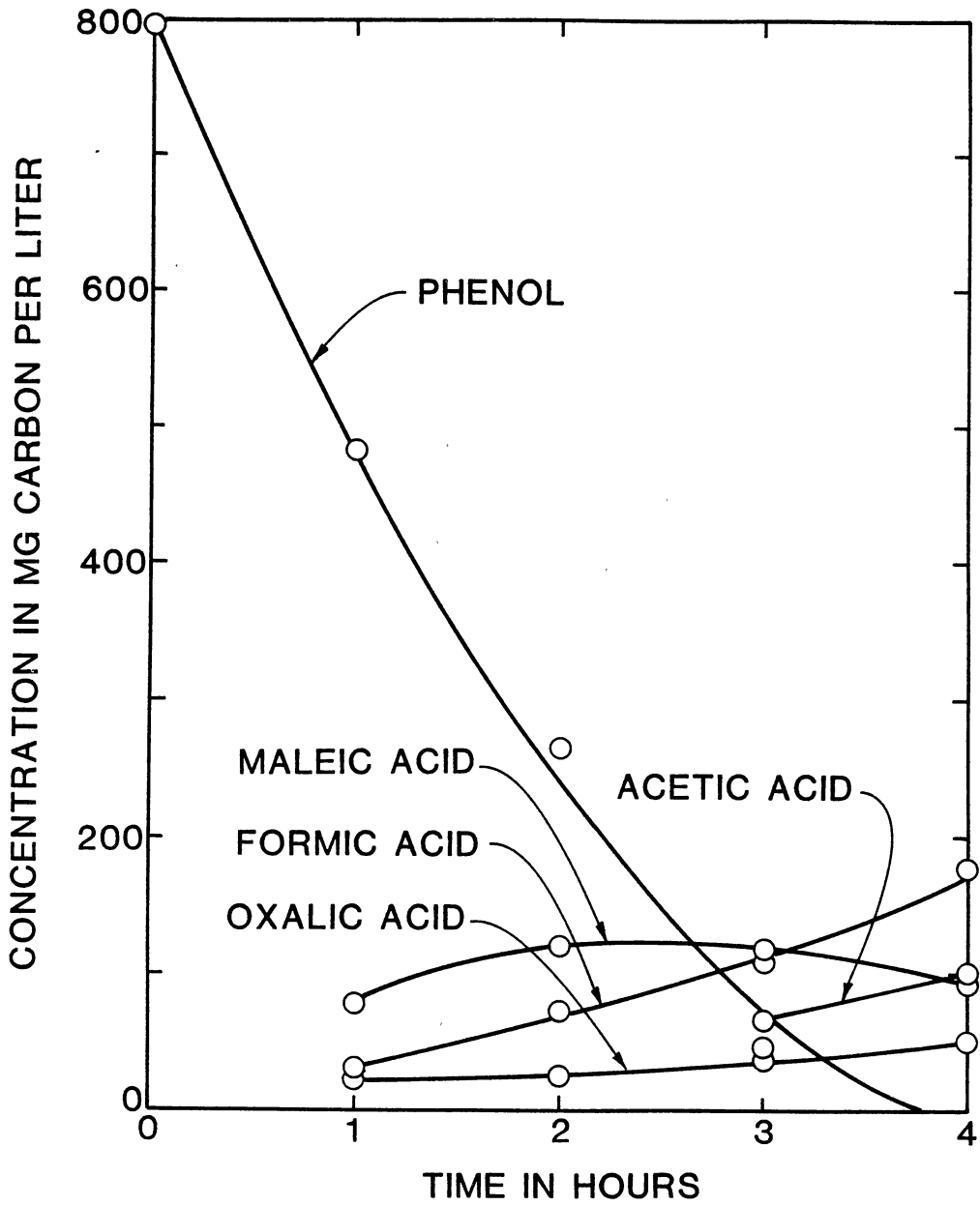
Figure 16. Concentration With Time for Run 3

phase. The mass transfer equation used in performing the calculations is:

$$k_L a = \frac{N_A}{V \, (c_A^* - c_A)_L}$$

(74)

and

$$(c_A^* - c_A)_L = \frac{[(c_{A_2}^* - c_{A_2}) - (c_{A_1}^* - c_{A_1})]}{\ln \frac{(c_{A_2}^* - c_{A_2})}{(c_{A_1}^* - c_{A_1})}}$$

(75)

The value for $k_L a$ is calculated every hour for each run. The volume of the reaction is taken to be an average between the volume at the beginning of the time period and the volume at the middle of the time period. In calculating the milligrams of ozone transferred per hour, N_A, the values for the inlet gas concentration, the offgas concentration, and the gas flowrate are used. Two values for the inlet gas concentration are taken for each run, one at the beginning of the experiment and the other at the end of the experiment. Since the beginning concentration is consistently lower than the ending concentration, it is assumed that the concentration of ozone in the inlet gas increases linearly with time. To calculate the milligrams of ozone transferred during the first hour, the value of the inlet gas concentration at time equal 0.5 hour is calculated and the value of the offgas at 0.5 hour is used. The same method is used to calculate N_A for the second, third, and fourth hours of the experiment. The general equation to calculate the milligrams of ozone transferred is:

$$N_A = ([O_3]_o - [O_3]_f) \, G \qquad (76)$$

where G is the gas flowrate.

Henry's Law equation is used to calculate the equilibrium ozone concentrations, $C_{A_1}^*$ and $C_{A_2}^*$. The equation used in the calculations is:

$$P_{O_3} = M_{O_3} \, K_H \qquad (77)$$

where

K_H = Henry's Law constant in units of atm M^{-1};

M_{O_3} = molar concentration of ozone in the liquid phase; and

P_{O_3} = partial pressure of the ozone in the gas phase.

The value for K_H is found from experiments done by Kosak-Channing and Heiz [23]. In their experiments, the K_H values were measured at temperatures between 5 and 30°C. The following equation was derived from the experimental results:

$$\ln K_H = -2297 \, T^{-1} + 2.659\mu - 6.880 \, \mu T^{-1} + 12.19 \qquad (78)$$

where μ is the molar ionic strength, and T is the temperature in Kelvin. The K_H values used for the calculations had to be extrapolated from the Kosak-Channing and Heiz equation. The K_H values obtained for 65°C, 70°C, and 90°C are 220 atm M^{-1}, 243 atm M^{-1}, and 351 atm M^{-1}, respectively. The values for K_H are also calculated using the Roth and Sullivan correlation [36]. The Roth and Sullivan values are consistently lower than the Kosak-Channing and Heiz values. For example, at 65°C the Roth and Sullivan value is calculated to be 213 atm M^{-1} compared with a value of 220 atm M^{-1} for the Kosak-Channing and Heiz equation.

To calculate the partial pressure of ozone, Raoult's Law is used as shown:

$$p_{O_3} = y_{O_3} P \qquad (79)$$

The mole fraction of ozone is calculated by using the concentration of ozone in the gas phase and converting it to moles/min, and by using the gas flowrate and converting it to moles/min with the ideal gas equation. When these conversions are combined, the equation to calculate the mole fraction is:

$$y_{O_3} = \frac{[O_3] (0.08206) (293)}{48,000} \qquad (80)$$

After calculating the partial pressure of ozone, p_{O_3}, and Henry's Law constant, K_H, the molar concentration of equilibrium ozone in the liquid phase, M_{O_3}, can be calculated using Equation (77). This value is then converted to mg/L which is C_A^*. The only value left to find in order to calculate the mass transfer coefficient in Equation (74) is the concentration of ozone in the main liquid. This is assumed to be zero, since the results of other investigators showed that phenol reacts fast with ozone. A summary of the mass transfer values is listed in Table XXVII. The values of the ozone transferred, volume, and resistance are shown in Appendix C.

The enhancement factor is the ratio of the mass transfer coefficient with chemical reaction and the mass transfer coefficient without chemical reaction. The mass transfer coefficient with chemical reaction and with the interfacial area per unit volume is calculated from Equation (74). To calculate the mass transfer coefficient without chemical reaction, the Hughmark correlation is used [21]. The Hughmark equation is as follows:

TABLE XXVII

SUMMARY OF THE VALUES FOR THE MASS TRANSFER COEFFICIENT

Time (hr)	Run 1 (10/20/82)	Run 2 (1/26/83)	Run 3 (4/1/83)	Run 4 (6/29/83)	Run 5 (7/6/83)	Run 6 (7/13/83)	Run 7 (7/20/83)	Run 8 (8/4/83)	Run 9 (8/8/83)	Run 10 (7/25/83)	Run 11 (7/27/83)	Run 12 (7/30/83)
1	46.3	31.6	39.3	40.8	62.1	53.6	42.6	34.4	44.0	60.1	61.9	72.8
2	60.5	53.1	45.8	54.1	61.6	78.1	54.2	48.8	69.5	85.2	63.8	62.3
3	58.7	57.2	68.6	46.5	64.0	79.9	61.8	72.8	71.1	107.0	105.0	103.5
4	69.6	70.1	70.2	75.8	75.9	81.7	55.7	74.5	72.7	109.3	107.3	106.2

$$Sh = 2 + 0.0187 \ [Re^{0.484} \ Sc^{0.339} \ (d_B \ g^{0.333}/D_{o_3}^{0.667})^{0.072}]^{1.61}$$

(81)

The values of the bubble diameter, the bubble velocity, the liquid viscosity, the density of the liquid, and the diffusivity of ozone are needed to be able to use the Hughmark equation.

The viscosity and density of the liquid are assumed to be that of pure water. To calculate the diffusivity of ozone, the Wilke-Chang correlation in Treybal's book [45] is used. The diffusivity of ozone is calculated at 70°C to be $5.25 \times 10^{-5} \ cm^2/s$, and at 90°C to be 7.12×10^{-5} cm^2/s. The value of the bubble size is estimated to be 2.0 mm by visual inspection.

The value of the bubble slip velocity is calculated from the gas holdup. The following equation is used to calculate the gas holdup:

$$h = \frac{L_f - L_o}{L_f}$$

(82)

where

L_f = the height of liquid in the column when there is recycling and gas bubbling; and

L_o = the height of liquid in the column when there is recycling and no gas bubbling.

The gas holdup is calculated at conditions of 70°C, 110 psia, and 0.01 M acetic acid, and is found to have a value of 0.0342.

The bubble slip velocity is calculated by the following equation:

$$U_s = \frac{G}{h} - \frac{V_{SL}}{1 - h}$$

(83)

where G is the velocity of the gas, and V_{SL} is the velocity of the re-cycle liquid in cocurrent direction. The value for G is assumed to be the average of the measured gas flowrates for all the runs. The value is calculated to be 6.8×10^{-3} ft/s. The value for V_{SL} is calculated during the gas holdup experiment and found to be 0.123 ft/s. From these values and the value calculated for the gas holdup, the bubble slip velocity is calculated to be 0.326 ft/s.

This is enough information to calculate the mass transfer coefficient from the Hughmark equation. The mass transfer coefficient at 70°C is calculated to be .0152 cm/s and at 90°C is calculated to be 0.0187 cm/s. To compare the experimental mass transfer coefficient and the Hughmark mass transfer coefficient, the interfacial area per unit volume is needed. The equation to calculate the interfacial area is:

$$a = \frac{6}{d_B} h \qquad (84)$$

The value for the interfacial area is calculated to be 1.03 cm^2/cm^3.

The value for $k_L a$ without chemical absorption is calculated to be 60.0 hr^{-1} at 70°C and 69.0 hr^{-1} at 90°C. These values are compared with the values in Table XXVII. Some of the values of the mass transfer coefficient with chemical reaction are lower than the calculated values of the mass transfer coefficient without chemical reaction.

The equation to calculate the theoretical enhancement factor for the reaction is:

$$E = \sqrt{1 + M} \qquad (85)$$

and

$$M = \frac{D_A k C_B}{k_L^2} \qquad (86)$$

The values for k_L are the values calculated from the Hughmark equation. The values for the rate constant are extrapolated from Li and Kuo [26] and Hoigné and Bader [19]. Li and Kuo found a rate constant at 70°C to be 20,000 and at 90°C to be 30,000. Hoigné and Bader found a rate constant at 70°C to be 4,300 and at 90°C to be 23,300. The enhancement factor using Li and Kuo's data is calculated to be 9.6 at 70°C and to be 11.0 at 90°C, and using Hoigné and Bader's data is calculated to be 5.5 at 70°C and 11.9 at 90°C.

The theoretical gas holdup value can be calculated by rearranging Equation (83) and using a chart in Govier and Aziz's book [13]. If the value for the gas holdup is small, then Equation (83) can be written as:

$$h = \frac{G}{U_s + V_{SL}} \qquad (87)$$

From Govier and Aziz's chart, the bubble slip velocity can be found from the diameter of the bubble. For a bubble diameter of 2 mm, the slip velocity is found to be 0.9 ft/sec. Using this value and the values for the gas and recycle flowrate, the theoretical gas holdup is calculated to be 0.0088. The bubble rise velocity is based on a temperature of 20°C.

CHAPTER V

DISCUSSION

Stoichiometry

There are four different sets of conditions for runs 1 through 12. The conditions are labeled as: condition 1, no acetic acid and 65°C; condition 2, 0.15 M acetic acid and 70°C; condition 3, 0.01 M acetic acid and 70°C; and condition 4, 0.01 M acetic acid and 90°C. From the data in Tables XIX and XX, an average stoichiometric value is calculated. This is done to try and compare the different conditions. The average stoichiometric values are listed in Tables XXVIII and XXIX. . It is observed that the stoichiometric ratio of moles ozone consumed per mole phenol oxidized is similar at conditions 1 and 4. Conditions 1 and 4 have a better stoichiometric ratio compared with conditions 2 and 3. Condition 1 has the best phenol stoichiometry initially. This is probably because it has the highest initial pH. Toward the end of the experiment as all the pH values decrease, condition 4 has the best phenol stoichiometry. This is probably because it is at the highest temperature. Conditions 2 and 3 have similar stoichiometry throughout the run. Initially, condition 3 has a better phenol stoichiometry. This is probably due to the pH effect. Toward the end of the experiment, when the pH values are approximately the same, condition 2 has the better phenol stoichiometry. This could be caused by the more concentrated acetic acid in condition 2. The acetic acid was found by visual inspection to reduce the

TABLE XXVIII

AVERAGE STOICHIOMETRIC VALUE OF MOLES OZONE
CONSUMED PER MOLE PHENOL OXIDIZED

Time (hr)	Condition 1	Condition 2	Condition 3	Condition 4
1	2.11	2.36	2.31	2.14
2	2.51	2.77	2.73	2.47
3	2.86	3.12	3.13	2.89
4	3.64	3.68	3.78	3.59

TABLE XXIX

AVERAGE STOICHIOMETRIC VALUE OF MG OZONE CONSUMED
PER MG CHANGE IN CHEMICAL OXYGEN DEMAND

Time (hr)	Condition 1	Condition 2	Condition 3	Condition 4
1	1.27	1.88	1.58	1.57
2	1.29	1.48	1.56	1.40
3	1.30	1.41	1.56	1.38
4	1.33	1.37	1.51	1.34

bubble size which increases the mass transfer of ozone. Similar trends as the ones just discussed are found in comparing the stoichiometry of ozone consumed per change in COD. It is concluded that the pH and temperature have a definite effect on the stoichiometry of the reaction.

For the overall reaction, the stoichiometric ratio of ozone consumed per change in chemical oxygen demand has a range of 1.24 to 1.59. Anderson [1] found a stoichiometric ratio of 2 (using a continuous reactor and an initial phenol concentration of 1000 mg/L) when the pH was 6.6 and a stoichiometric ratio of 1 when the pH was 11.4. Niegowski [31] found a stoichiometric ratio of 1.4 when the pH was 12 (initial phenol concentration of 100 mg/L). To explain the pH effects, Hoigné and Bader [18] proposed a two path reaction mechanism where the direct reaction is predominant at low pH and the hydroxyl radical reaction is predominant at high pH. It is possible that each pathway could have a different stoichiometric value. Since the pH values are low in the experiment, the direct reaction is expected to dominate. In comparing the stoichiometric ratios with Anderson's values at a pH of 6.6, the values in this experiment are lower. The stoichiometric values of this experiment compare more closely to the values that Anderson and Niegowski obtained at a high pH. This can be explained by two reasons: the ozone molecules decompose in the aqueous solution at the elevated temperature and pressure forming hydroxyl radicals, thus the reaction pathway is similar to the pathway at a high pH; and/or some of the diatomic oxygen molecules react with the organic compounds, causing the stoichiometric ratio of ozone consumed per change in chemical oxygen demand to decrease.

The overall stoichiometric ratio of moles ozone fed per mole phenol oxidized has a range of 3.4 to 4.0. Bauch et al. [5] and Eisenhauer

[9] had a stoichiometric ratio of 5.5 (initial phenol concentration of 19 mg/L) and 4.0 (initial phenol concentration of 200 mg/L), respectively when 99 percent of the phenol was oxidized and there was no pH adjustment. When Niegowski [31] adjusted the initial pH to 12.3, the stoichiometric ratio was 3.7 at 99 percent phenol reduction. In the present experiment, when the temperature was 90°C and the initial pH was 3.45, the stoichiometric ratio was close to the value of the stoichiometric ratios that other investigators found at the high pH. When the temperature was at 70°C and the initial pH was 3.40, the stoichiometric value was between Eisenhauer's value (no pH adjustment) and Niegowski's value (initial pH 12). The same reasons that are used to explain the improvement in the stoichiometric ratio for chemical oxygen demand are used to explain the improvement of the phenol stoichiometric ratio.

The acetic acid with no phenol experiment, run 13, shows a resistance to oxidation with ozone. Thus in runs 1 through 12, the change in chemical oxygen demand can be attributed mostly to the oxidation of phenol and its intermediate products. In run 14, there was no obvious oxidation of the organics. This concludes that very little of the oxygen is entrained in the initial reaction of phenol oxidation.

The efficiency of the ozone absorption is 99 percent for all four different conditions. For the acetic acid run with no dissolved phenol, the efficiency of the ozone absorption is 60 percent. The efficiency of the ozone absorption from other investigators ranged from 5 to 99 percent. Anderson [1] found a 99 percent efficiency of absorption when the pH was 11.4 but had a 76 percent efficiency when the pH was 7.0. The 99 percent efficiency of his system is probably due to the ozone decomposition at high pH. Bauch et al. [5] obtained a 99 percent efficiency in

their experiments. They had a length to diameter ratio of 20/1 and had an initial phenol concentration of 19 mg/L.

In the present experiment the phenol concentration was around 940 mg/L and the length to diameter ratio was 125/1. The high efficiency in this reaction is probably due to the high concentration of the phenol, the recycle of the liquid (4.9 L/min), the contact time of the ozone, and the pressure of the column.

Isotachophoresis

The analysis of the isotachophoresis data is based on limited experience with the new analytical technique. In making the analysis of the data, the findings of previous investigators had a significant influence in selecting known compounds for comparison with the unknown compounds in the experimental samples. Previous investigators have found muconic acid, muconaldehyde, maleic acid, maleinaldehyde, tartaric acid, propionic acid, glyoxylic acid, acetic acid, glycolic acid, oxalic acid, and formic acid to be reaction products.

In run 1, a total of four different peaks are found in the isotachophoresis data. One peak is found in all the hourly samples and is tentatively identified as formic acid. This peak could also be fumaric acid or tartaric acid, since the potential gradients are very similar and the difference of the three compounds cannot be distinguished by isotachophoresis. The reason for choosing this peak to represent formic acid is from the results of previous investigators. No investigator has determined fumaric acid to be a reaction product and only one investigator [5] has found tartaric acid to be a product and that was in minor concentrations. Formic acid, however, is found to be a major product in

several experiments [4, 24, 44]. In run 1, the peak identified as formic acid is a major product of the reaction.

In the second, third, and fourth hour samples, a peak is tentatively identified as maleic acid. The measured relative peak height is within the range of the relative peak height of pure maleic acid. The concentration of the peak identified as maleic acid reaches a maximum between the third and fourth hour sample and then begins to decline. Baillod et al. [4] found maleic acid as a reaction product that reached a maximum early in the reaction and then declined.

An unknown peak is found in the first and second hour samples. The unknown peak has a relative peak height value between the relative peak heights of maleic acid and acetic acid. There is already a peak identified as maleic acid and if the peak was acetic acid, it would be assumed that the width from peak to peak would increase throughout the reaction, which did not happen. Acetic acid is a two-carbon compound resistant to further oxidation. Therefore, once it initially appears it is not expected to disappear until after much further oxidation. A possible explanation for the unknown peak is that it is muconic acid. Muconic acid is expected to be an initial reaction product which would disappear after a short oxidation time. Muconic acid was also found by Yamamoto et al. [46] when they did analysis of phenol ozonation products by isotachophoresis.

In the third hour sample of run 1, a peak appears with a relative peak height similar to the relative peak height of oxalic acid. In Yamamoto's et al. [46] analysis of the products of phenol ozonation, the oxalic acid did not initially appear and when it was detected it increased slowly in concentration (Figure 2). The peak identified as oxalic

acid varies in concentration similar to the oxalic acid in Yamamoto's experiment.

In run 2, there are two peak heights close to the peak height of oxalic acid. The first peak appears in all four samples of run 2 whereas the second peak appears in only the third and fourth hour samples. The first peak is closer to the realtive peak height of pure oxalic acid. The concentration of the first peak is relatively high in the first hour sample. It reaches a maximum concentration around the third hour sample and then begins to decrease. The way the second peak varies in concentration is similar to the concentration of the peak identified as oxalic acid in run 1 and is also similar to the oxalic concentration in Yamamoto's et al. [46] experiments. In both Yamamoto's et al. [46] and Baillod's et al. [4] experiments, the formic acid concentration reaches a maximum before the oxalic acid concentration. In run 2, the first peak reaches a maximum concentration much earlier than the peak identified as formic acid. If the identification is based on relative peak heights, the first peak would be identified as oxalic acid. If the identification is based on the way the concentration varies with time, the second peak would be identified as oxalic acid. The first peak is tentatively identified as oxalic acid since its relative peak height is so close to that of oxalic acid.

An unidentified peak appears in the third and fourth hour samples of run 2. From the relative peak height it is tentatively identified as acetic acid. The relative peak height of the sample is slightly higher than the relative peak height of the pure acetic acid. As mentioned earlier, when a mixture of acetic acid and gloxylic acid is analyzed by isotachophoresis, only one peak appears. This peak is between the heights

of acetic acid and glyoxylic acid. Thus since the relative peak height of the sample is slightly higher than the relative peak height of acetic acid, the presence of glyoxylic acid could be indicated.

Peaks identified as maleic acid and formic acid are also found in run 2. They follow a pattern similar to the pattern in run 1. The concentration of formic acid increases throughout the reaction and the concentration of maleic acid reaches a maximum and then decreases. The unidentified peak in run 1 is not found in run 2.

In run 3, all peaks are tentatively identified. The maleic acid and formic acid followed a concentration pattern similar to runs 1 and 2. The acetic acid followed a concentration pattern similar to the one found in run 2. The relative peak height of the acetic acid in the fourth hour sample is higher than the relative peak height of pure acetic acid. This could be because glyoxylic acid is a product and influences the peak height. The oxalic acid in run 3 is found in all four samples, similar to the peak identified as oxalic acid in run 2. The concentration of oxalic acid in run 3 never reaches the amount found in run 2 but is similar to the concentrations found in run 1. The oxalic acid concentration in run 3 never reaches a maximum concentration as it did in run 2 but it continues to increase as in run 1. The unknown compounds found in runs 1 and 2 are not found in run 3.

Baillod et al. [4] found that oxalic acid was a major product in phenol ozonation but not in wet air oxidation of phenol. It was also found that acetic acid was a major product in wet air oxidation of phenol but not in phenol ozonation. In this experiment, oxalic acid is one of the major products, indicating the effect of ozonation on the reaction. Acetic acid was tentatively identified toward the latter part of

the reaction. This could indicate the effect that the diatomic oxygen had on the reaction.

The calculated concentrations of the different compounds are a rough approximation. More work on the operating conditions and analytical procedures is needed. Since this is a preliminary investigation, some of the chemicals were not at a high quality. Also, since the peak-to-peak distance is small for measurement by ruler, the accuracy of the measurement is low. The concentrations of formic acid are not known; therefore, a value of 1.4 cm for the width is used for a 1000 mg/L solution of formic acid. This value is an average of the width from the other components measured at 1000 mg/L.

Mass Transfer

Initially, the enhancement factor was going to be calculated using the mass transfer values of the acetic acid run (Table XVII). The mass transfer coefficient of the acetic acid run is assumed to be due to physical absorption only, since very little acetic acid is oxidized. During this run, the calculated dissolved ozone concentration in equilibrium with the gas ozone concentration was found to be less than the measured dissolved ozone concentration. This is a physical impossibility (implying a negative driving force for mass transfer). Either the dissolved ozone gas measurement is too high, the calculated equilibrium concentration is too low, or an interfering oxidant other than ozone is present in solution. Singer and Gurol [42] concluded that the potassium iodide test for dissolved ozone was invalid because of significant interference by some of the ozonation products of phenol.

Investigators have concluded that ozone reacts quickly with phenol. In this experiment with the initial phenol concentration being high, it is not expected that any substantial ozone will be present in the liquid until the phenol concentration goes below 5 mg/L [43]. The dissolved ozone concentration in this experiemnt is observed to be high when the phenol concentration is well above 5 mg/L. This lends support to the conclusion that the dissolved ozone gas measurement is in error. The dissolved ozone is assumed to be zero throughout the entire reaction.

The mass transfer coefficient depends on the driving force, $\overline{(C_A^* - C_A)}_L$, the amount of ozone transferred, N_A, and the volume of the reaction, V. The amount of ozone transferred increases slightly throughout the time of the reaction. This is due in part to the concentration of ozone produced gradually increasing throughout the reaction. The volume decreases during the time of the reaction. The combination of these two variables, the ozone transferred and the reaction volume, causes the mass transfer coefficient to increase approximately 10 percent during the reaction. The variable that had the most effect on the mass transfer coefficient is the driving force. The driving force depends upon the inlet ozone concentration, the outlet ozone concentration, and the dissolved ozone concentration. The dissolved ozone, as mentioned earlier, is assumed to be zero throughout the entire reaction and therefore it did not have an influence on the change of the value of the mass transfer coefficient. The concentration change of the inlet gas is small and had very little influence on the change of the value of the driving force. The percent change of the value of the outlet gas is large. The value ranges from approximately 1.5 to 0.06 mg/L. The range has a large effect on the value of the driving force.

Since the value of the outlet ozone concentration is small, a slight error in measurement affects the value of the mass transfer coefficient. The values of the mass transfer coefficient show a slight randomness, due probably to the sensitivity of the outlet gas measurement, but in general the mass transfer values increase during the experimental runs.

In calculating a theoretical enhancement factor, the data used were extrapolated. In both, Li and Kuo's [26] data and Hoigné and Bader's [19] data, the kinetic values were measured between 5 and 30°C, whereas the values extrapolated to calculate the enhancement factor are at 70°C and 90°C. The graph is an Arrhenius function of temperature versus kinetic rate constant. The Arrhenius equation is accurate over a small temperature range; therefore, the extrapolation of the kinetic values could be in error.

CHAPTER VI

CONCLUSIONS

The following conclusions are made:

1. The value of the stoichiometric ratio for the chemical oxygen demand (mg ozone/mg COD) at temperature 90°C, pressure 655 kPag, pH 3.45, concentration 0.01 M phenol and 0.01 M acetic acid was 1.34. This compares to a value of 2.0 from previous investigators at a pH of 6.6 [1]. The value of the stoichiometric ratio for 99 percent removal of phenol (mole ozone/mole phenol) at the conditions listed above was 3.59. This compares to values of 4.0 and 5.5 for a pH of 6.5 from previous investigators [9, 5]. This concludes that the stoichiometric value for chemical oxygen demand and for phenol oxidation showed a slight improvement when comparing what other investigators found at higher pH but lower temperatures and pressures.

2. The limited experience with isotachophoresis shows this to be a promising analytical technique. The technique to operate the isotachophoresis is simple and there is no pretreatment involved, whereas to analyze the organic acids by chromatography derivatives would have to be made of the acids. More work is required to better understand the different operating conditions and the effect these conditions have on the qualitative and quantitative data.

3. The general trend of the mass transfer coefficient was to increase during the reaction. This is contrary to what was expected. As

phenol oxidizes, it was expected that the mass transfer coefficient would decrease.

4. The gas holdup with liqid reflux (V_{SL} = 0.0375 m/sec) was calculated to be 0.034. The theoretical value without liquid reflux was calculated to be approximately 0.009. This shows that the reflux increased the gas holdup by over 300 percent.

5. The ratio of ozone absorbed per ozone fed was between 97 to 99 percent. This showed a high efficiency of the ozone utilization.

6. The theoretical enhancement factor was higher than the experimental enhancement factor. The theoretical enhancement factor using rate constants from Li and Kuo [26] is 9.6 at 70°C, 756 kPa, and 0.01 M acetic acid; and is 11.0 at 90°C, 756 kPa, and 0.01 M acetic acid. The theoretical enhancement factor using rate constants from Hoigné and Bader [19] is 5.5 at 70°C, 756 kPa, and 0.01 M acetic acid; and is 11.9 at 90°C, 756 kPa, and 0.01 M acetic acid. The experimental enhancement factor ranged from 0.87 to 1.3 at 70°C, 756 kPa, and 0.01 M acetic acid; and ranged from 0.94 to 1.6 at 90°C, 756 kPa, and 0.01 M acetic acid.

A SELECTED BIBLIOGRAPHY

[1] Anderson, G. L. "Ozonation of High Levels of Phenol in Water." AIChE Symposium Series, Vol. 73, No. 166 (1976), pp. 265-271.

[2] Astarita, G. Mass Transfer With Chemical Reactions. Amsterdam: Elsevier Publishing Co., 1967.

[3] Augugliaro, V., and L. Rizzuti. "The pH Dependence of the Ozone Absorption Kinetics in Aqueous Phenol Solutions." Chemical Engineering Science, Vol. 33 (1978), pp. 1441-1447.

[4] Baillod, C. R., B. M. Faith, and O. Masi. "Fate of Specific Pollutants During Wet Oxidation and Ozonation." Environmental Progress, Vol. 1, No. 3 (1982), pp. 217-226.

[5] Bauch, H., H. Buchard, and H. M. Arsovic. "Ozone as an Oxidative Disintegrant for Phenols in Aqueous Solutions." Gesundheits-Ingenieur, Vol. 91, No. 9 (1970), pp. 258-261.

[6] Chen, J. W. "Catalytic Oxidation in Advanced Waste Treatment." AIChE Symposium Series, Vol. 69, No. 129 (1972), pp. 61-69.

[7] Danckwerts, P. V. Gas-Liquid Reactions. New York: McGraw-Hill, Inc., 1970.

[8] Day, D. C., R. R. Hudgins, and P. L. Silveston. "Oxidation of Propionic Acid Solutions." Can. Jour. of Chem. Eng., Vol. 51 (1973), pp. 733-740.

[9] Eisenhauer, H. R. "The Ozonization of Phenolic Wastes." J. Water Poll. Control Fed., Vol. 40, No. 11 (1968), pp. 1887-1899.

[10] Eisenhauer, H. R. "Increased Rate and Efficiency of Phenolic Waste Ozonization." J. Water Poll. Control Fed., Vol. 43, No. 2 (1971), pp. 200-208.

[11] Franson, M. A., ed. Standard Methods for the Examination of Water and Wastewater. 14th ed. Washington, D.C.: American Public Health Association, 1976.

[12] Gould, J. P., and W. J. Weber, Jr. "Oxidation of Phenols by Ozone." J. Water Poll. Control Fed., Vol. 48, No. 1 (1976), pp. 48-60.
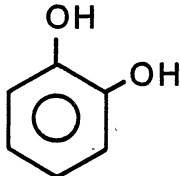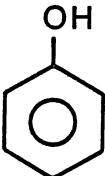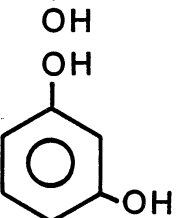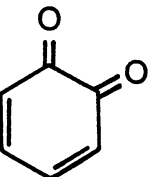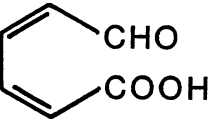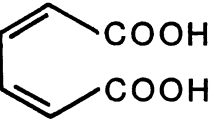
[13] Govier, G. W., and K. Aziz. The Flow of Complex Mixtures in Pipes. New York: Van Nostrand Reinhold Company, 1972.

[14] Hill, A. G., and J. B. Howell. Symposium on Advanced Ozone Technology. Toronto: International Ozone Institute, November, 1977.

[15] Hill, A. G. "Reaction of Ozone With Trace Organics in a Pressurized Bubble Column." (Unpub. Ph.D. dissertation, Louisiana Tech University, 1980.)

[16] Hill, A. G., J. B. Howell, J. Wagner, S. L. Burks, and C. Reece. "Ozone Pretreatment of Refinery Sour Water Stripper Effluent/ Laboratory Feasibility Study." Paper No. 42, presented at the Cleveland AIChE Meeting, Cleveland, Ohio, August 30, 1982.

[17] Himmelblau, D. M. "Solubilities of Inert Gases in Water." J. of Chem. and Eng. Data, Vol. 5, No. 1 (1960), pp. 10-15.

[18] Hoigné, J., and H. Bader. "Ozonation of Water: Selectivity and Rate of Oxidation of Solutes." Ozone: Science and Engineering, Vol. 1, No. 1 (1979), pp. 73-85.

[19] Hoigné, J., and H. Bader. "Rate Constants of Reactions of Ozone With Organic and Inorganic Compounds in Water--I. Non-Dissociating Organic Compounds." Water Res., Vol. 17 (1983), pp. 173-183.

[20] Hoigné, J., and H. Bader. "Rate Constants of Reactions of Ozone With Organic and Inorganic Compounds in Water--II. Dissociating Organic Compounds." Water Res., Vol. 17 (1983), pp. 185-194.

[21] Hughmark, G. A. "Holdup and Mass Transfer in Bubble Columns." I&EC Process Design and Development, Vol. 6, No. 2 (1967), pp. 218-220.

[22] Hurwitz, E., and W. A. Dundas. "Wet Oxidation of Sewage Sludge." J. Water Poll. Control Fed., Vol. 32, No. 9 (1960), pp. 918-929.

[23] Kosak-Channing, L. F., and G. R. Heiz. "Solubility of Ozone in Aqueous Solutions of 0-0.6 M Ionic Strength at 5-30°C." Environ. Sci. Technol., Vol. 17, No. 3 (1983), pp. 145-149.

[24] Kuo, C. H. "Mass Transfer in Ozone Absorption." Environmental Progress, Vol. 1, No. 3 (1982), pp. 189-194.

[25] Legube, B., B. Langlais, B. Sohm, and M. Dore. "Identification of Ozonation Products of Aromatic Hydrocarbon Micropollutants: Effect on Chlorination and Biological Filtration." Ozone: Science and Engineering, Vol. 3, No. 1 (1981), pp. 33-48.

[26] Li, K. Y., and C. H. Kuo. "Absorption and Reactions of Ozone in Phenolic Solutions." AIChE Symposium Series, Vol. 76, No. 197 (1979), pp. 161-168.

[27] Li, K. Y., C. H. Kuo, and J. L. Weeks, Jr. "A Kinetic Study of Ozone-Phenol Reaction in Aqueous Solutions." AIChE Journal, Vol. 25, No. 4 (1979), pp. 583-591.

[28] McPhee, W. T., and A. R. Smith. "From Refinery Wastes to Pure Water." Engineering Bull, Ser. 109, Purdue Univ. Eng. Ext. (1962), pp. 311-326.

[29] Nakayama, S., K. Esaki, K. Namba, Y. Taniguchi, and N. Tabata. "Improved Ozonation in Aqueous Systems." Ozone: Science and Engineering, Vol. 1, No. 2 (1979), pp. 119-132.

[30] Nebel, C., R. D. Gottschling, J. L. Holmes, and P. C. Unangst. Ozone Oxidation of Phenolic Effluents. Philadelphia: Welsbach Ozone Systems Corp., 1975.

[31] Niegowski, S. J. "Destruction of Phenols by Oxidation With Ozone." Industrial and Engineering Chemistry, Vol. 45, No. 3 (1953), pp. 632-634.

[32] Oyeka, S., J. Wallace, A. Alladin, and J. Fernandes. "Controlling Regime in the Ozonation of Aqueous Phenol in a Stirred Tank." Addendum to Proceedings of the Sixth Ozone World Congress, Ruston, La.: Louisiana Tech Univ., 1983.

[33] Peppler, M. L., and G. R. H. Fern. "A Laboratory Study of Ozone of Refinery Phenolic." Oil in Canada, Vol. 11, No. 27 (1959), pp. 84-90.

[34] Pruden, B. B., and H. Le. "Wet Air Oxidation of Soluble Components in Waste Water." Can. J. Chem. Engr., Vol. 54 (1979), pp. 319-324.

[35] Rice, R. G., C. M. Robson, G. W. Miller, and A. G. Hill. "Uses of Ozone in Drinking Water Treatment." AWWA J., Vol. 73, No. 1 (1981), pp. 44-57.

[36] Roth, J. A., and D. E. Sullivan. "Solubility of Ozone in Water." Ind. Eng. Chem. Fundam., Vol. 20, No. 2 (1981), pp. 137-140.

[37] Roustan, M., J. Mallevialle, H. Roques, and J. P. Jones. "Mass Transfer of Ozone to Water: A Fundamental Study." Ozone: Science and Engineering, Vol. 2, No. 4 (1980), pp. 337-344.

[38] Schmidt, L. I. "Liquid-Phase Oxidation of Phenol in Waste Waters at Elevated Temperatures and Pressures." Zhurnal Prikladnor Khimin, Vol. 43, No. 9 (1970), pp. 2123-2126.

[39] Sharifov, R. R., L. A. Mamediorova, and E. V. Shults. "Treatment of Wastewater Containing Petroleum Products." *Azer. Neft. Khoz.*, Vol. 53, No. 4 (1973), pp. 36-38.

[40] Shibaeva, L. V., D. I. Metelitsa, and E. T. Denisov. "Oxidation of Phenol With Molecular Oxygen in Aqueous Solutions--I. The Kinetics of the Oxidation of Phenol With Oxygen." *Kenet. Catal.*, Vol. 10, No. 5 (1969), pp. 832-836.

[41] Shimadzu Scientific Instruments, Inc. *Basic Isotachophoresis.* Columbia, Md.: Shimadzu, n.d.

[42] Singer, P. C., and M. D. Gurol. "Dynamics of the Ozonation of Phenol--I. Experimental Observations." *Water Res.*, Vol. 17, No. 9 (1983), pp. 1163-1171.

[43] Singer, P. C., and M. D. Gurol. "Dynamics of Ozonation of Phenol --II. Mathematical Simulation." *Water Res.*, Vol. 17, No. 9 (1983), pp. 1173-1181.

[44] Teletzke, G. H. "Wet Air Oxidation." *Chemical Engineering Progress*, Vol. 60, No. 1 (1964), pp. 33-38.

[45] Treybal, R. E. *Mass-Transfer Operations.* 2nd ed. New York: McGraw-Hill Book Co., Inc., 1968.

[46] Yamamoto, Y., E. Niki, H. Shiokawa, and Y. Kamiya. "Ozonation of Organic Compounds--2. Ozonation of Phenol in Water." *Jour. Org. Chem.*, Vol. 44, No. 13 (1979), pp. 2137-2142.

APPENDIX A

CHEMICAL STRUCTURES OF REACTION PRODUCTS

1. PHENOL

2. CATEHOL

3. HYDROQUINONE

4. RESORCINAL

5. O-QUINONE

6. MUCONALDEHYDE

7. MUCONIC ACID

8. MALEINALDEHYDE

$HOOC-CH=CH-C\diagdown_{H}^{O}$

9. MALEIC ACID

$HOOC-CH=CH-COOH$

10. TARTARIC ACID

$$\begin{matrix} & OH & OH & \\ & | & | & \\ HOOC- & CH- & CH- & COOH \end{matrix}$$

11. FUMARIC ACID

$$\begin{matrix} & & H & & & \\ & & | & & & \\ HO-C- & C & = & C- & C-OH \\ \| & & & | & & \| \\ O & & & H & & O \end{matrix}$$

12. PROPIONIC ACID

$$\begin{matrix} HO-C- & CH_2- & CH_3 \\ \| & & \\ O & & \end{matrix}$$

14. CETAMALONIC ACID

$$\begin{matrix} HOOC- & C- & COOH \\ & \| & \\ & O & \end{matrix}$$

15. ACETIC ACID

$$\begin{matrix} HO-C- & CH_3 \\ \| & \\ O & \end{matrix}$$

16. GLYOXAL

$$\begin{matrix} & O \\ & \| \\ HC- & C-H \\ \| & \\ O & \end{matrix}$$

17. GLYOXYLIC ACID

$$\begin{matrix} & O \\ & \| \\ HO-C- & C-H \\ \| & \\ O & \end{matrix}$$

18. OXALIC ACID

$$\begin{matrix} & O \\ & \| \\ HO-C- & C-OH \\ \| & \\ O & \end{matrix}$$

19. FORMIC ACID

$$\begin{matrix} H-C-OH \\ \| \\ O \end{matrix}$$

APPENDIX B

ISOTACHOPHEROGRAMS
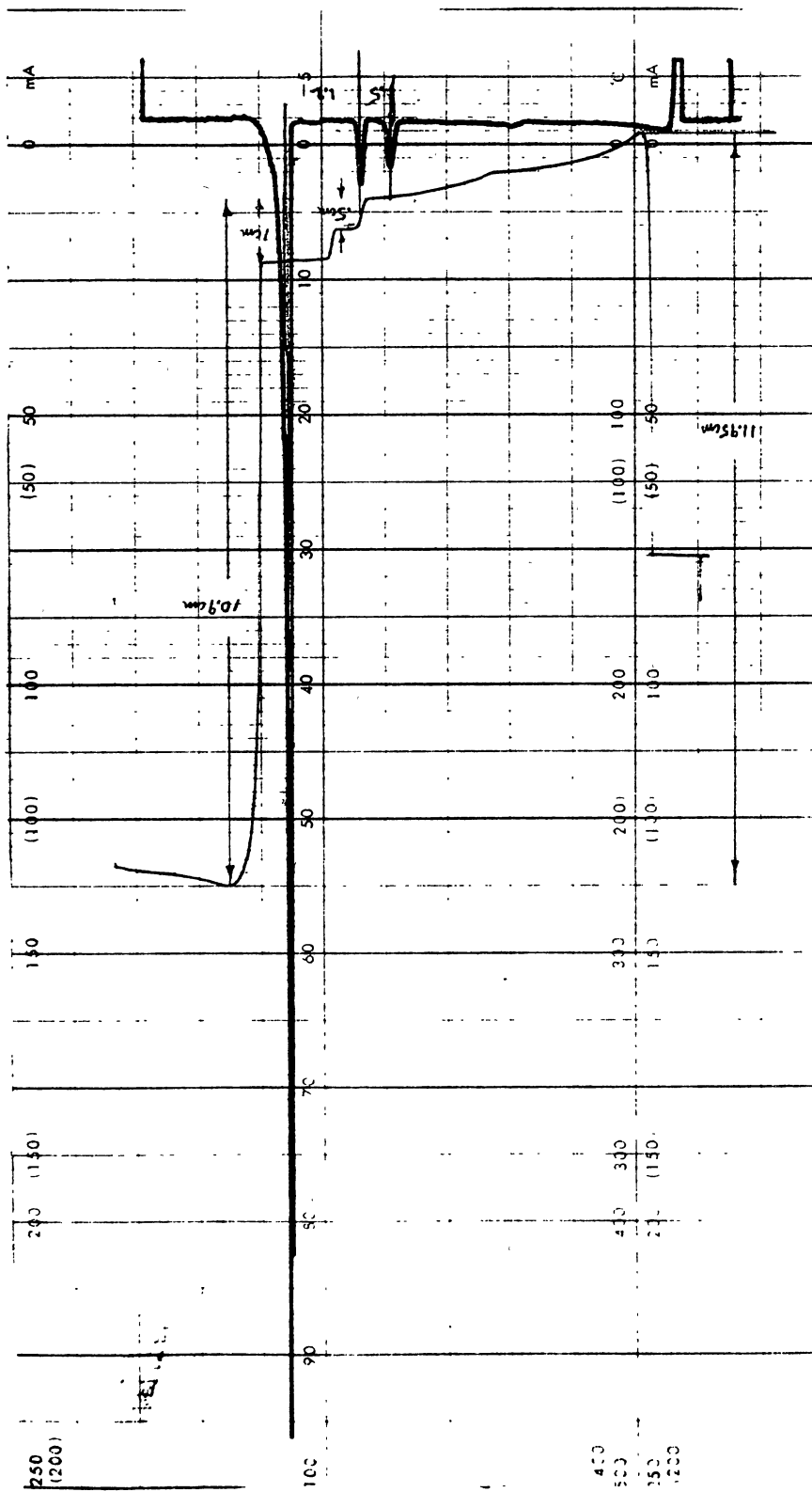
Oxalic acid, 1000 mg/L.
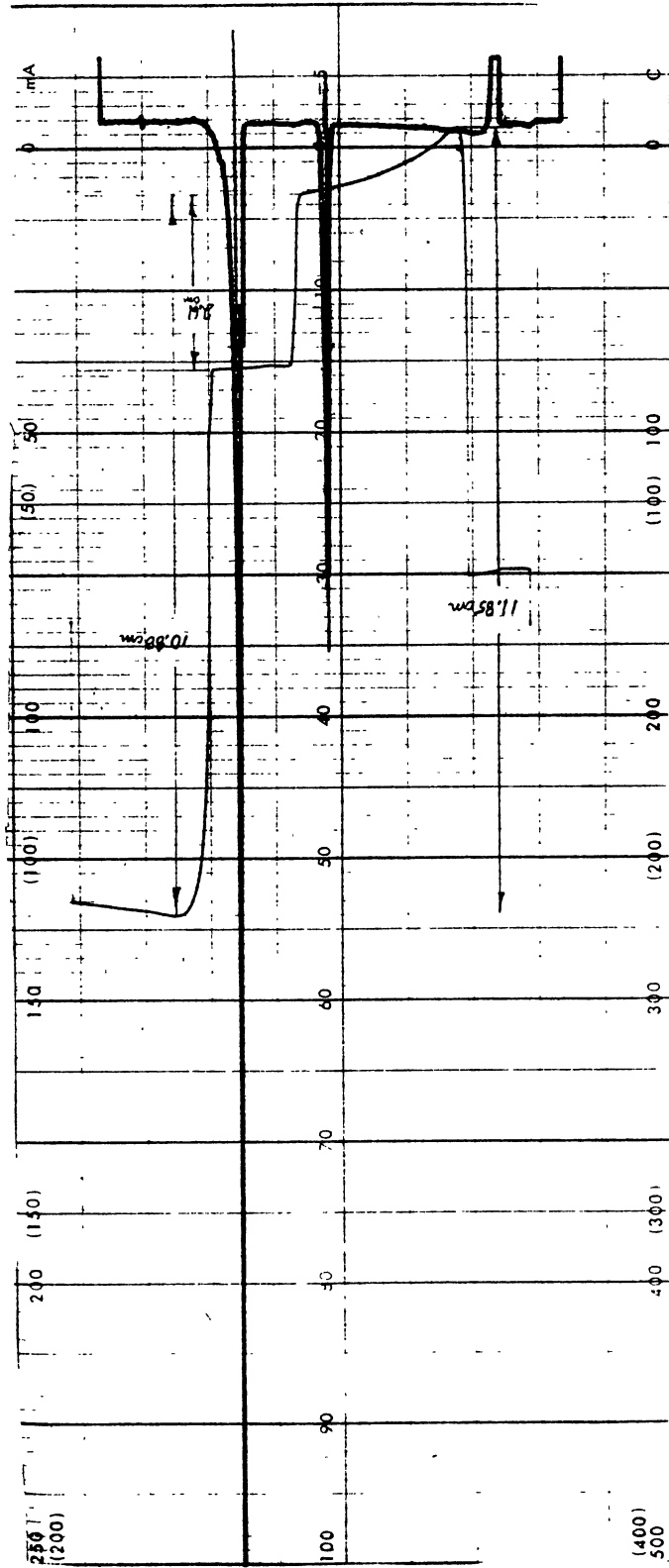
Tartaric acid, 1000 mg/L.

mA

3.58mm
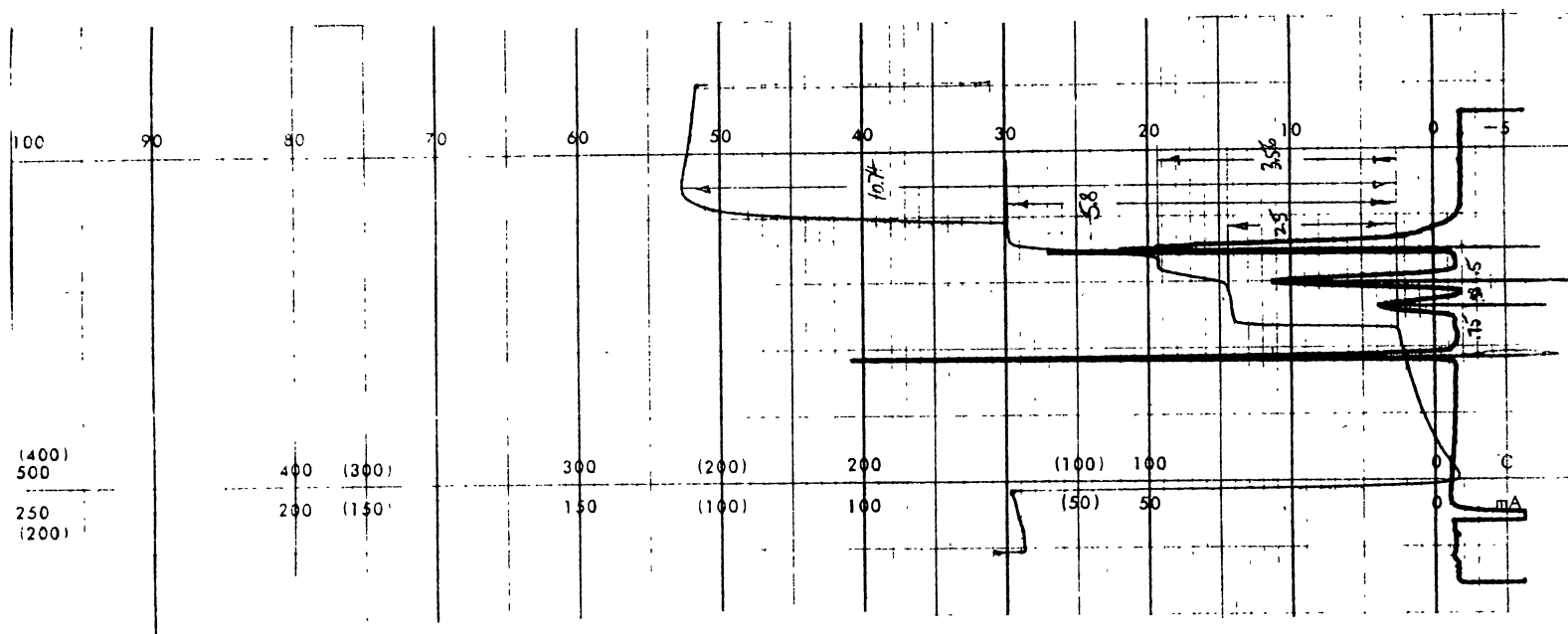
10.87mm

7.4mm

11.80mm
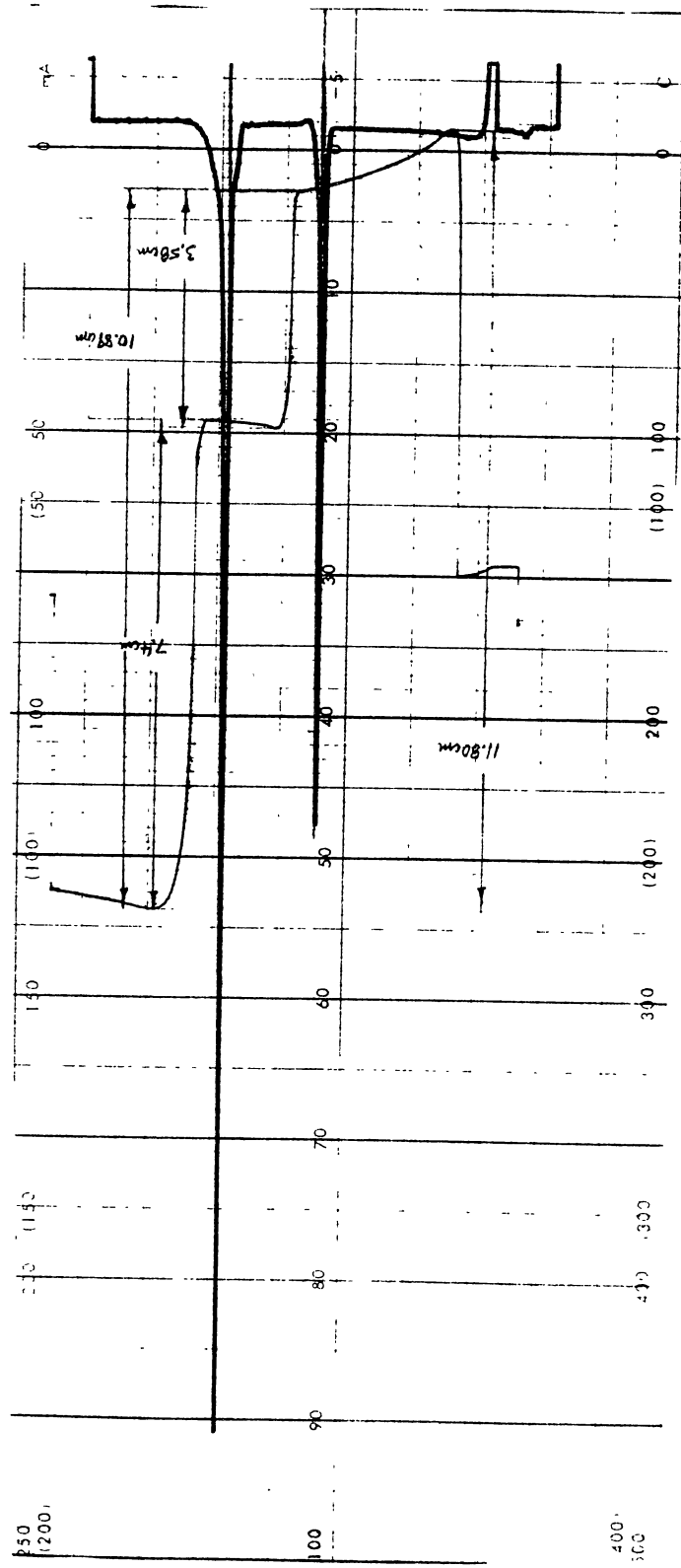
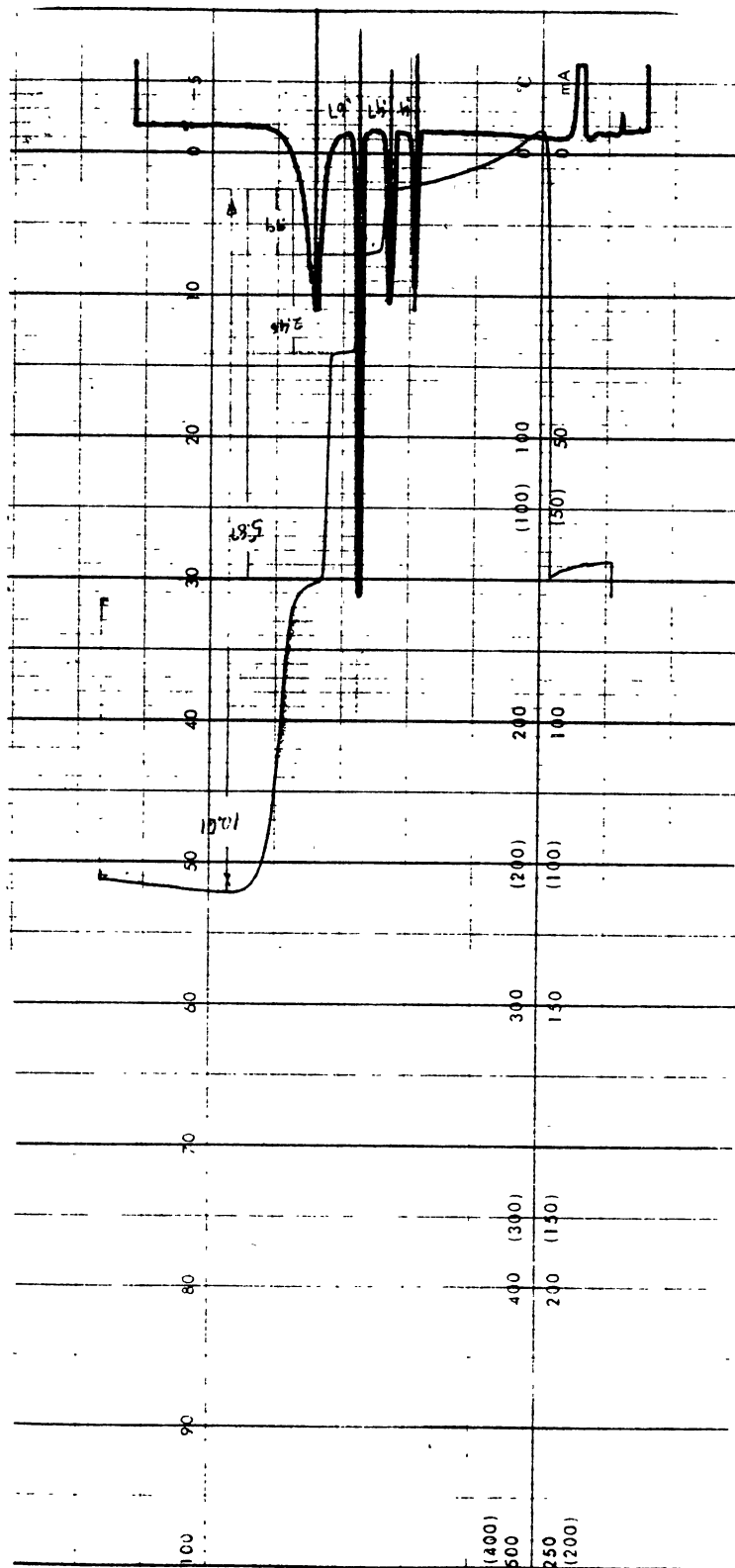Malaic acid, 1000 mg/L.
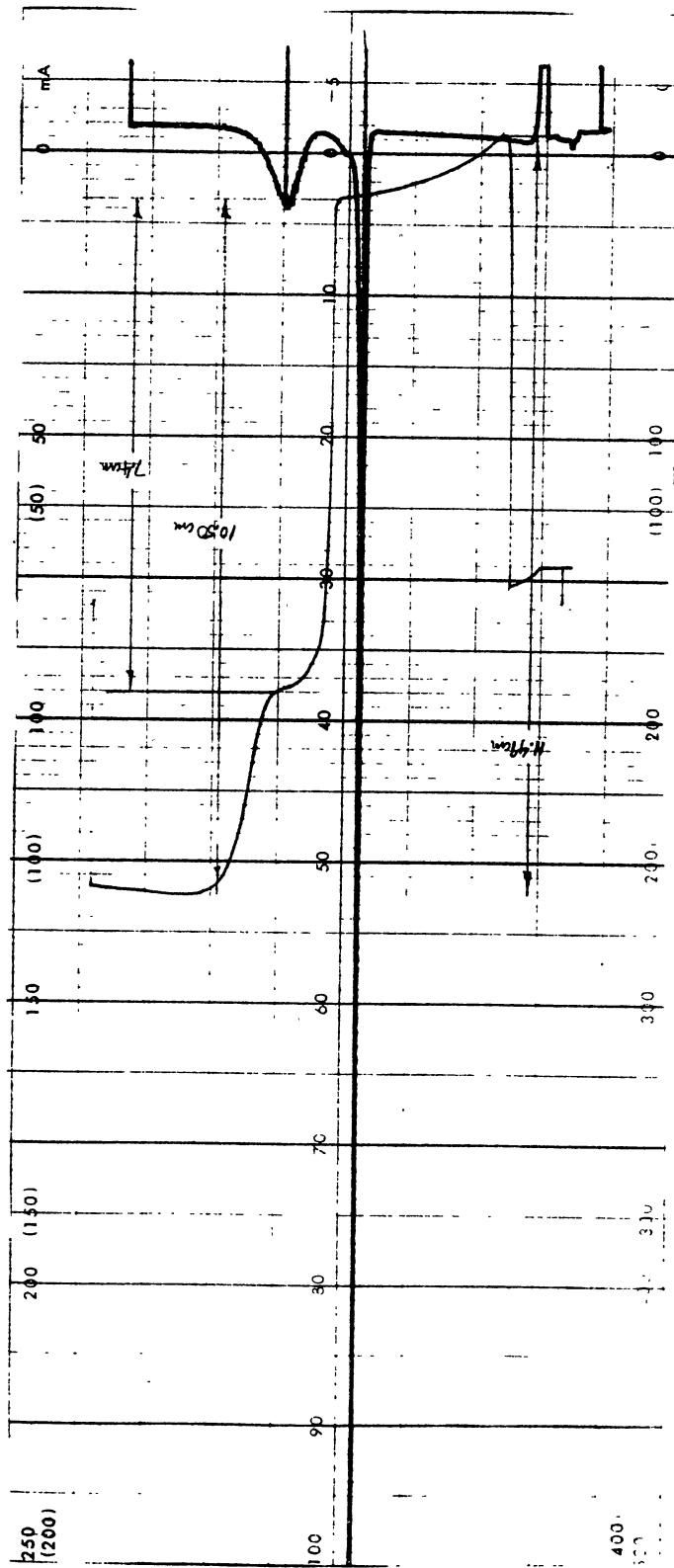
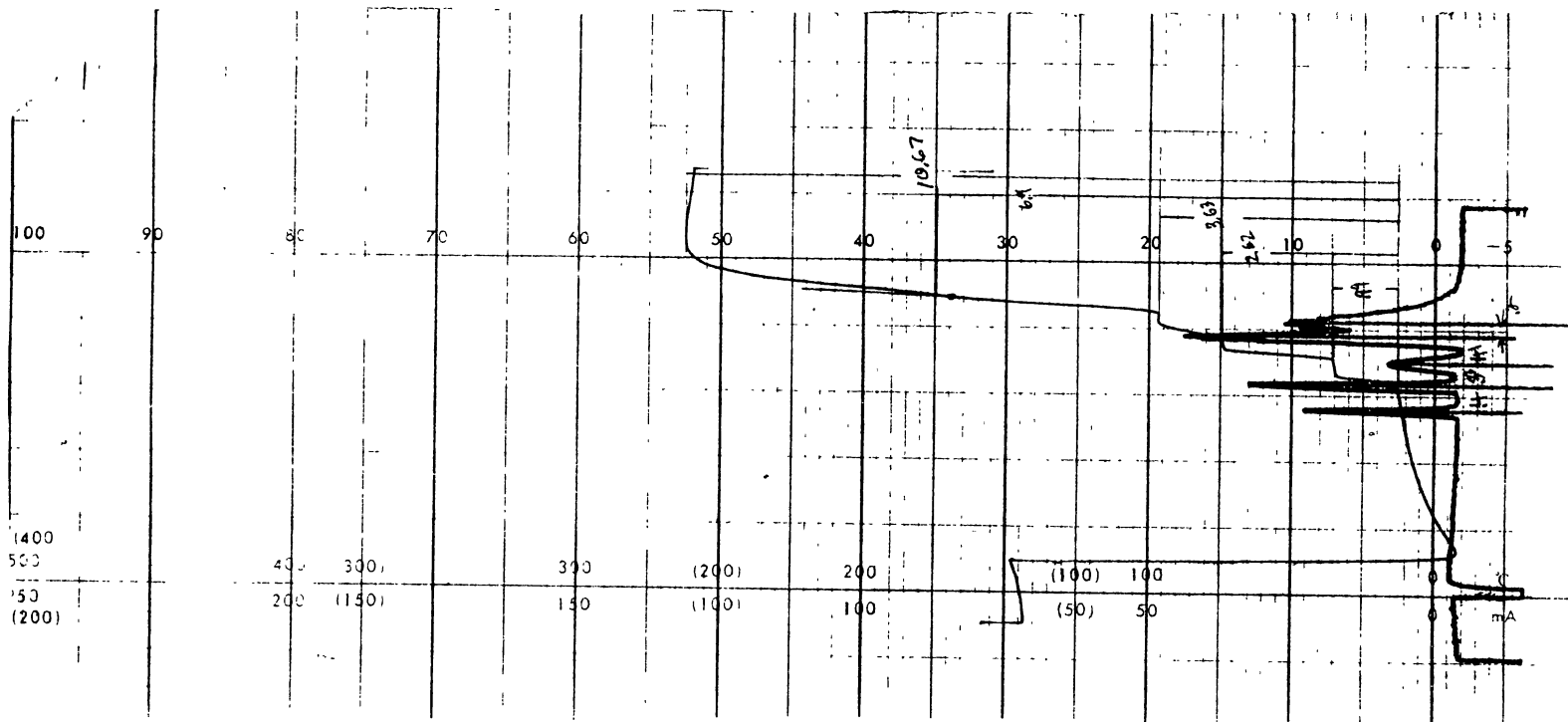Glyoxylic acid, 1000 mg/L.
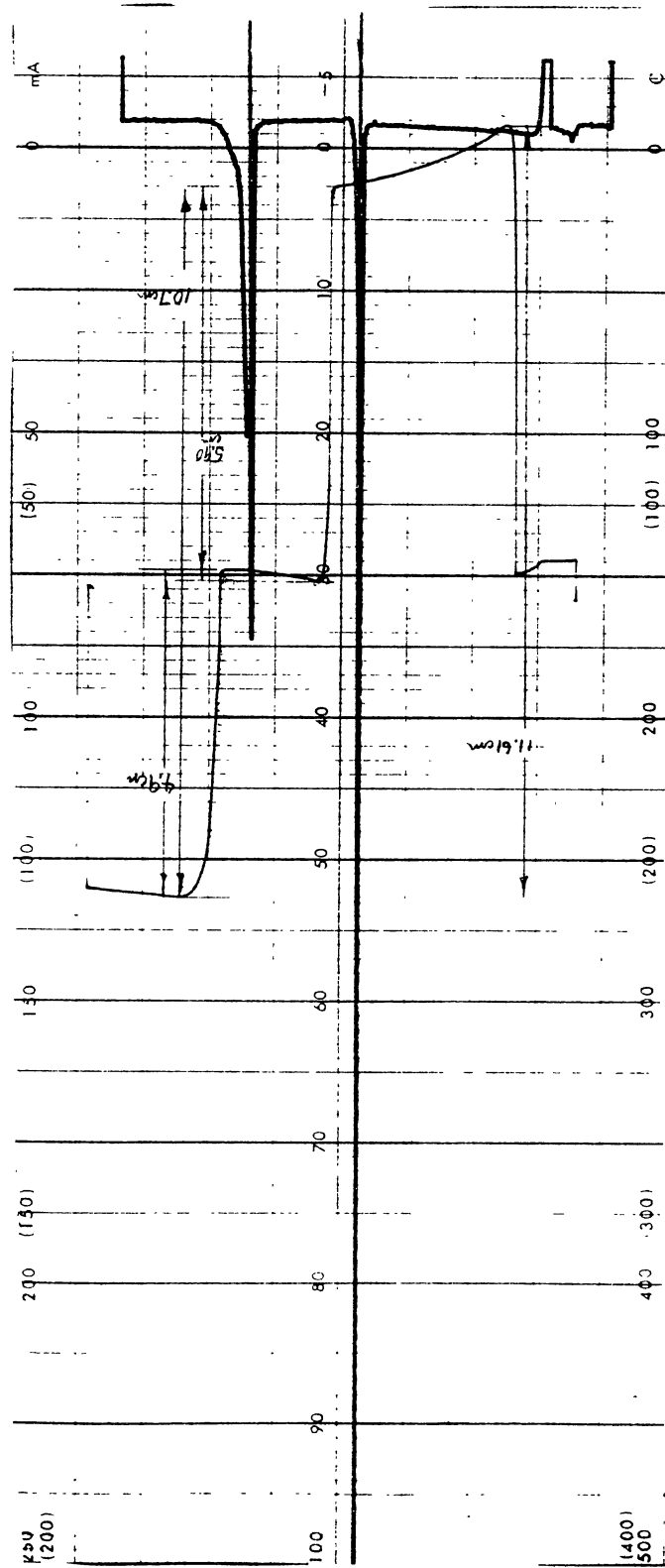
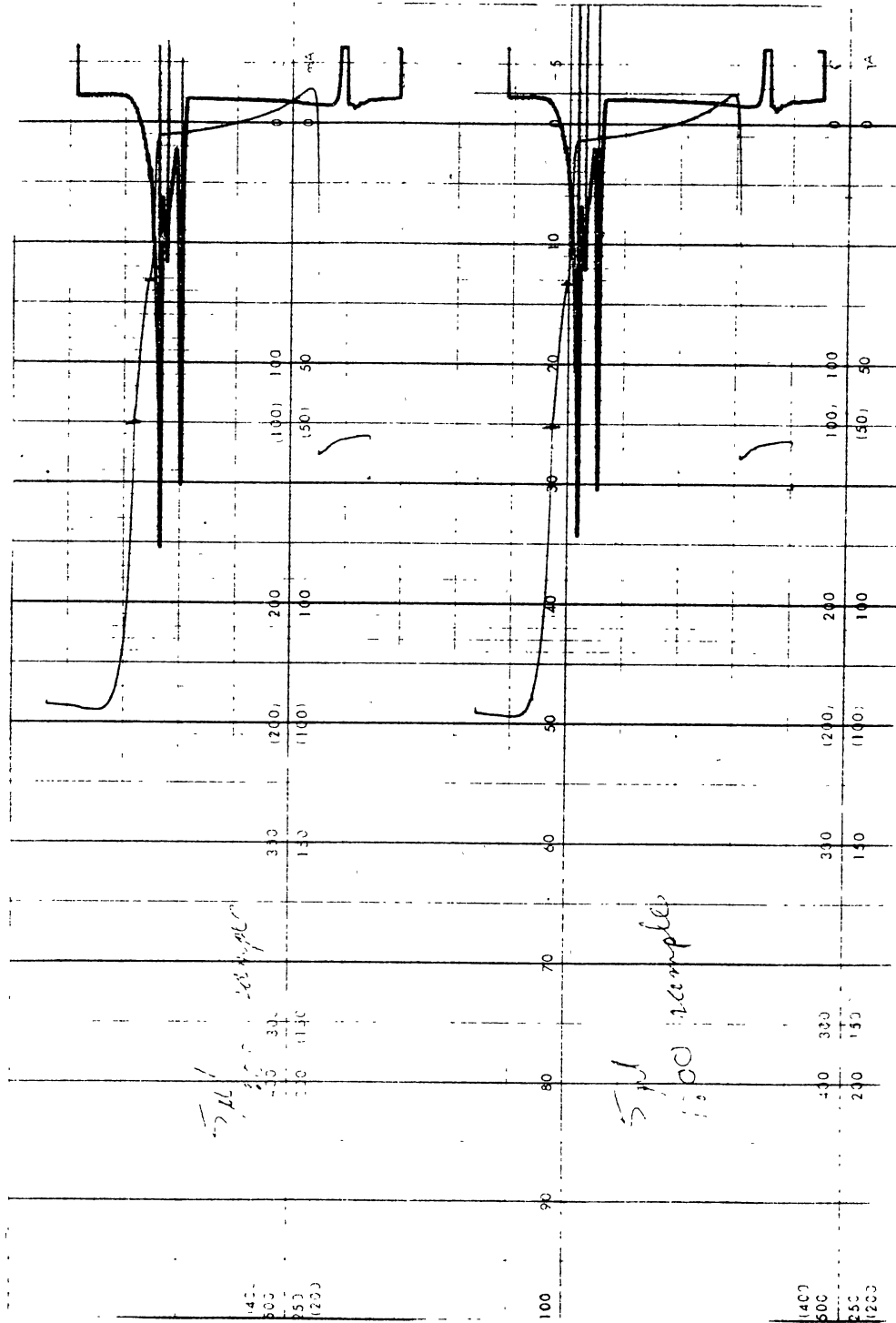Acetic acid, 1000 mg/L.
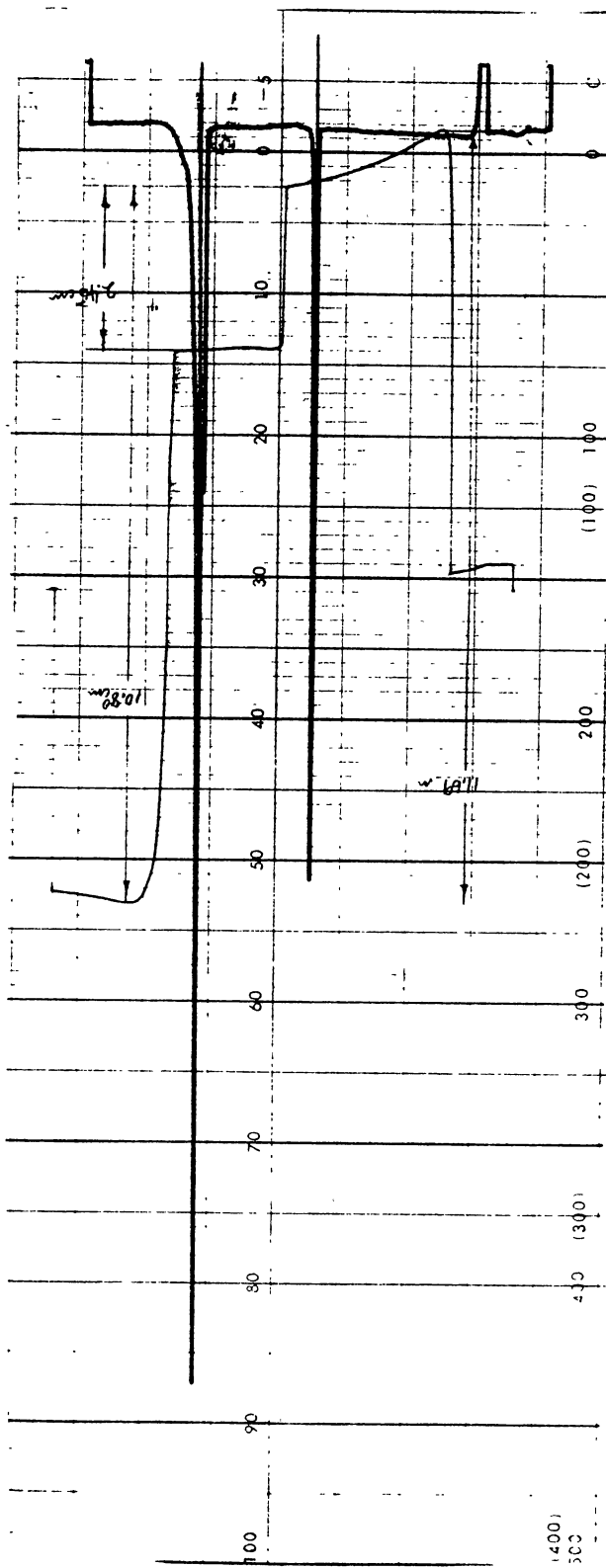
Fumaric acid, 1000 mg/L.

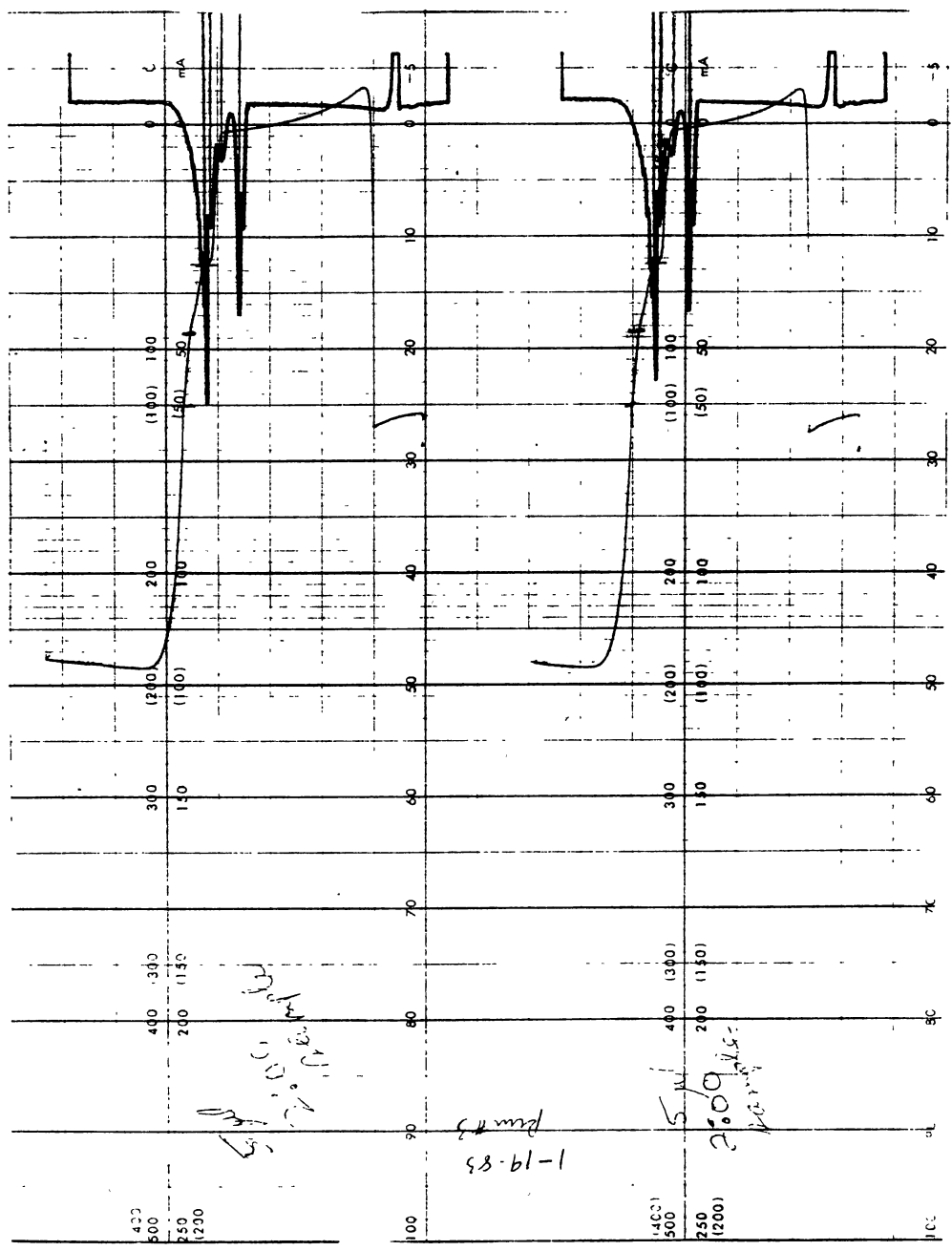Acetic acid, maleic acid, tartaric acid, and fumaric acid, 250 mg/L each.

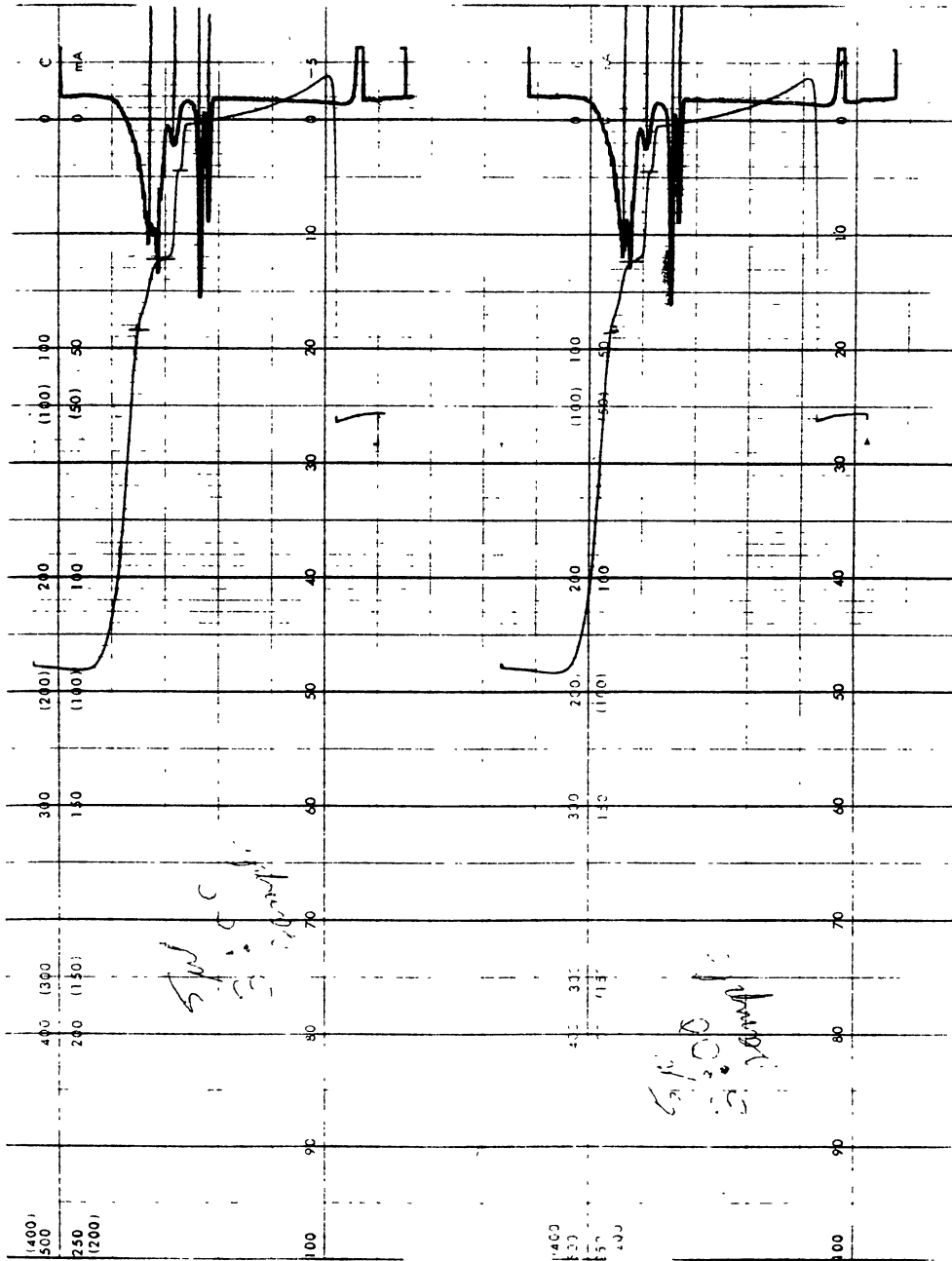Fumaric acid, acetic acid, glyoxylic acid, and oxalic acid, 250 mg/L each.

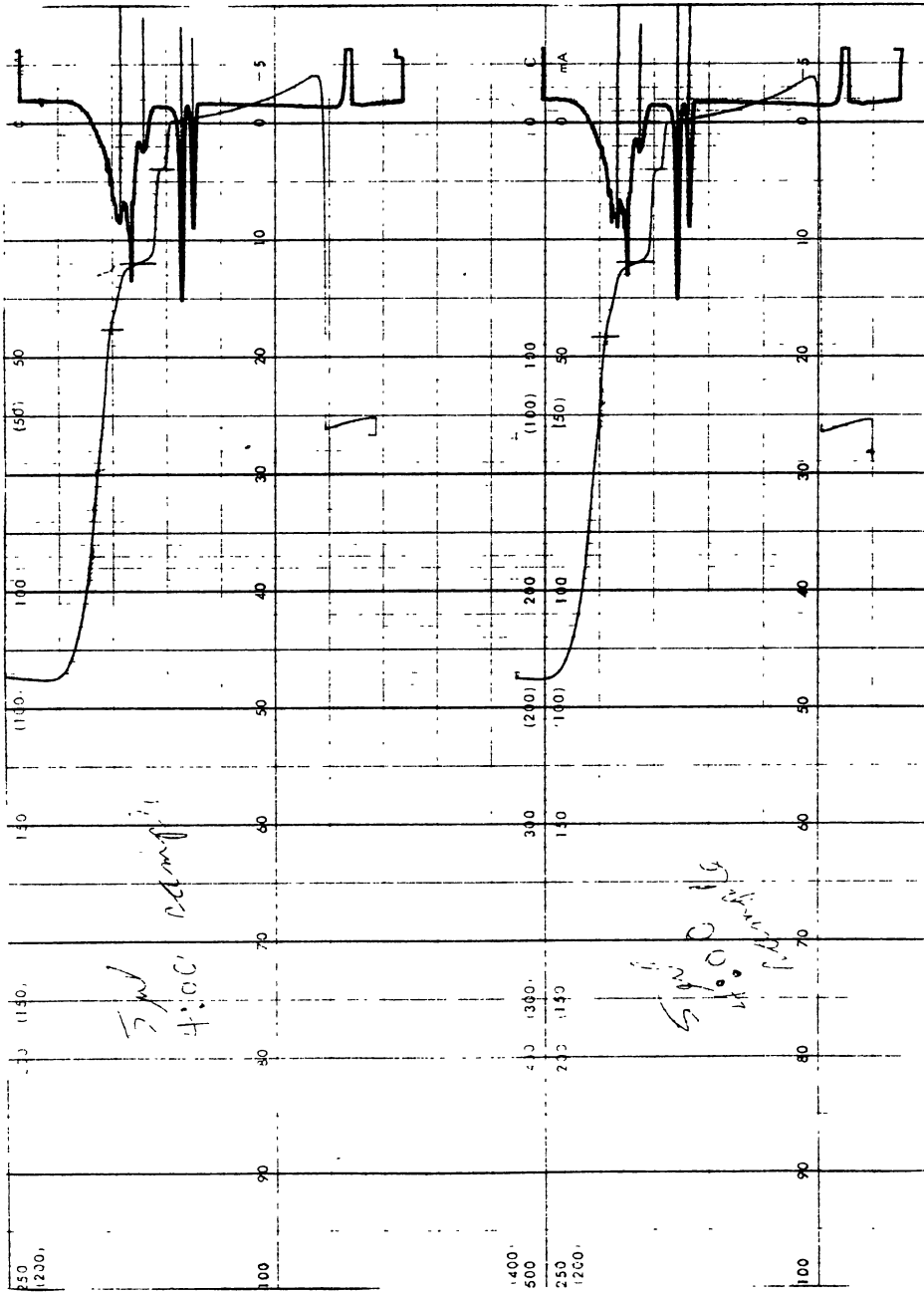Glyoxylic acid, tartaric acid, oxalic acid, and maleic acid, 250 mg/L each.
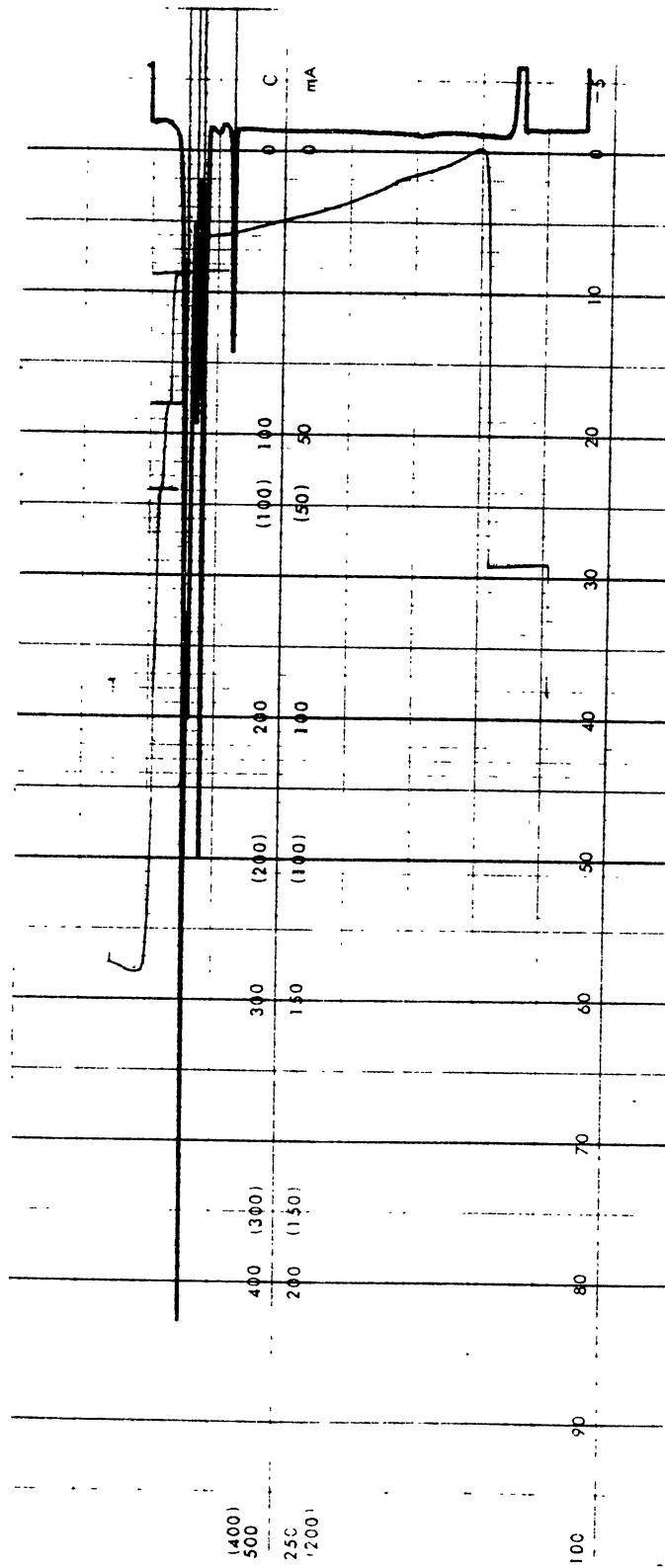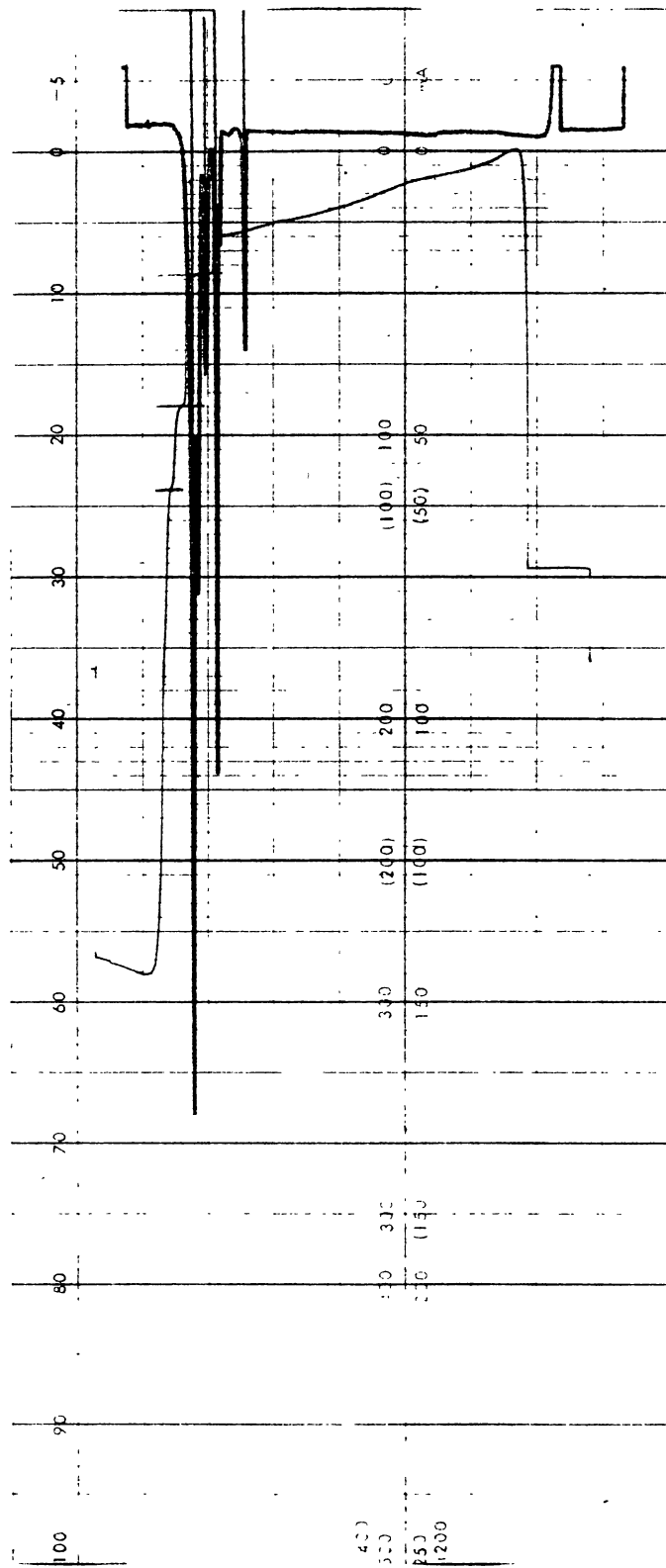
Run 1, 1st hour sample.

Run 1, 2nd hour sample.

Run 1, 3rd hour sample.

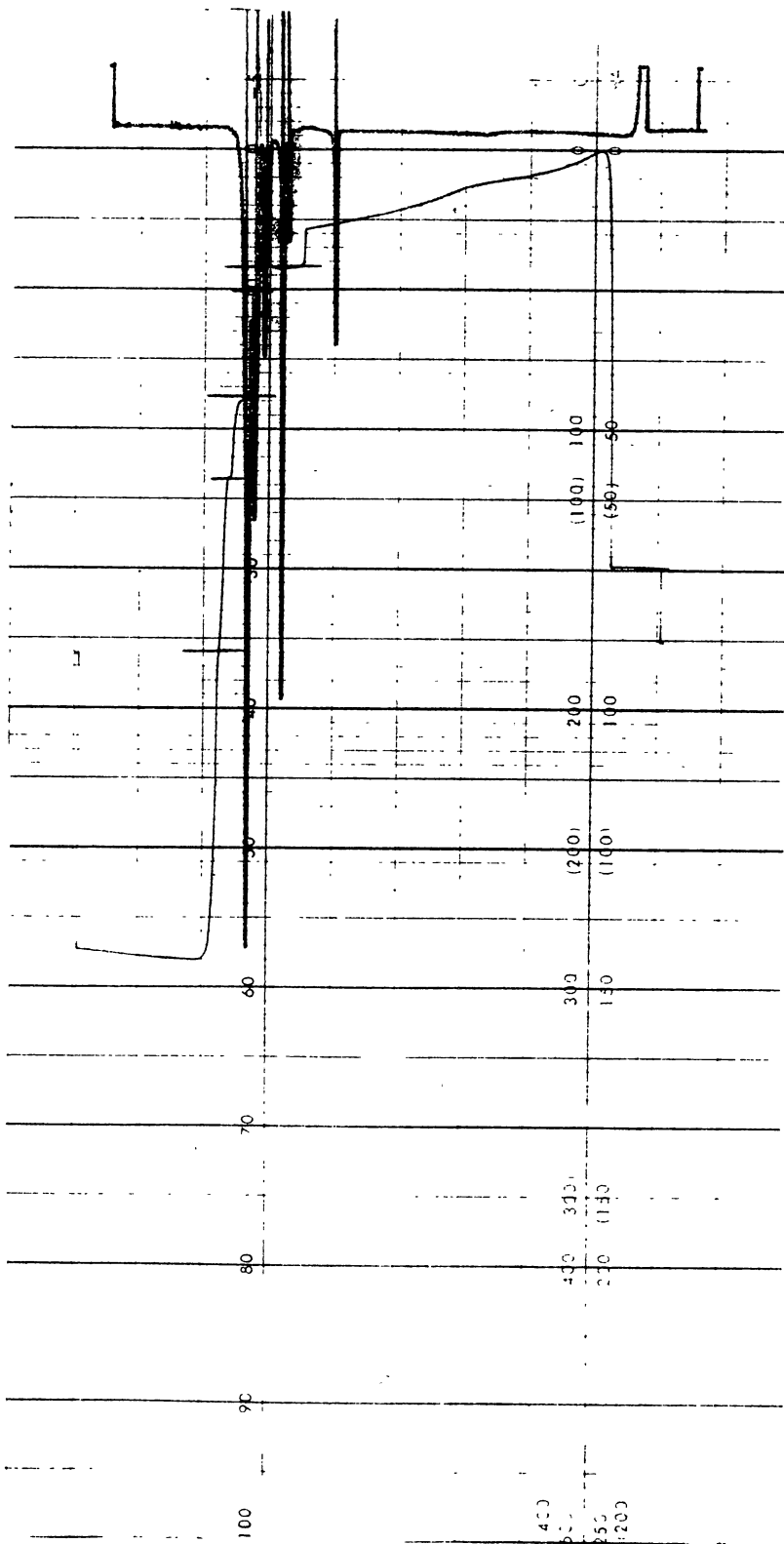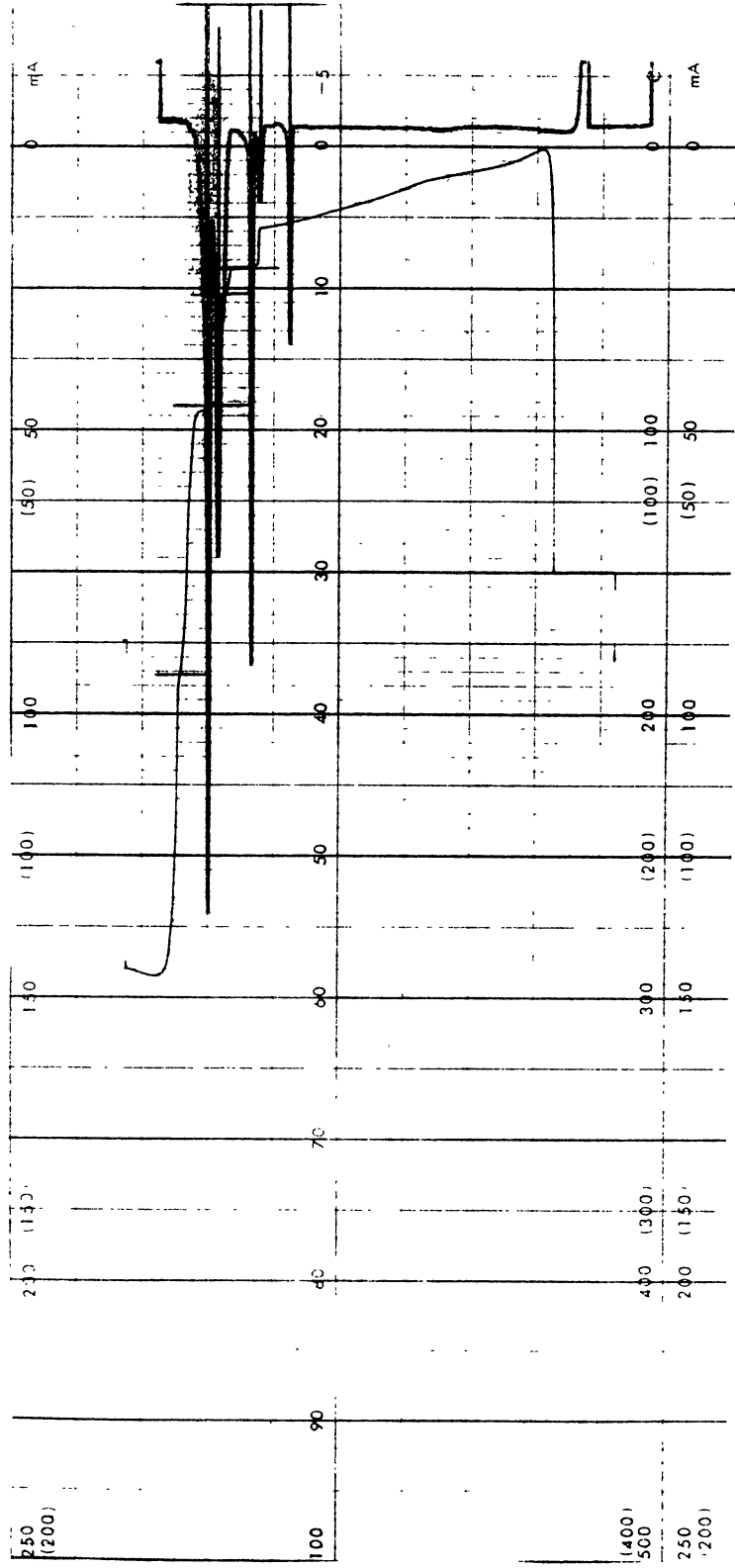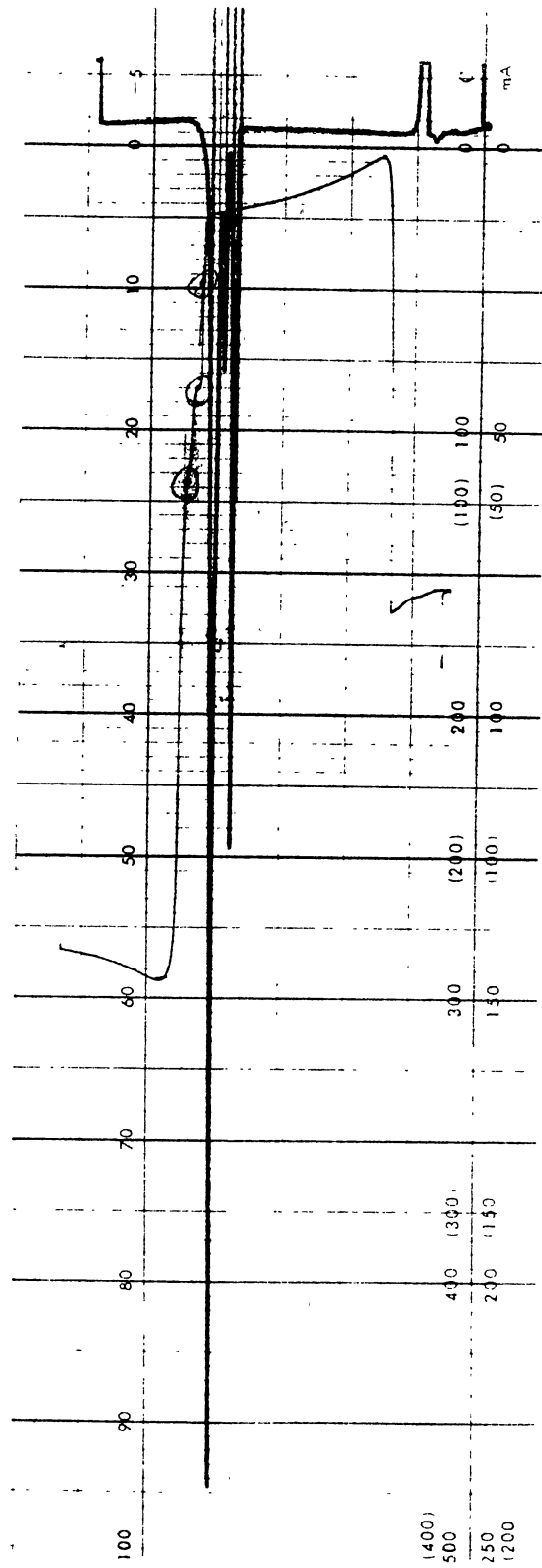Run 1, 4th hour sample.

Run 2, 1st hour sample.

Run 2, 2nd hour sample.

132

Run 2, 3rd hour sample.

Run 2, 4th hour sample.

Run 3, 1st hour sample.
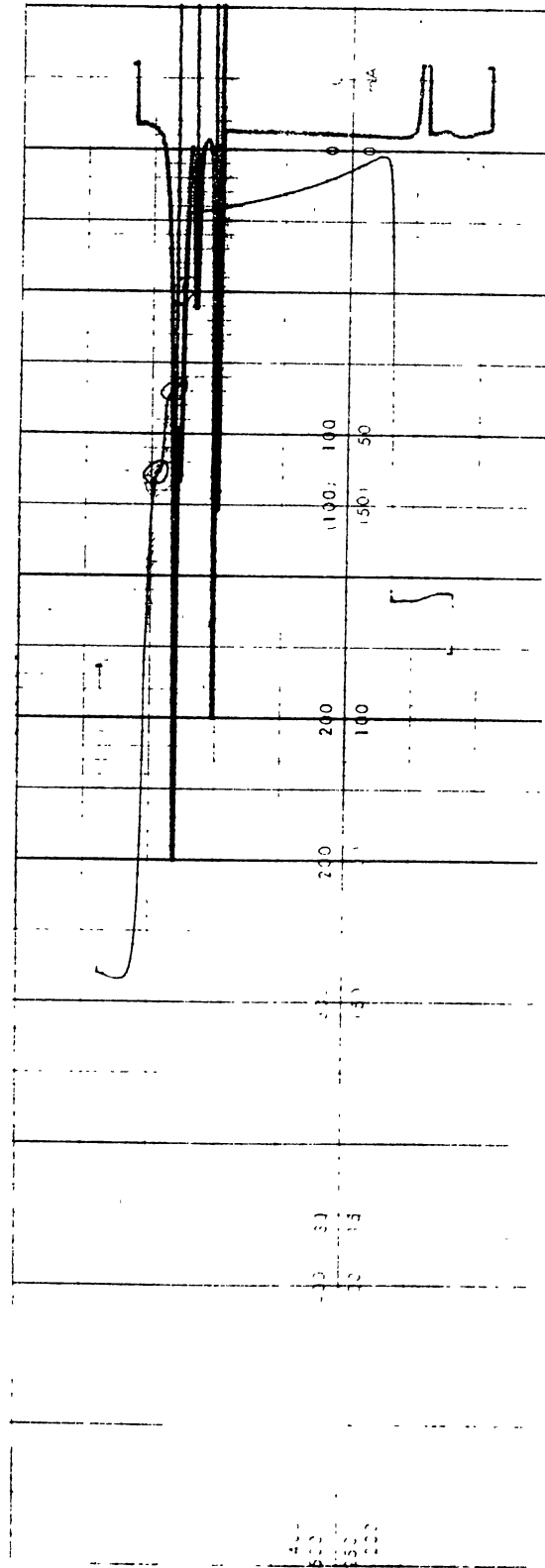
Run 3, 2nd hour sample.
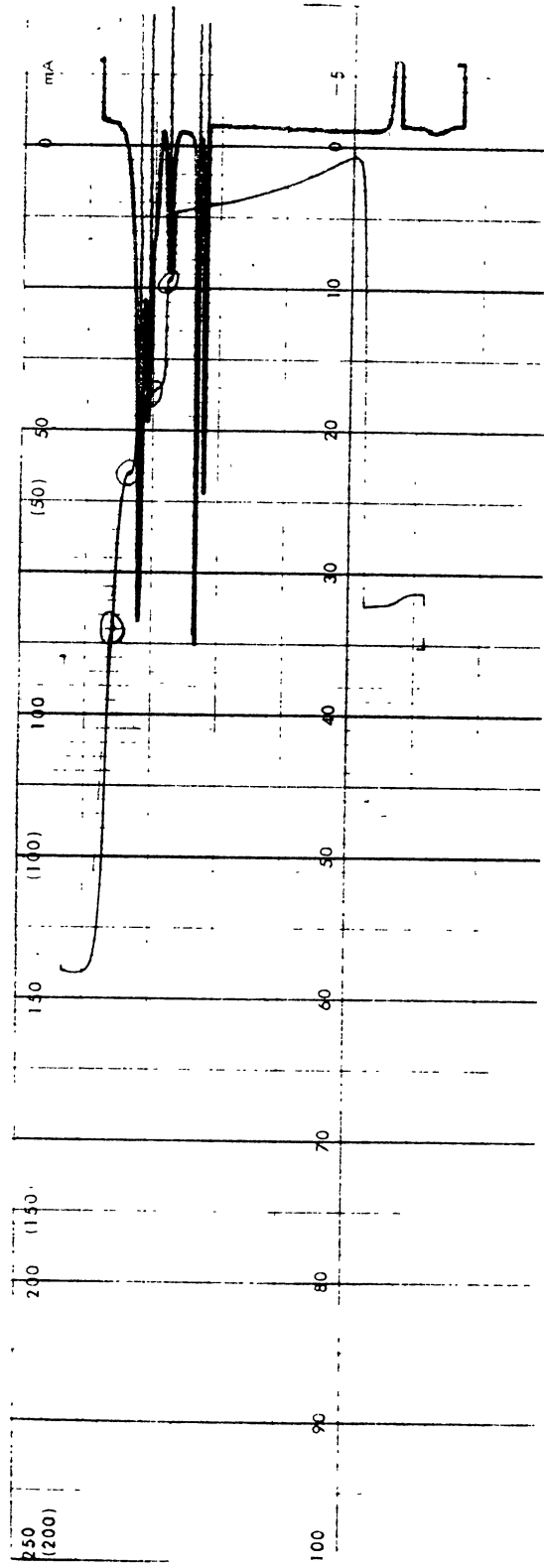
Run 3, 3rd hour sample.
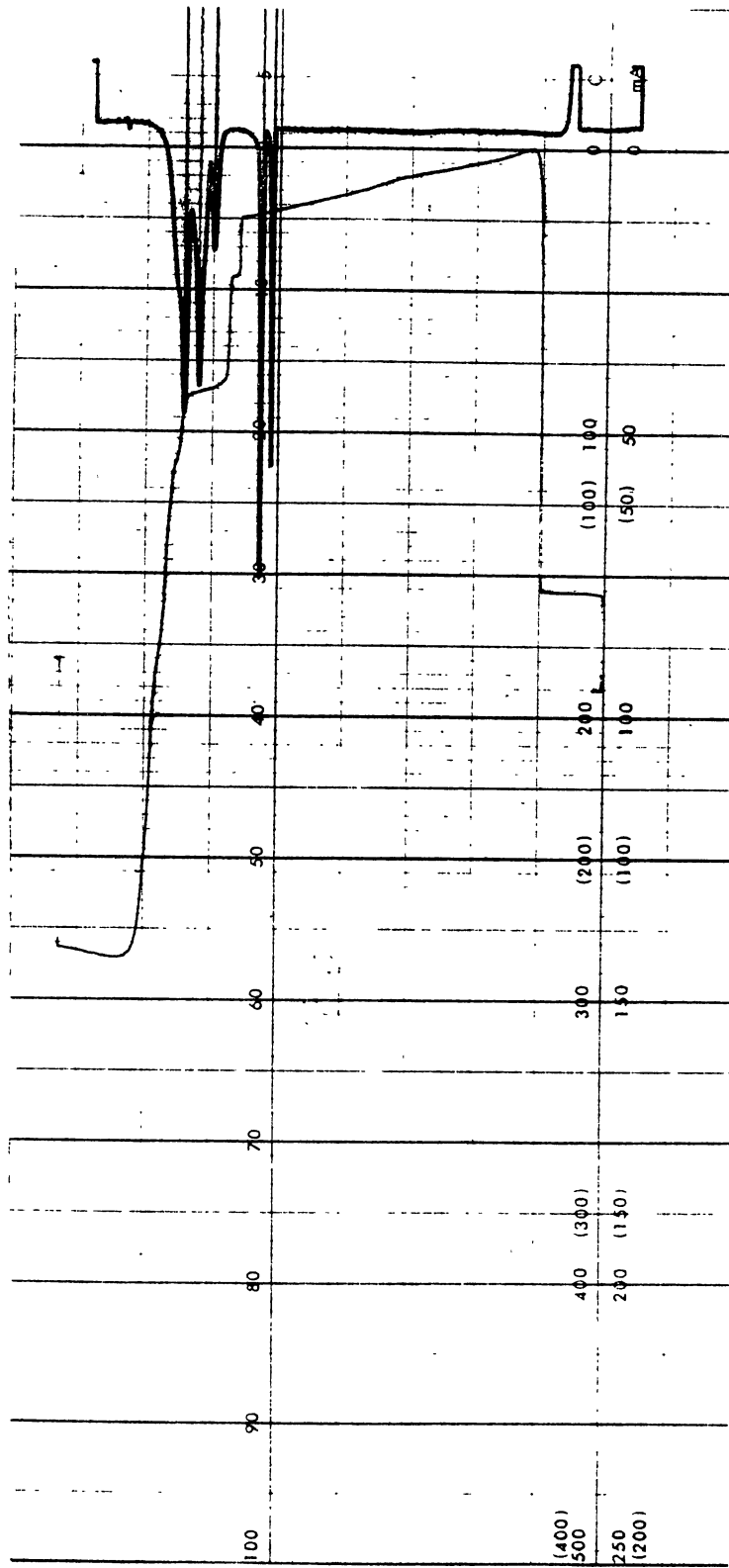
Run 3, 4th hour sample.

APPENDIX C

MASS TRANSFER COEFFICIENT DATA

138

TABLE XXX

DATA FOR MASS TRANSFER COEFFICIENTS, RUN 1

Time (hr)	V (L)	N_A (mg/L)	$c^*_{A_1}$ (mg/L)	$c^*_{A_2}$ (mg/L)	$\overline{(c^*_A - c_A)}_L$ (mg/L)	$k_L a$ (hr^{-1})
1	12.4	5075	42.4	0.36	8.81	46.3
2	12.2	5150	42.7	0.94	6.97	60.5
3	12.0	5180	43.0	0.13	7.38	58.7
4	11.7	5235	43.4	0.05	6.43	69.6

TABLE XXXI

DATA FOR MASS TRANSFER COEFFICIENTS, RUN 2

Time (hr)	V (L)	N_A (mg/L)	$c^*_{A_1}$ (mg/L)	$c^*_{A_2}$ (mg/L)	$\overline{(c^*_A - c_A)}_L$ (mg/L)	$k_L a$ (hr^{-1})
1	12.4	4015	34.6	1.32	10.2	31.6
2	12.2	4620	38.4	0.18	7.13	53.1
3	12.0	5090	42.3	0.15	7.43	57.2
4	11.7	5565	46.1	0.05	6.78	70.1

TABLE XXXII

DATA FOR MASS TRANSFER COEFFICIENTS, RUN 3

Time (hr)	V (L)	N_A (mg/L)	$c^*_{A_1}$ (mg/L)	$c^*_{A_2}$ (mg/L)	$\overline{(c^*_A - c_A)}_L$ (mg/L)	$k_L a$ (hr^{-1})
1	12.4	5230	44.08	0.77	10.70	39.3
2	12.2	5340	44.66	0.44	9.55	45.8
3	11.9	5460	45.24	0.05	6.66	68.6
4	11.7	5530	45.81	0.05	6.73	70.2

TABLE XXXIII

DATA FOR MASS TRANSFER COEFFICIENTS, RUN 4

Time (hr)	V (L)	N_A (mg/L)	$c^*_{A_1}$ (mg/L)	$c^*_{A_2}$ (mg/L)	$\overline{(c^*_A - c_A)}_L$ (mg/L)	(hr^{-1})
1	12.6	4485	35.1	0.68	8.73	40.76
2	12.4	4765	38.9	0.17	7.13	54.08
3	12.1	4925	37.5	0.55	8.74	46.50
4	11.9	5205	39.0	0.05	5.79	75.79

TABLE XXXIV

DATA FOR MASS TRANSFER COEFFICIENTS, RUN 5

Time (hr)	V (L)	N_A (mg/L)	$c_{A_1}^*$ (mg/L)	$c_{A_2}^*$ (mg/L)	$\overline{(c_A^* - c_A)}_L$ (mg/L)	$k_L a$ (hr^{-1})
1	12.7	5040	37.3	0.11	6.37	62.1
2	12.5	5045	34.4	0.19	6.55	61.6
3	12.2	5070	37.5	0.12	6.48	64.0
4	12.0	5100	37.7	0.05	5.62	75.9

TABLE XXXV

DATA FOR MASS TRANSFER COEFFICIENTS, RUN 6

Time (hr)	V (L)	N_A (mg/L)	$c_{A_1}^*$ (mg/L)	$c_{A_2}^*$ (mg/L)	$\overline{(c_A^* - c_A)}_L$ (mg/L)	$k_L a$ (hr^{-1})
1	12.9	5375	36.8	0.34	7.79	53.5
2	12.6	5490	37.3	0.05	5.57	78.1
3	12.4	5555	37.7	0.05	5.62	79.9
4	12.1	5620	38.2	0.05	5.68	81.7

TABLE XXXVI

DATA FOR MASS TRANSFER COEFFICIENTS, RUN 7

Time (hr)	V (mg/L)	N_A (mg/L)	$c^*_{A_1}$ (mg/L)	$c^*_{A_2}$ (mg/L)	$\overline{(c^*_A - c_A)}_L$ (mg/L)	$k_L a$ (hr^{-1})
1	12.4	5120	40.4	0.66	9.65	42.6
2	12.2	5210	40.4	0.25	7.88	54.2
3	11.9	5240	40.4	0.14	7.10	61.8
4	11.7	5250	40.4	0.28	8.05	55.7

TABLE XXXVII

DATA FOR MASS TRANSFER COEFFICIENTS, RUN 8

Time (hr)	V (L)	N_A (mg/L)	$c^*_{A_1}$ (mg/L)	$c^*_{A_2}$ (mg/L)	$\overline{(c^*_A - c_A)}_L$ (mg/L)	$k_L a$ (hr^{-1})
1	12.5	4630	37.2	1.36	10.82	34.4
2	12.2	4800	37.5	0.38	8.08	48.8
3	11.9	4900	37.9	0.05	5.64	72.8
4	11.7	4950	38.2	0.05	5.69	74.5

TABLE XXXVIII

DATA FOR MASS TRANSFER COEFFICIENTS, RUN 9

Time (hr)	V (L)	N_A (mg/L)	$c_{A_1}^*$ (mg/L)	$c_{A_2}^*$ (mg/L)	$\overline{(c_A^* - c_A)}_L$ (mg/L)	$k_L a$ (hr^{-1})
1	12.5	4585	36.6	0.49	8.37	44.0
2	12.2	4700	37.1	0.05	5.54	69.5
3	11.9	4755	37.5	0.05	5.60	71.1
4	11.7	4810	37.9	0.05	5.65	72.7

TABLE XXXIX

DATA FOR MASS TRANSFER COEFFICIENTS, RUN 10

Time (hr)	V (L)	N_A (mg/L)	$c_{A_1}^*$ (mg/L)	$c_{A_2}^*$ (mg/L)	$\overline{(c_A^* - c_A)}_L$ (mg/L)	$k_L a$ (hr^{-1})
1	12.4	5120	27.6	0.53	6.84	60.1
2	12.2	5210	27.7	0.11	5.01	85.2
3	11.9	5240	27.7	0.03	4.10	107.0
4	11.7	5250	27.8	0.03	4.10	109.3

TABLE XL

DATA FOR MASS TRANSFER COEFFICIENTS, RUN 11

Time (hr)	V (L)	N_A (mg/L)	$c_{A_1}^*$ (mg/L)	$c_{A_2}^*$ (mg/L)	$\overline{(c_A^* - c_A)}_L$ (mg/L)	$k_L a$ (hr^{-1})
1	12.4	5120	28.1	0.43	6.64	61.9
2	12.2	5130	28.2	0.42	6.60	63.7
3	11.9	5215	28.2	0.03	4.16	104.9
4	11.7	5220	28.3	0.03	4.17	107.3

TABLE XLI

DATA FOR MASS TRANSFER COEFFICIENTS, RUN 12

Time (hr)	V (L)	N_A (mg/L)	$c_{A_1}^*$ (mg/L)	$c_{A_2}^*$ (mg/L)	$\overline{(c_A^* - c_A)}_L$ (mg/L)	$k_L a$ (hr^{-1})
1	12.4	5210	28.8	0.20	5.75	72.8
2	12.2	5175	28.9	0.44	6.81	62.3
3	11.9	5244	28.9	0.03	4.25	103.5
4	11.7	5277	29.0	0.03	4.25	106.2

2

VITA

Victoria Lynn Milam

Candidate for the Degree of

Master of Science

Thesis: OZONOLYSIS OF AQUEOUS PHENOL AND ACETIC ACID IN A PRESSURIZED BUBBLE COLUMN

Major Field: Chemical Engineering

Biographical:

Personal Data: Born in Oklahoma City, Oklahoma, November 22, 1958, the daughter of Mr. and Mrs. James A. Milam.

Education: Graduated from U. S. Grant High School, Oklahoma City, Oklahoma, in May, 1977; received the Bachelor of Science in Chemical Engineering degree from Oklahoma State University in 1981; completed requirements for the Master of Science degree at Oklahoma State University in July, 1984.

Professional Experience: Roustabout, Mobil Oil Co., summer, 1980; summer engineer, Dowel Co., summer, 1981; graduate research and teaching assistant, Oklahoma State University, August, 1982, to May, 1984.